SNSB Bayerische Staatssammlung für Paläontologie und Geologie

■ München, 2020

■ Manuscript:
received:
25.08.2020
revision:
accepted, 02.09.2020
available online, 17.11.2020

■ ISSN 0373-9627

■ ISBN 978-3-946705-08-6

A summary of the Jurassic System in North and East-Central Iran

Kazem Seyed-Emami[1]*, Markus Wilmsen[2] & Franz T. Fürsich[3]
with contributions by Mahmoud R. Majidifard[4], Ahmad Raoufian[5] & Jafar Taheri[6]

[1] *School of Mining Engineering, College of Engineering, University of Tehran, Iran*
[2] *Senckenberg Naturhistorische Sammlungen Dresden, Museum für Mineralogie und Geologie, Sektion Paläozoologie, Germany*
[3] *GeoZentrum Nordbayern, Fachgruppe PaläoUmwelt, Friedrich-Alexander-Universität Erlangen-Nürnberg, Germany*
[4] *Research Institute for Earth Sciences, Geological Survey of Iran, Box 131851-1494 Tehran, Iran*
[5] *Daneshvar Center, Farhangian University, Neyshapour, Iran*
[6] *Geological Survey of Iran, NE Branch, P.O. Box 91735-1166, Mashad, Iran*

**Author for correspondence and reprint requests; E-mail:* kemami@ut.ac.ir

Zitteliana 94, 99–156.

Abstract

The rocks of the Jurassic System in North and Central Iran are represented by very thick sedimentary successions reflecting the deposition during two tectono-stratigraphic megacycles, bounded by three important unconformities. The older (Early to early Middle Jurassic) cycle starts, after the Late Triassic closure of the Palaeotethys and the collision of the Iran Plate with the southern margin of Eurasia (Turan Plate), with an abrupt uplift of the Cimmerian Mountains around the Triassic–Jurassic boundary (Main-Cimmerian Event) and is terminated by the Mid-Cimmerian Tectonic Event in the mid-Bajocian. The predominantly siliciclastic sediments of this tectono-stratigraphic cycle are accommodated in the Ab-e-Haji Subgroup of the (upper) Shemshak Group. The Ab-e-Haji Subgroup consists of thick and widespread, partly coal-bearing siliciclastic strata and also records some important marine ingressions, especially in the Toarcian and Aalenian. The younger tectono-stratigraphic cycle starts with an extensive marine transgression in the Late Bajocian and ends around the Jurassic-Cretaceous boundary with the Late Cimmerian Tectonic Event. In the aftermath of the Mid-Cimmerian Tectonic Event, the Iran Plate was dissected into several structural units, the geological histories of which differed and so did their facies patterns. Thus, in North Iran two main sedimentary areas developed, namely the Alborz and Koppeh Dagh basins, which show moderate differences in lithology and thicknesses. However, the differentiation is much more pronounced on the Central-East Iranian Microcontinent, which comprises three N–S-oriented and independent structural units, i.e., from east to west the Lut, Tabas and Yazd blocks. During the Jurassic Period, the sea mostly covered the Tabas and Lut blocks, whereas the Yazd Block remained largely emergent. The lithologically diverse and numerous formations of the area are combined in the Magu and Bidou groups. Early to Early Middle Jurassic ammonite faunas of North and Central Iran are palaeobiogeographically closely related to Northwest European (Subboreal) ammonite faunas, allowing a similar biozonation. Concurrent with the Late Bajocian transgression, there is an abrupt change in faunal composition and the Middle and Late Jurassic ammonite faunas of North and Central Iran are much more similar to those of epicontinental seas bordering the northern margin of the western Tethys and occupy an intermediate position between the Mediterranean and the Submediterranean Province. The results of the studies on ammonoid palaeobiogeography are in line with Early Jurassic palaeogeographic reconstructions that place the Iran Plate at fairly high palaeo-latitudes of about 45°N, followed by a rapid southward shift throughout the Middle and Late Jurassic to a position of about 30°N.

Keywords: Jurassic System, Iran Plate, Lithostratigraphy, Biostratigraphy, Ammonite faunas, Palaeo(bio)geography.

1 Introduction

Jurassic rocks show a wide distribution in North and Central Iran, attain great thicknesses and are commonly superbly exposed. The present paper is a short synopsis of the extensive investigations of the sedimentary strata of the Jurassic System in North and East-Central Iran, carried out over the last 20 years by teams from Iran (University of Tehran and Geological Survey of Iran) and Germany (universities of München, Würzburg and Erlangen-Nürnberg as well as the Senckenberg Natural History Collections in Dresden). The manifold results of these studies have been published in numerous papers (see text and references), which are summarized herein. The biostratigraphy is based on systematically collected, described, and published ammonites that fortunately occur in most of the studied formations, allowing

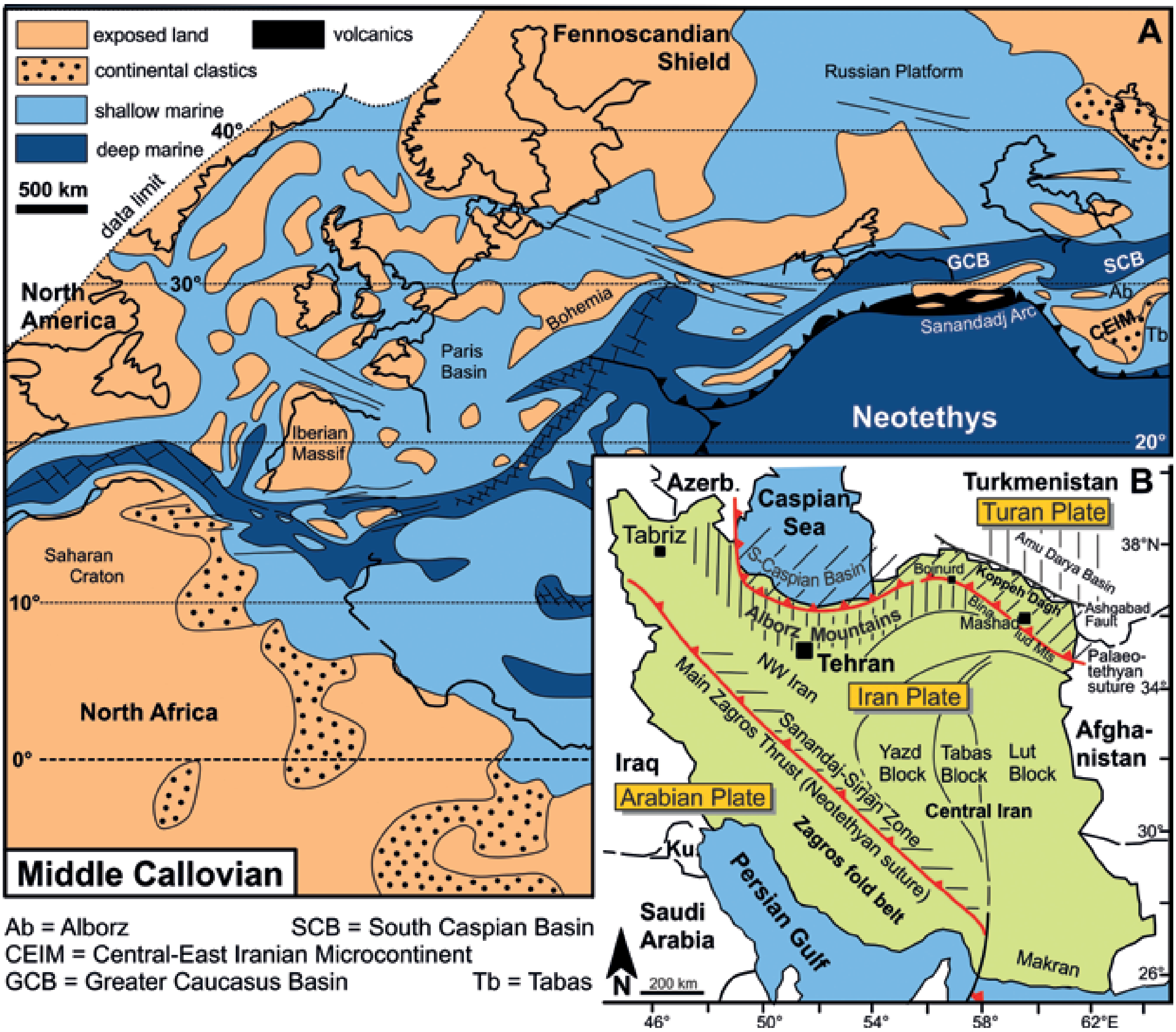

Figure 1: Structural and palaeogeographic framework of Iran. A, Middle Callovian palaeogeography of the western Tethyan area (modified after Thierry 2000). B, main structural units and sutures of Iran (modified after Wilmsen et al. 2009a).

an accurate chronostratigraphic calibration of the lithostratigraphic units as well as precise intra- and interbasinal correlations. Therefore, special emphasis is put herein on the extensive and diverse Jurassic ammonite fauna collected over the years.

2 Geological overview

Iran is characterized by a very diverse Phanerozoic geology. The Central-East Iranian Microcontinent (CEIM; Takin 1972), consisting of the Yazd, Tabas, and Lut blocks, together with North/Northwest Iran forms the Iran Plate, which occupies a structural key position in the Middle East (Fig. 1a, b; Wilmsen et al. 2009a). As an element of the Cimmerian microplate assemblage, it became detached from Gondwana during the Late Permian and collided with Eurasia (Turan Plate) during the early Late Triassic, closing the Palaeotethys Ocean. The resulting Palaeotethys suture runs approximately E–W in northern Iran, bending southeastwards into Afghanistan (Fig. 1b). Towards the southwest, the Iran Plate is bounded by the Neotethyan suture, separating it from the Arabian Plate. Palaeogeographic reconstructions for the Middle Jurassic (e.g., Barrier & Vrielynck 2008) place the Iran Plate at the northern margin of the Neotethyan Ocean at subtropical palaeo-latitudes of ca. 30°N (Fig. 1a).

The Jurassic System in North and Central Iran (Iran Plate) consists of two large tectono-sedimentary cycles. The older cycle begins, after the closure of the Palaeotethys and the collision of the Iran Plate with the active southern margin of Eurasia during the Late Triassic (Eo-Cimmerian Event; Stöcklin 1974; Sengör et al. 1988; Wilmsen et al. 2009a), with the so-called Main-Cimmerian Event at the Triassic-Jurassic boundary (Fürsich et al. 2009a; Wilmsen

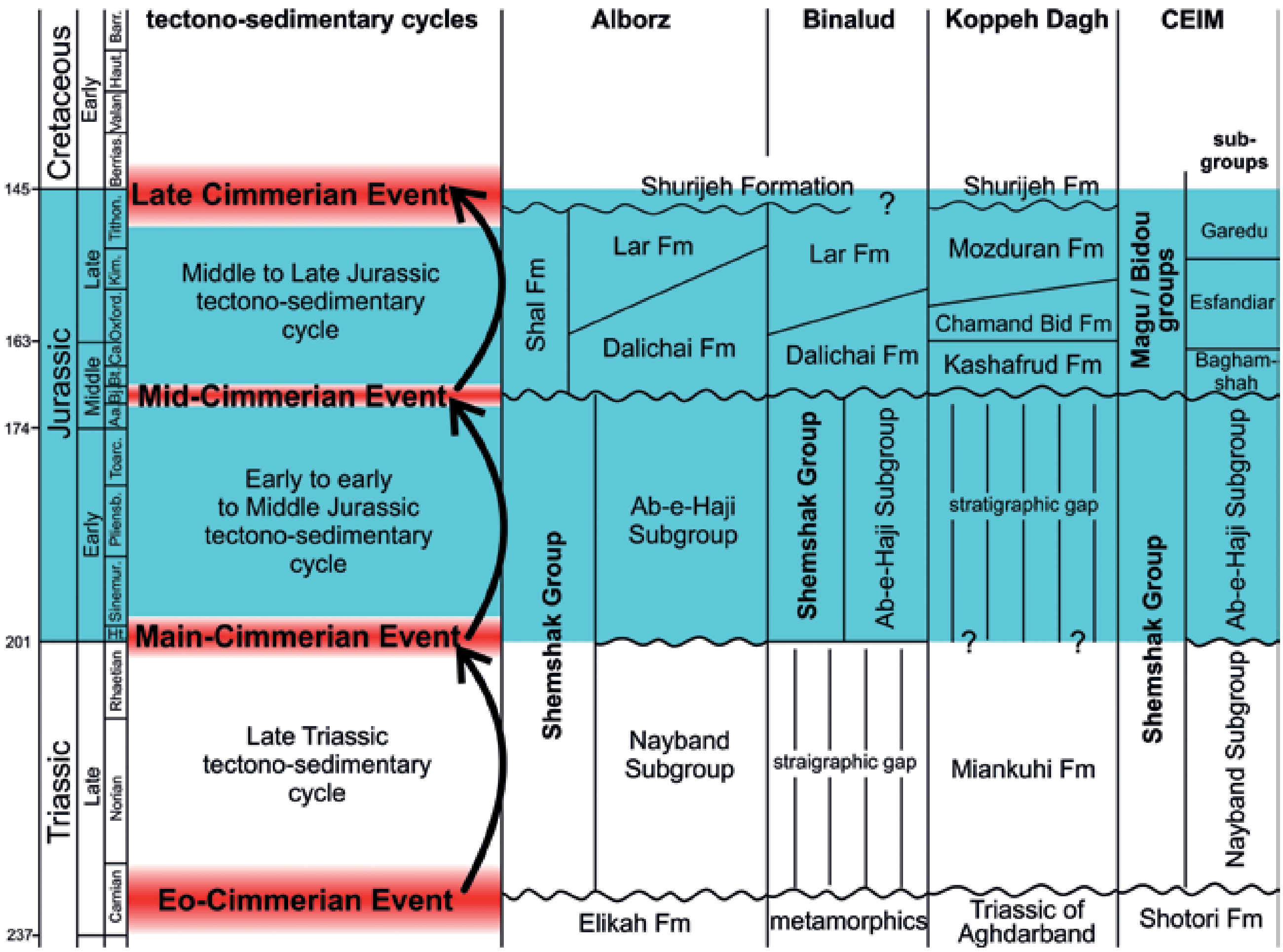

Figure 2: Late Triassic to Jurassic tectono-sedimentary and lithostratigraphic framework of Iran (compiled after Seyed-Emami et al. 2004a and Wilmsen et al. 2009a). The Jurassic System with its two tectono-stratigraphic megacycles is highlighted in blue. CEIM: Central-East Iranian Microcontinent.

et al. 2009a; Fig. 2). This Early to early Middle Jurassic tectono-sedimentary cycle is represented by the predominantly siliciclastic rocks of the Ab-e-Haji Subgroup (new) of the Shemshak Group (Fürsich et al. 2009a; Wilmsen et al. 2009b, c). The cycle was terminated by the Mid-Cimmerian Event, around the early/late Bajocian boundary (Seyed-Emami & Alavi-Naini 1990; Brunet et al. 2003; Seyed-Emami et al. 2004a; Fürsich et al. 2009b; Wilmsen et al. 2009a; Fig. 2). The younger cycle started with an extensive transgression in the late Bajocian and is terminated by the Late Cimmerian Event, around the Jurassic-Cretaceous boundary (Wilmsen et al. 2003, 2009b, 2010; Fig. 2). In East-Central Iran, this Middle to Late Jurassic tectono-sedimentary cycle includes the deposits of the Magu and Bidou groups (Wilmsen et al. 2009b), while in northern Iran it is represented by a lithologically diverse complex of lithostratigraphic units comprising the Shal, Dalichai, Kashafrud, Chaman Bid, Lar, Mozduran and Shurijeh formations (e.g., Lassemi 1995; Majidifard 2008; Taheri et al. 2009; Hosseinyar et al. 2019; Fig. 2).

During Late Triassic to early Middle Jurassic, the Iran Plate acted more or less as a coherent mass and the sedimentary rocks are widely similar. The Shemshak Group (former Shemshak Formation of Assereto 1966a) in North as well as in Central Iran (Iran Plate) is an up to 4000-m-thick siliciclastic succession, widely distributed across the Iran Plate (Figs. 2, 3). It is bounded at the base and at the top by two important unconformities, caused by the Early and Mid Cimmerian tectonic events. For better comparison with Central Iran, Assereto (1966a) proposed to raise the Shemshak Formation to the rank of a group. During a symposium on this matter at the Geological Survey of Iran in 1984, it was largely accepted to combine the Nayband, Ab-e-Haji, Badamu, and Hojedk formations within the Shemshak Group (Aghanabati 1998). Fürsich et al. (2009a) raised the Shemshak Formation of the Alborz Mountains formally into the rank of a group and subdivided it from base to the top into nine formations: Ekrasar, Shahmirzad, Laleband, Kalariz, Alasht, Javaherdeh, Shirindasht, Fillzamin and Dansirit (Figs. 3, 4). However, Krystyn et al. (2019) excluded the Norian-Rhaetian Nayband Formation from the Shemshak Group, based on lithostratigraphic and facies differences, as well as on the occurrence of the Main-Cimmerian event at the

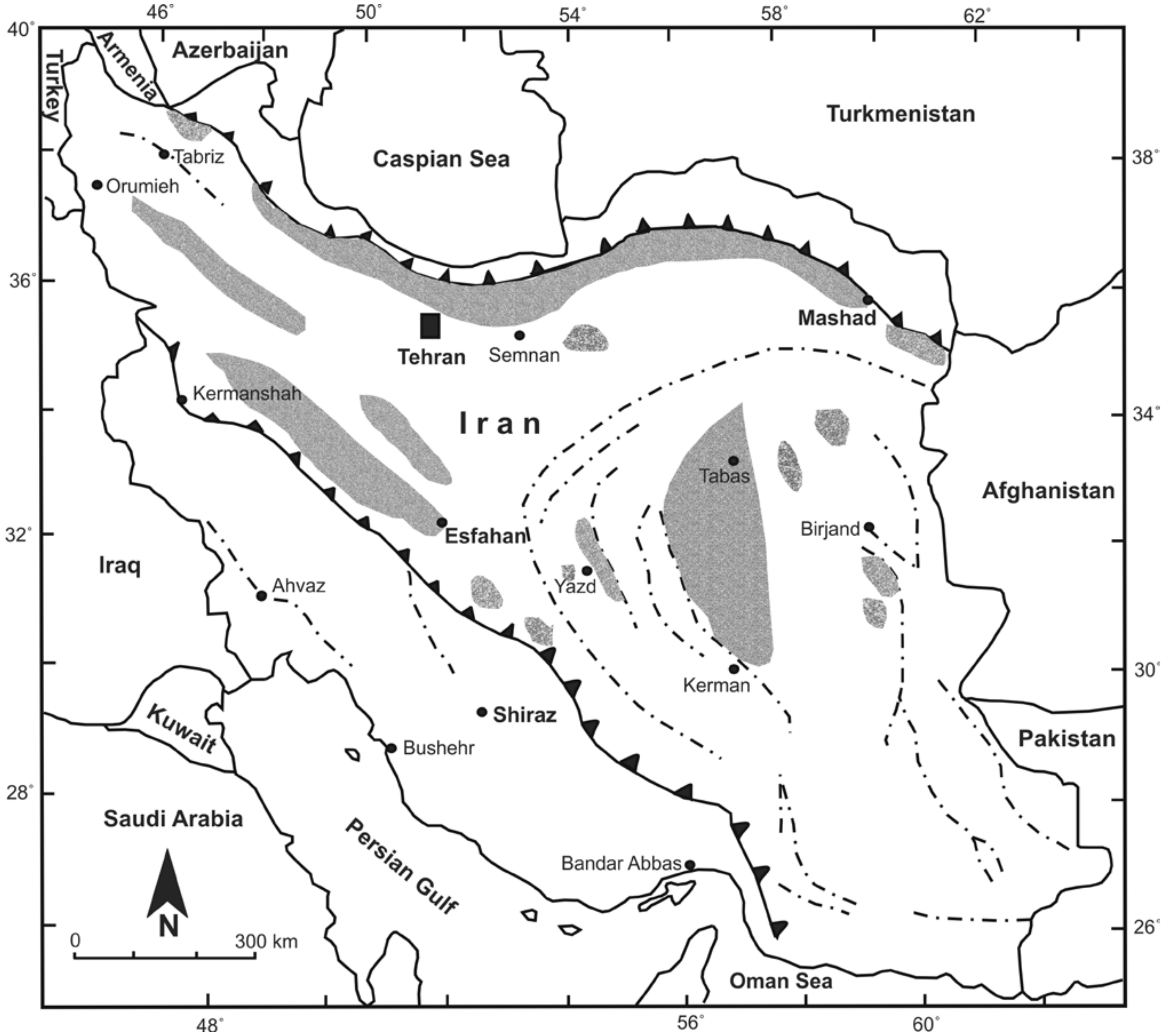

Figure 3: Distribution of the Shemshak Group (grey-shaded areas) in Iran.

Triassic-Jurassic boundary. As a compromise, we still keep the Shemshak Group as originally defined, but separate the Triassic part as the Nayband Subgroup (new) from the Jurassic part as the Ab-e-Haji Subgroup (new), to take into account the unconformity at the base of the Jurassic succession, but also to stress the predominantly siliciclastic nature of the Upper Triassic and Lower to lower Middle Jurassic rocks.

3 Lithostratigraphy

3.1 North Iran (Alborz, Koppeh Dagh, and Binalud Mountains)

3.1.1 Lower to lower Middle Jurassic strata (Ab-e-Haji Subgroup, Shemshak Group)

Alborz—The Ab-e-Haji Subgroup of the Shemshak Group is not developed in the Koppeh Dagh area, where the Kashafrud Formation transgresses with angular unconformity on older rocks (the Norian–Rhaetian Miankuhi Formation represents the Nayband Subgroup in this area; Fig 2). The Kashafrud Basin of the Koppeh-Dagh is thought to have been deposited in a rift basin, which formed as the southeastern extension of the South Caspian Basin after the Mid-Cimmerian Event in early Late Bajocian times (Taheri et al. 2009). Therefore, the following account of the Ab-e-Haji Subgroup of the Shemshak Group refers solely to the Alborz Mountains.

The Ab-e-Haji Subgroup is widely distributed in the Alborz Mountains and exhibits a distinct facies change from north to south. In the north, the subgroup locally rests with an angular unconformity on the Rhaetian Kalariz Formation. Towards the south it forms a sharp boundary with the Upper Triassic Shahmirzad Formation. Contrary to its monotonous appearance and common belief, the environmental framework of the Ab-e-Haji Subgroup is very com-

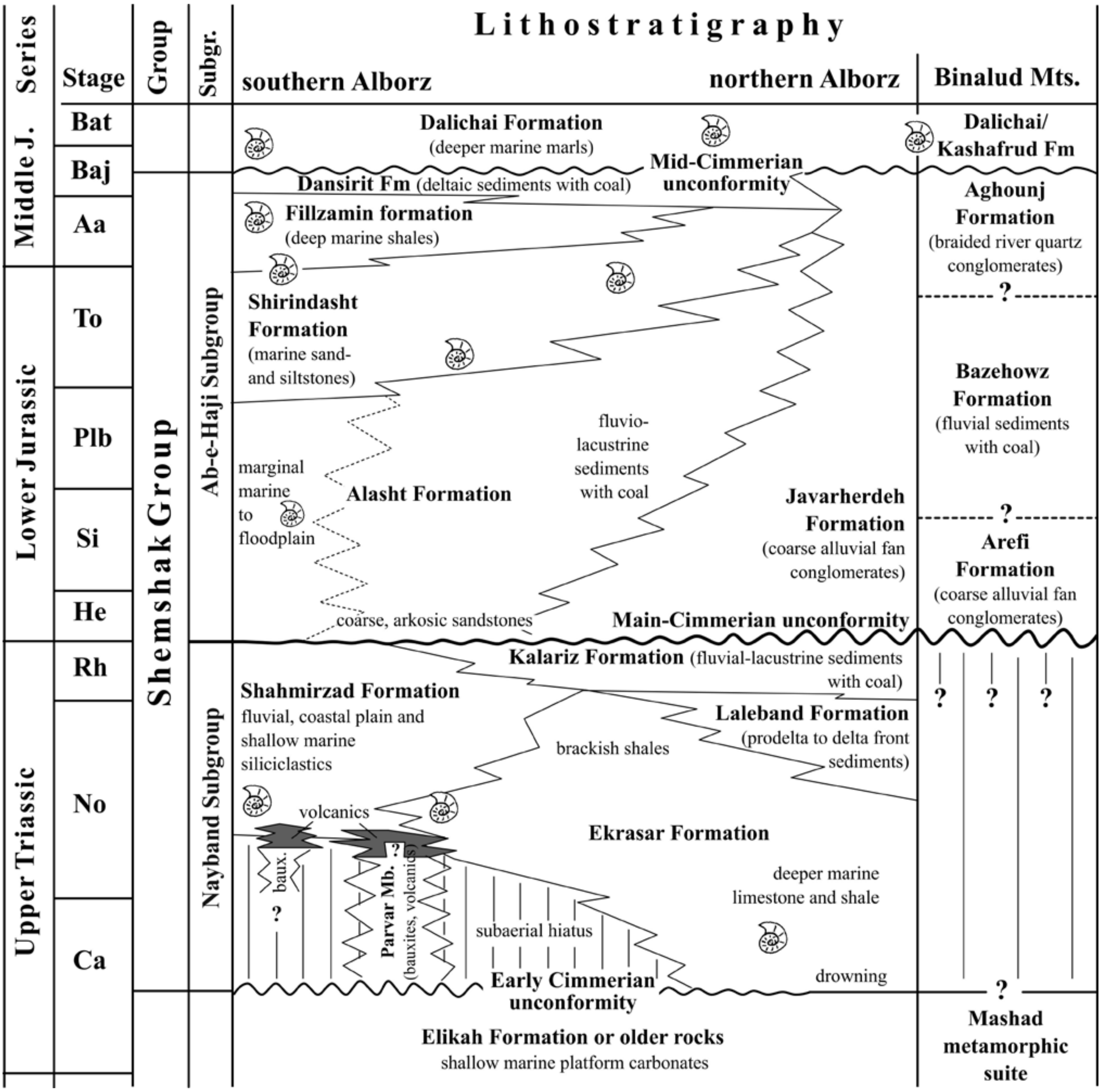

Figure 4: Lithostratigraphic scheme of the Shemshak Group in the Alborz and Binalud mountains (modified after Fürsich et al. 2009a and Wilmsen et al. 2009c).

plex, including alluvial fans, fluvial-lacustrine, coastal plains, prodelta-delta front, marginal-marine, to storm-dominated shelf and even relatively deep-marine environments (Fürsich et al. 2005, 2009a).

In the northern Alborz, close to the Cimmerian mountain range, the subgroup is represented by the Javaherdeh Formation, an approximately 1000-m-thick succession of polymict conglomerates, composed mainly of rounded quartzite, milk quartz, volcanic, and metamorphic pebbles. Towards the south the thickness diminishes rapidly and the formation grades into the sandy Alasht Formation. The conglomerates form several-metres-thick lenticular packages separated by coarse-grained to gravelly sandstone layers and locally contain tree trunks. The deposits represent partly debris flows, partly braided streams of mid- to distal humid alluvial fans.

The Hettangian to ?Toarcian Alasht Formation, decreasing in thickness towards the west from approximately 1700 m to 300 m, replaces the Javaherdeh Formation towards the south. The predominantly fine- to coarse-grained arkosic sandstones are, in places, pebbly or conglomeratic and form decametre-thick packages, which commonly fine upwards. Rootlets, mottled siltstones, and ferricretes are common pedogenic features. Carbonaceous silt and coals seams are common within finer-grained (silt to argillaceous silt) intercalations. Towards the west, trace fossils and occasional bivalves document some marine influence. This is also the case in the topmost part of the formation. The Alasht Formation represents largely meandering stream deposits and floodplain environments with small lakes and swamps. Towards the west, the non-marine succession interfingers with marginal and shallow marine deposits, partly delta-front sandstones. Similarly, towards the top of the formation marine ingressions repeatedly flooded the coastal plains.

The base and top of the upper Pliensbachian to Aalenian Shirindasht Formation (110–550 m) are distinctly time-transgressive. The dominant lithology is dark-grey to olive-grey fine-grained siliciclastics (silt, argillaceous silt, fine-grained sandstones), which are commonly organized in small coarsening-upward parasequences. Pervasive bioturbation, common bivalves, and ammonites indicate a fully marine environment. The sandstones are usually parallel-bedded and hummocky cross-stratified and indicate a water depth above the storm wave-base and below the fair-weather wave-base.

The overlying Aalenian to Lower Bajocian Fillzamin Formation increases in thickness southward and reaches 680 m in the southern Alborz. Towards the north it grades into the Shirindasht and Dansirit formations. Its boundaries are again time-transgressive. Lithologically, it is composed of bioturbated, monotonous, argillaceous to fine-sandy silt but in the eastern Alborz sandstone intercalations with parallel lamination and hummocky cross-stratification are common towards the top. The depositional depth was below the storm wave-base, but shallowed towards the top to represent a pro-delta or in some areas even a lower delta-front regime.

The top of the Shemshak Group is formed by the Lower Bajocian Dansirit Formation. Its thickness varies strongly, ranging from 10 to 320 m. The formation is composed of cross-bedded, highly immature arkoses, between which carbonaceous silt and coal layers are intercalated, which contain a rich flora. The top of the formation is an unconformity. In most areas, the Dansirit Formation represents delta-plain to marginal marine environments, but locally corresponds to delta-front or nearshore bar settings. It documents a distinct shallowing of the basin and a marked sea-level fall.

The thick siliciclastic sediments of the Ab-e-Haji Subgroup were deposited in a fast-subsiding sedimentary basin and at the same time required vast erosional areas. It records syn- and post-collisional processes of the Cimmerian Orogeny as well as the opening of a Neotethys back-arc rift basin (Fürsich et al. 2005, 2009b; Wilmsen et al. 2009a). Ammonites document several significant marine transgressions. These occurred in the late Sinemurian, late Pliensbachian and the most extensive one in the Toarcian–Aalenian and early Bajocian. Strikingly, these transgressive phases do not necessarily follow the global sea-level fluctuations (Hallam 1988; Hardenbol et al. 1998), but apparently were greatly influenced by the local and regional synsedimentary tectonic activity (Fürsich et al. 2005).

Ammonites occur at several levels within the subgroup. More than 70 taxa have been described so far from the Alborz Basin (Seyed-Emami et al. 2008),

Plate 1 (Page 105): Ammonites from the Shemshak Group, Badamu Formation, SW Ravar, Central Iran. **(1a, b)** *Brasilia bradfordensis* (Buckman, 1881). Middle Aalenian, Murchisonae Zone (Seyed-Emami et al. 1993, p. 19, pl. 3, fig. 3). **(2a, b)** *Graphoceras* (*Ludwigella*) *arcitenens* (Buckman, 1902). Upper Aalenian, Concavum Zone (Seyed-Emami et al. 1993, p. 20, pl. 2, fig. 3). **(3a, b)** *Ludwigia murchisonae* (Sowerby, 1829). Middle Aalenian, Murchisonae Zone (Seyed-Emami et al. 1993, p. 18, pl. 3, fig. 2). **(4a, b)** *Leioceras comptum* (Reinecke, 1818). Lower Aalenian, Opalinum Zone (Seyed-Emami et al. 1993, pl. 2, fig. 2). **(5a, b)** *Leioceras crassicostatum* Rieber, 1963. Lower Aalenian, Opalinum Zone (Seyed-Emami et al. 1993, pl. 1, fig. 8). **(6a, b)** *Dumortieria moorei* (Lycett, 1857). Upper Toarcian, Levesquei Zone (Seyed-Emami et al. 1993, pl. 1, fig. 2). **(7a, b)** *Tmetoceras scissum* (Benecke, 1865) Lower Aalenian, Opalinum Zone (Seyed-Emami et al. 1993, pl. 1, fig. 4).

Plate 2 (Page 106): Ammonites from the Shemshak Group, Badamu Formation, of the Kerman-Ravar area, Central Iran. **(1)** *Bredyia brancoi* (Prinz, 1904). Lower Aalenian, Opalinum Zone (Seyed-Emami 1967, p.83, pl. 10, fig. 1). **(2a, b)** *Parsemileites liebi* (Maubeuge, 1955). Lower Bajocian, Laeviuscula Zone (Seyed-Emami 1967, p. 125, pl. 13, fig. 1a, b). **(3a, b)** *Geczyceras tipperi* Seyed-Emami, 1967. Upper Toarcian, Pseudoradiosa Zone (Seyed-Emami 1967, p. 72, fig. 1a, b). **(4a, b)** *Bradfordia inclusa* Buckman, 1910. Lower Bajocian, ?Laeviuscula Zone (Seyed-Emami 1967, p. 124, pl. 12, fig. 18). **(5a–c)** *Malladaites kermanensis* (Seyed-Emami, 1967). Upper Aalenian-Lower Bajocian, ?Laeviuscula Zone (Seyed-Emami 1967, p. 104, pl. 12, fig. 13; 1971, p. 37, pl. 12, fig. 13). **(6a, b)** *Haplopleuroceras subspinatum* Buckman, 1901. Upper Aalenian-Lower Bajocian, ?Laeviuscula Zone (Seyed-Emami 1967, p. 102, pl. 12, fig. 15). **(7)** *Witchellia laeviuscula* (Sowerby, 1824). Lower Bajocian, Laeviuscula Zone (Seyed-Emami 1967, p. 110, pl. 12, fig. 3). **(8a, b)** *Pelekodites macer* (Buckman, 1888). Lower Bajocian, Laeviuscula Zone (Seyed-Emami 1967, p. 117, pl. 12, fig. 11). **(9a, b)** *Pelekodites varicosa* (Sowerby, 1825). Lower Bajocian, laeviuscula Zone (Seyed-Emami 1967, p. 121, pl. 12, fig. 5). **(10)** *Sonninia* (*Euhoploceras*) *adicra* (Waagen, 1867). Lower Bajocian, Laeviuscula Zone (Seyed-Emami 1967, p. 107, pl. 12, fig. 2). **(11a, b)** *Abbasitoides modestum* (Vacek, 1886) (for *Erycites spathi* Seyed-Emami, 1967). Aalenian, Murcisonae Zone (Seyed-Emami 1967, p. 99, pl. 10, fig. 8; 1971, p. 36, pl. 10, fig. 8).

Plate 3 (Page 107): Ammonites from the Shemshak Group, Badamu Formation, Central Iran. **(1a, b)** *Otoites cf. sauzei* (d'Orbigny, 1846). Lower Bajocian, Laeviuscula Zone, Tabas area (Seyed-Emami et al. 2000, p. 260, fig. 3(7)). **(2a, b)** *Witchellia connata* (Buckman, 1927 [m]. Lower Bajocian, Laeviuscula Zone, Tabas area (Seyed-Emami et al. 2000, p. 258, fig. 3(2)). **(3a, b)** *Emileia* sp.; Lower Bajocian, Sauzei Zone, west Kerman (Seyed-Emami 1988b, p. 84, fig. 22). **(4)** *Witchellia* sp. ex gr. *W. laeviuscula* (Sowerby, 1824). Lower Bajocian, Laeviuscula Zone, northern Lut Block (Seyed-Emami et al. 2004b, p. 88, pl. 3, fig. 2). **(5)** *Witchellia platymorpha* Buckman, 1925. Lower Bajocian, Laeviuscula Zone, northern Lut Block (Seyed-Emami et al. 2004b, p. 90, pl. 3, fig. 3). **(6a, b)** *Kummatostephanus* sp. Lower Bajocian, Laeviuscula Zone, west Kerman (Seyed-Emami 1988b, p. 84, fig. 41). **(7)** *Pseuaptetoceras amplectens* (Buckman, 1889). Upper Aalenian, Concavum Zone, Kerman area (Seyed-Emami 1967, p. 90, pl. 11, fig. 4; 1971, pl. 11, fig. 4). **(8)** *Otoites contractus* (Sowerby, 1825). Lower Bajocian, Laeviuscula Zone, Kerman area (Seyed-Emami 1967, p. 130, pl. 13, fig. 4). **(9a, b)** *Pseudaptetoceras amaltheiforme* (Vacek, 1886). Upper Aalenian, Concava Zone, Kerman area (Seyed-Emami 1967, p. 91, pl. 11, fig. 1; 1971, pl. 11, fig. 1).

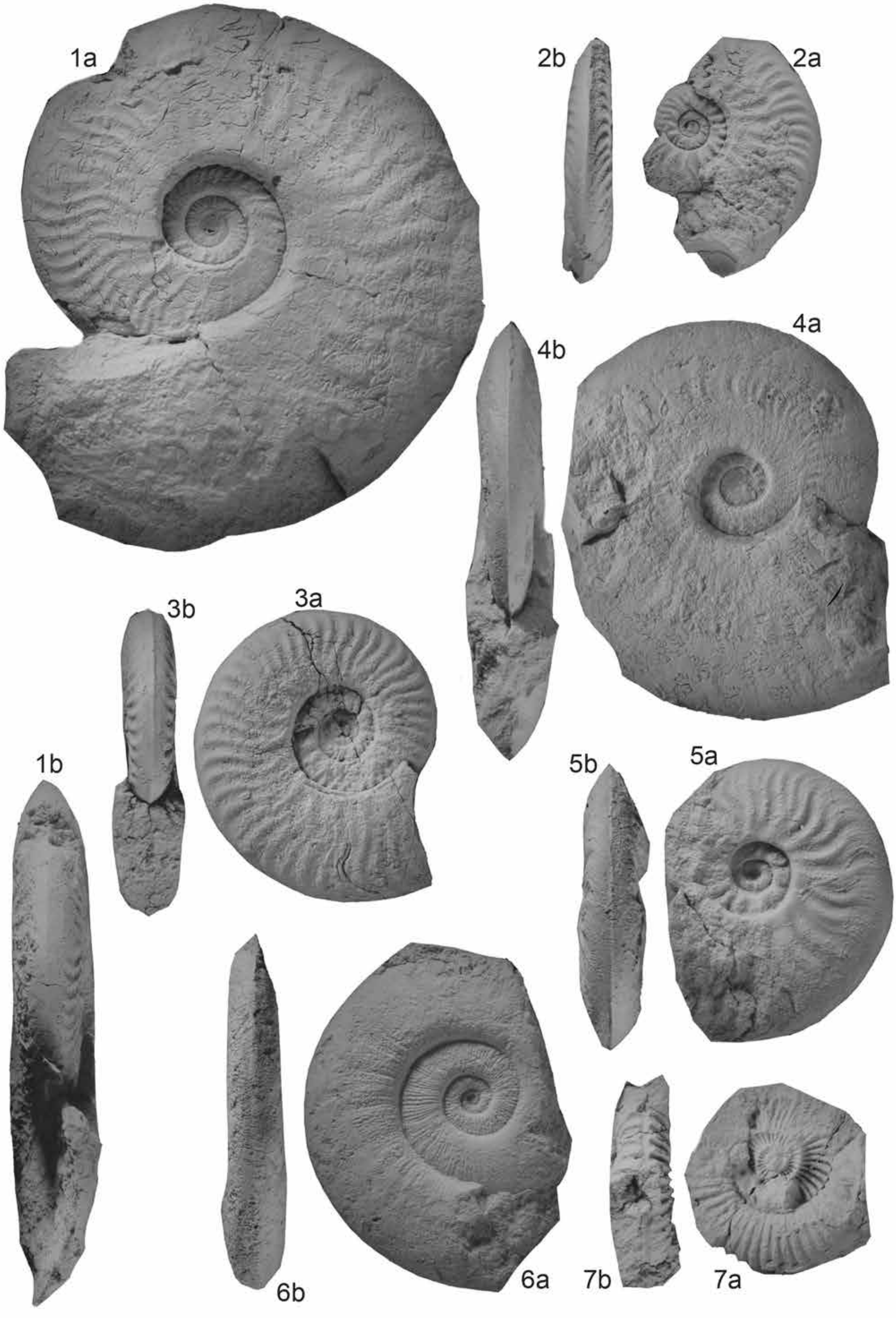
1a
2b
2a
4b
4a
3b
3a
1b
5b
5a
6b
6a
7b
7a

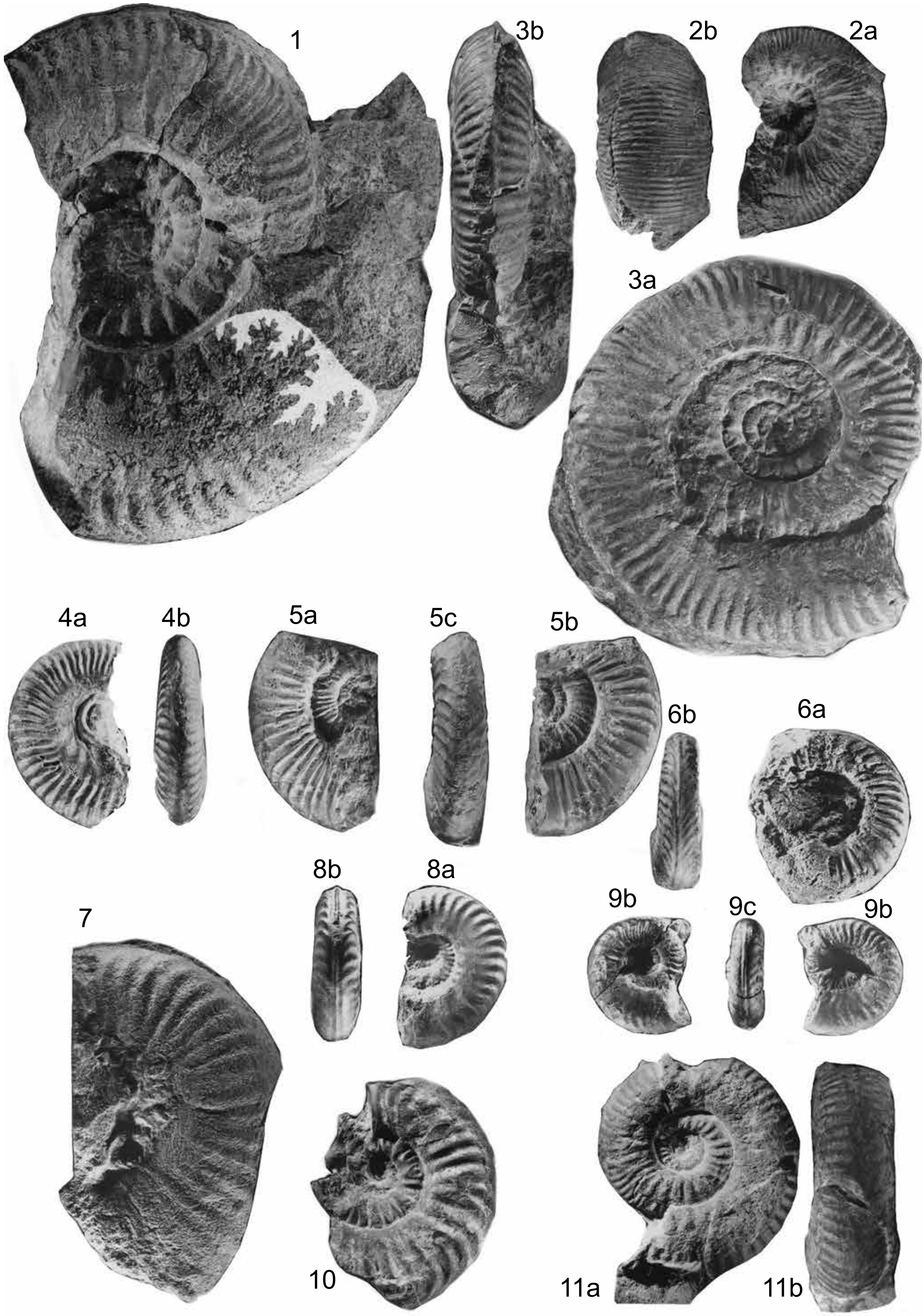
1
3b
2b
2a
3a
4a
4b
5a
5c
5b
6b
6a
8b
8a
7
9b
9c
9b
10
11a
11b

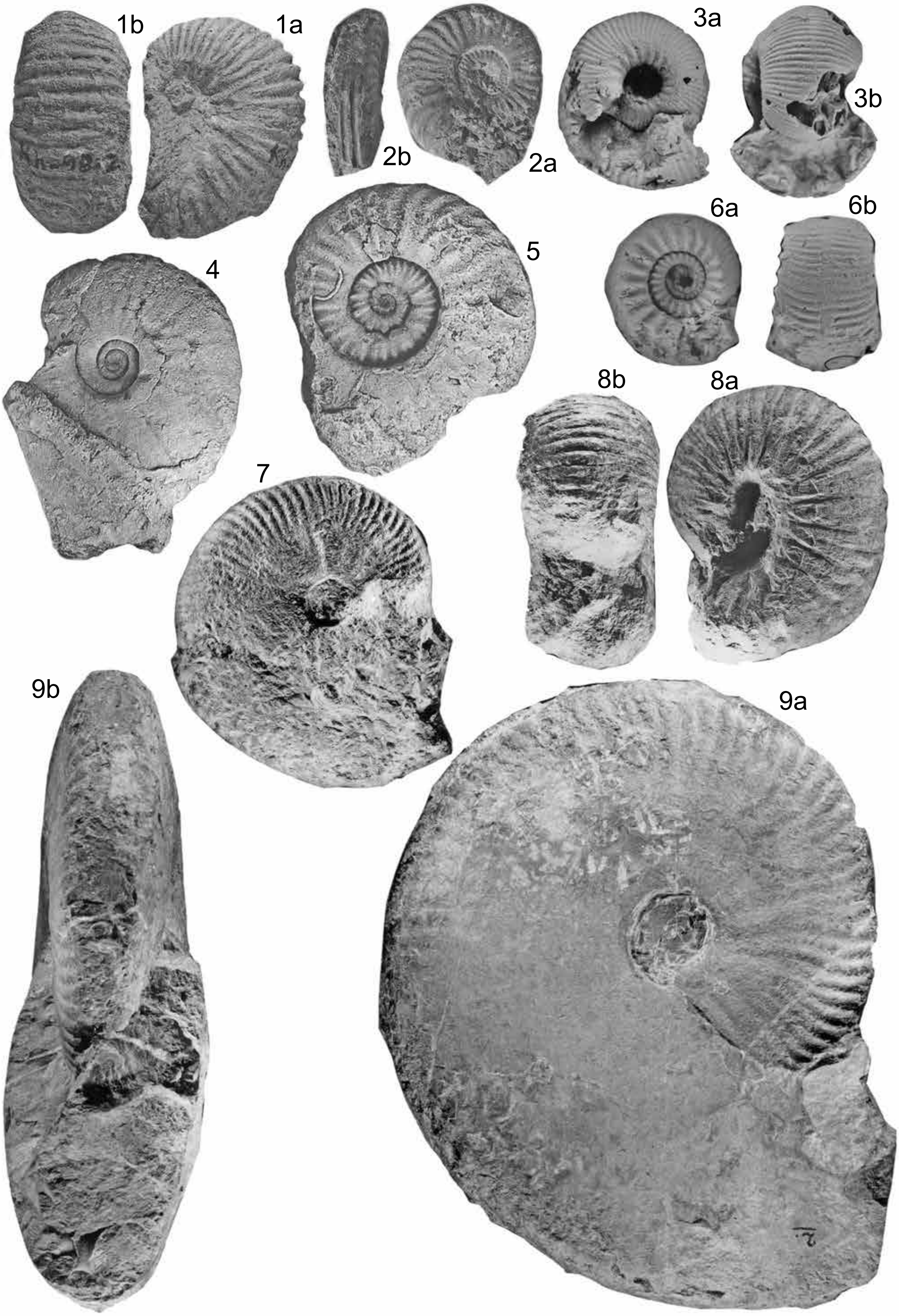
1b
1a
2b
2a
3a
3b
4
5
6a
6b
7
8b
8a
9b
9a

among them the following families: Cymbitidae, Echioceratidae, Amaltheidae, Dactylioceratidae, Hildoceratidae, Graphoceratidae, Hammatoceratidae, Erycitidae, and Stephanoceratidae (Nabavi & Seyed-Emami 1977; Seyed-Emami & Nabavi 1985; Seyed-Emami et al. 2005, 2006, 2008).

Apart from a few endemic taxa, the ammonite fauna is closely related to that of northwestern Europe (Subboreal Province), allowing a similar biozonation. The nearly total absence of Tethyan Lytoceratidae and the scarcity of Phylloceratidae are remarkable. The close lithological and faunistic relationships between North and Central Iran during deposition of the Ab-e-Haji Subgroup indicate that palaeogeographically the two areas were close to each other. According to Early Jurassic palaeogeographic maps (Thierry 2000; Golonka 2007), North Iran occupied a comparatively high latitude around 44°N at the northeastern margin of the western Tethys. During the Middle Jurassic, it shifted further southward to about 30°N.

Eastern Binalud Mountains—The Lower and lower Middle Jurassic strata in the easternmost part of the Binalud Mountains (the southeastern extension of the Alborz chain) consist of a thick, non-marine, coarse-grained siliciclastic sedimentary succession, which corresponds to the Jurassic part of the Shemshak Group, i.e., the Ab-e-Haji Subgroup of the Alborz Mountains (Wilmsen et al. 2009a, c). The succession rests with angular unconformity on a Permo-Triassic metamorphic basement and has been subdivided in three formations, the Arefi, Bazehowz, and Aghounj Formation (Fig. 4).

The lowermost unit, the Arefi Formation, is up to 750 m thick and has been divided into two members. The lower member (Derekhtoot Member) consists of very coarse-grained, chaotic boulder beds, megabreccias and conglomerates, representing rock-fall, debris flow, and ephemeral stream deposits characteristic of upper to middle alluvial fans. The upper member (Kurtian Member) consists of more mature polymikt conglomerates with intercalated fine- to coarse-grained greywackes to subarkoses, which represent lower alluvial fan to proximal braided river deposits.

The overlying Bazehowz Formation is more than 1000 m thick and is composed of stacked m- to decam-thick fining-upward cycles of argillaceous to fine-sandy silt, rich in plant fossils and occasionally containing thin coal layers, alternating with medium- to coarse-grained sandstones and fine-grained conglomerates. They were deposited in the middle reaches of a braided river system (Wilmsen et al. 2009c).

The Aghounj Formation consists of more than 400 m of thick-bedded coarse quartz conglomerates, between which thinner sandstone beds are intercalated. It represents a proximal braided river system.

The Shemshak Group in the eastern Binalud Mountains reflects the erosion of a close-by high-relief source area situated in the northeast. It rests on Cimmerian basement, suggesting that the strata are intramontane deposits of the Cimmerian mountain chain in NE Iran (?Koppeh Dagh) and therefore correspond to Cimmerian molasse deposits (Wilmsen et al. 2009c).

3.1.2 Middle and Upper Jurassic strata

Following the Mid-Cimmerian Event and the subsequent Late Bajocian transgression there was an abrupt lithological change from the siliciclastics of the Ab-e-Haji Subgroup of the Shemshak Group to deeper marine marls, shales, limestones, and platform carbonates. During the Middle and Late Jurassic, two sedimentary areas can be recognized in North Iran, which slightly differ in lithology and thickness; i.e., the Alborz, with its eastern extension, the Binalud Mountains, and the Koppeh Dagh (Kopet Dagh) (Figs. 1, 5, 6). The differences between the two sedimentary areas are not very substantial, but become much more significant during the Cretaceous and Cenozoic periods.

Kashafrud Formation—At the southeastern margin of the Koppeh Dagh, a thick succession (up to 2000 m and more) of predominantly turbiditic siliciclastics is developed, the Kashafrud Formation (Madani 1977; Afshar-Harb 1994; Taheri et al. 2009). It overlies, with angular unconformity (expression of the Mid-Cimmerian Tectonic Event) and a basal conglomerate, various older rocks of the so-called Agh-Darband Window (Ruttner 1991) or Late Palaeozoic mafic-ultramafic (ophiolitic) rocks (Eftekharnezhad & Behroozi 1991; Seyed-Emami et al. 1994, 1996). In the western part of the range there is a gradual contact with the overlying Chaman Bid Formation, whereas in the southeasternmost part, it is overlain by the Mozduran Formation. The sedimentary environments of the Kashafrud Formation range from alluvial fans and braided rivers to the storm-dominated shelf, slope and a deep-marine basin (commonly with distal turbidites). The Kashafrud Formation

Plate 4: Ammonites from the Shemshak Group, Badamu Formation, Central Iran. **(1a, b)** *Witchellia* aff. *suttneri* (Branco, 1879). Lower Bajocian, Laeviuscula Zone, Tabas area (Seyed-Emami et al. 2000, p. 260, fig. 3(1)). **(2a, b)** *Kumatostephanus kumaterus persicus* Seyed-Emami, 1967. Lower Bajocian, Laeviuscula Zone, Kerman area (Seyed-Emami 1967, p. 132, pl. 14, fig. 1; 1971, pl. 14, fig. 1). **(3a, b)** *Emileia quenstedti* Westermann, 1964. Lower Bajocian, Laeviuscula Zone, Kerman area (Seyed-Emami 1967, p. 128, pl. 13, fig. 3; 1971, pl. 13, fig. 3). **(4a, b)** *Pseudaptetoceras amaltheiforme* (Vacek, 1886). Upper Aalenian, Concava Zone, SW Ravar (Seyed-Emami et al. 1993, p. 22, pl. 4, fig. 5). **(5a, b)** *Emileia* cf. *polyschides* (Waagen, 1867). Lower Bajocian, Laeviuscula Zone, southwest Ravar (Seyed-Emami et al. 1993, p. 22, pl. 4, fig. 3).

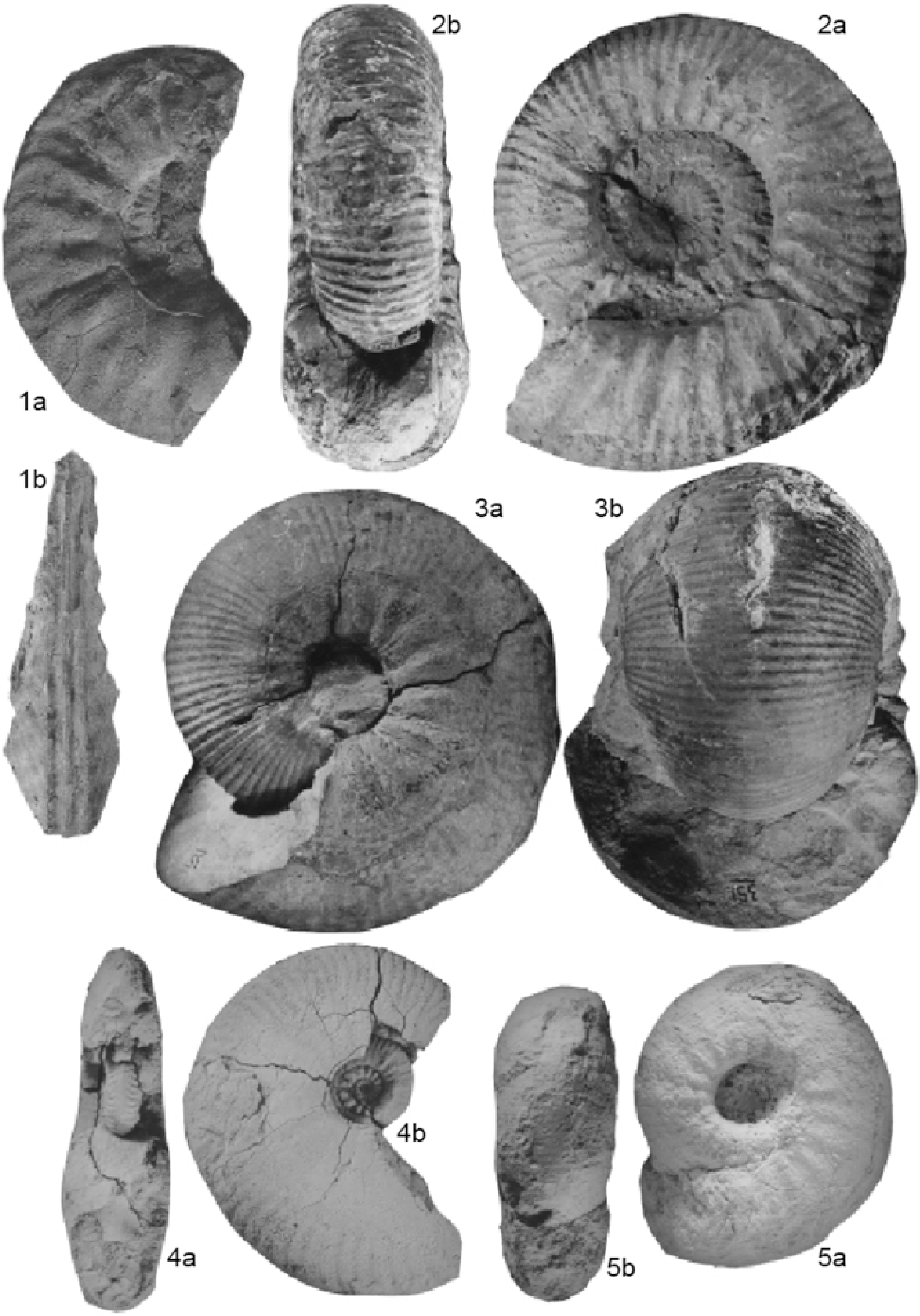
1a
1b
2a
2b
3a
3b
4a
4b
5a
5b

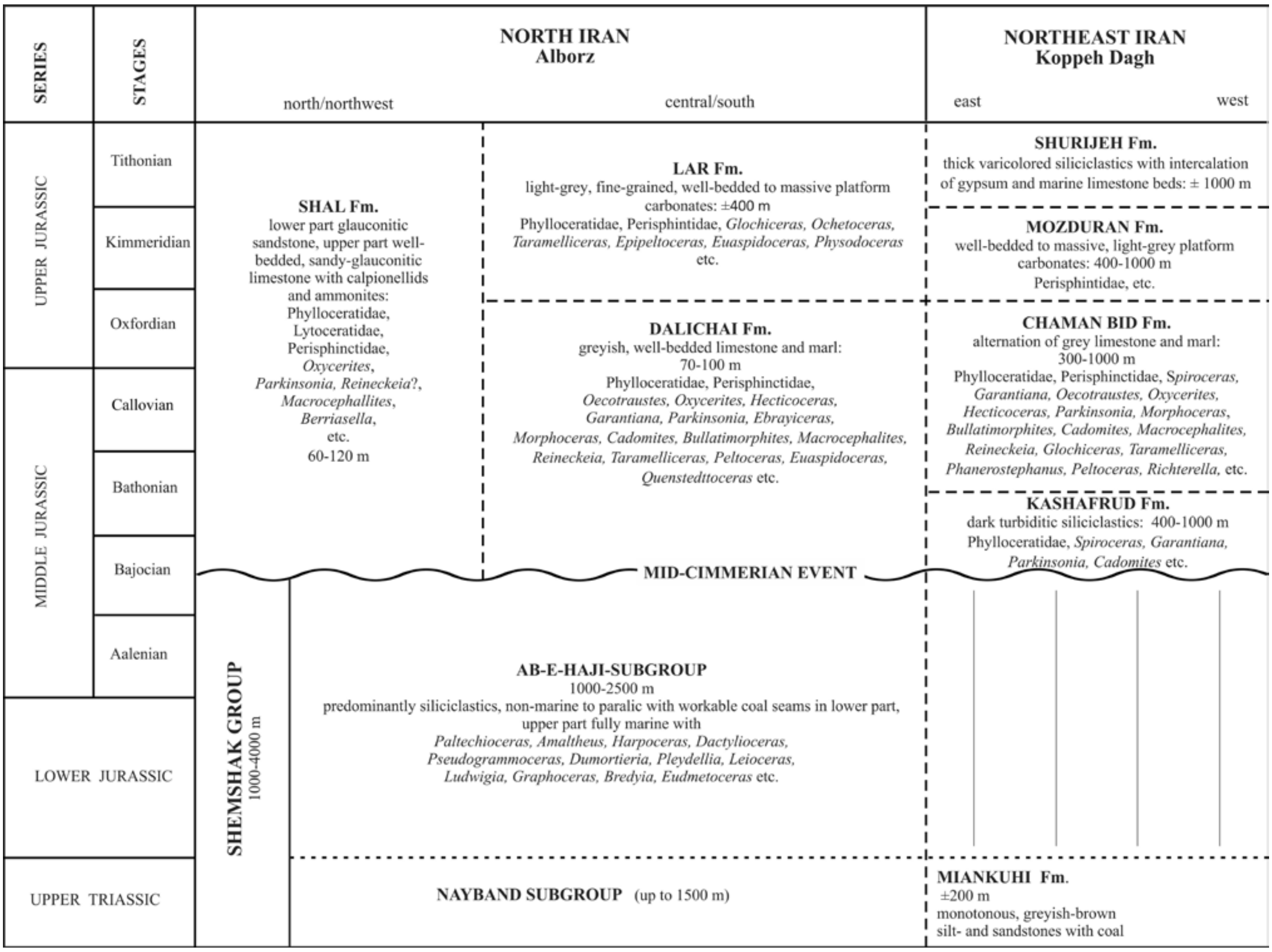

Figure 5: Generalized lithostratigraphic scheme of the Jurassic System in North Iran (Alborz and Koppeh Dagh).

represents the rapid infilling of a rapidly subsiding, narrow rift basin along the Palaeotethys suture at the southern margin of the Turan Plate (Seyed-Emami et al. 1994; Taheri et al. 2009; Robert et al. 2014; Sardar-Abadi et al. 2014; Poursoltani 2017). The interfingering of the Kashafrud and Dalichai formations in the southwestern Koppeh Dagh has been called "Bashkalateh Formation". It is characterized by some sandstone packages and finer-grained siliciclastics intercalated between the dominating carbonates (Majidifard 2008).

The Kashafrud Formation contains hardly any macrobenthic fossils, but a diverse ichnofauna (Taheri 2009) and a poor ammonite fauna of the following families: Phylloceratidae, Lytoceratidae, Stephanoceratidae, Parkinsoniidae and Perisphinctidae, indicating a Late Bajocian to Bathonian age (Seyed-Emami et al. 1994, 1996; Hoseiniun 1995).

Dalichai and Chaman Bid formations—In the Alborz Mountains, Middle Jurassic strata are represented by the Dalichai Formation and their equivalents and in the Koppeh Dagh by the Chaman Bid Formation. These consist largely of an alternation of greyish marls and limestones. In the western and central Alborz Mountains, the thickness of the Dalichai Formation is around 100 m but increases considerably towards the east (eastern Alborz and Binalud) to up to 500 m and more. The Chaman Bid Formation may reach 1000 m and more. The lower boundary of Dalichai/Chaman Bid formations with the underlying Shemshak Group is usually an unconformity, the expression of the Mid-Cimmerian Event, whereas the strongly diachronous boundary with the overlying Lar/Mozduran formations is gradual. Apart from marls and carbonate mudstones, the Dalichai Formation consists of wacke-, pack-, and grainstones, the latter commonly graded. Characteristic components are bioclasts, ooids, and intraclasts, occasionally with minor admixture of silt and quarz grains. Microbialites with *Tubiphytes*, siliceous sponges, and serpulids occur occasionally near the top of the Dalichai Formation. In the mudstones and wackestones, bioclasts consist mainly of radiolarians, *Saccocoma*, sponge spicules, and filaments (Majidifard 2008). In eastern areas, several-m-thick intercalations of fine-grained sandstones indicate the interfingering with the Kashafrud Formation.

A remarkable feature of the Dalichai Formation, especially in the eastern Alborz and Binalud mountains, is the occurrence of several red nodular limestone beds in "Ammonitico Rosso" facies. They repre-

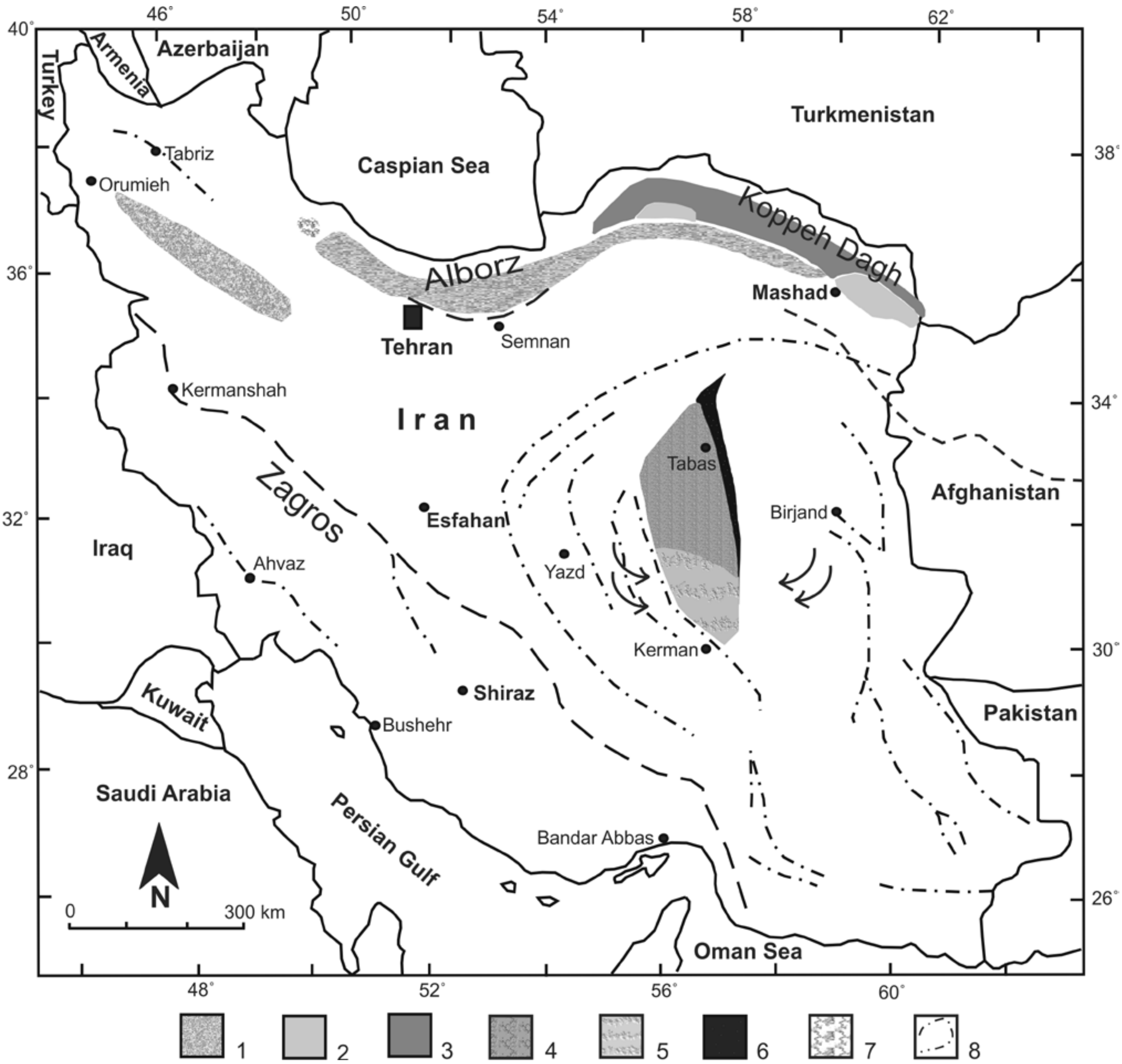

Figure 6: Distribution of Middle Jurassic strata in Iran. 1. Dalichai Formation; 2. Shal Formation; 3. Kashafrud Formation; 4. Chaman Bid Formation; 5. Baghamshah Formation; 6. Qal'eh Dokhtar Formation; 7. Bidou Formation; 8. Main tectonic lines; arrows: inferred directions of siliciclastic supply from land areas (east: Lut Block; west: Yazd Block).

sent condensation horizons, indicated by a strongly reduced thickness, presence of firmgrounds, iron crusts, and a concentration of ammonites (Seyed-Emami et al. 2013; Dietze et al. 2014). This lithology is widespread in the Alpine-Mediterranean Jurassic. The "Farsian formation" of Stampfli (1978) is a local variation of the condensed Dalichai Formation.

The depositional environments of the Dalichai and Chaman Bid formations range from upper to lower slope and even basinal settings. The pack- and grainstones are gravitationally transported sediments (allodapic limestones of turbidite origin) derived from carbonate platforms represented by the Lar and Mozduran formations. In the Koppeh Dagh, the slope sediments locally represent, apart from basinal facies, debris flows with olistholiths, mudflows, and slumps indicating a steep relief.

Ammonites are common elements and represented by the families Phylloceratidae, Spiroceratidae, Stephanoceratidae, Sphaeroceratidae, Parkinsoniidae, Morphoceratidae, Tuilitidae, Reineckeiidae, Pachyceratidae, Oppeliidae, Macrocephalitidae, Tulitidae, Perisphinctidae, Ataxioceratidae, Aspidoceratidae, Cardioceratidae, and Haploceratidae (Seyed-Emmami et al. 1985, 1989, 1995, 2013,2015, 2018; Schairer et al. 1991; Majidifard 2003; Seyed-Emami & Schairer 2010, 2011a, 2011b; Raoufian 2014; Raoufian et al. 2011, 2014, 2019; Dietze et al. 2010). They indicate a Late Bajocian age of the base of the formation in the Alborz Mountains and a Late Bathonian age in the Koppeh Dagh. The upper boundary is highly diachronous, ranging from the late Callovian to the early Tithonian, depending on the time the carbonate platforms became established and on the rate with which they prograded across the basinal and slope sediments.

Lar and Mozduran formations—The Upper Jurassic strata in the Alborz, Binalud (Lar Formation; Assereto 1966b), and in the Koppeh Dagh (Mozduran Formation; Afshar Harb 1994) consist largely of light yellow-grey to cream-coloured, well bedded to massive and cliff-forming shallow-water carbonates (Lassemi 1995). These constitute a vast carbonate platform throughout North and East-Central Iran. The "Abnak formation" (Assereto 1966b) is a local variant of the Lar Formation.

The boundary of the Lar/Mozduran formations with the underlying Dalichai/Chaman Bid formations is gradual. In fact, in the Koppeh Dagh the lower part of the Mozduran Formation as mapped and described in the literature is better accommodated in the Chaman Bid Formation, as it represents typical slope or even basinal sediments (see above). The upper boundary is marked by the onset of red and varicolored siliciclastic rocks with intercalations of gypsum and some volcanic rocks indicating the onset of the Late Cimmerian movements. Typical sediments of the Lar/Mozduran formations include mudstones, peloidal, oncoidal, or bioclastic wacke- to packstones, commonly with fenestral fabric. These low-energy carbonates correspond to inner parts of the carbonate platform and represent supratidal, tidal flat to lagoonal environments (Majidifard 2008; Aghaei et al. 2013). On the platform margins locally high-energy microfacies (pack- and grainstones with ooids, bioclasts, peloids, and intraclasts) prevailed (e.g., Kavoosi et al 2009). In other areas, the carbonate platform is developed as a homoclinal ramp (e.g., Aghaei et al. 2013, 2019).

Both formations contain a rather poor ammonite fauna of the following families: Oppeliidae, Glochiceratidae, Aspidoceratidae, and Perisphinctidae (Assereto et al. 1968; Fantini-Sestini et al. 1970; Schairer et al. 1991; Majidifard 2003; Seyed-Emami & Schairer 2010, 2011 b). They indicate Oxfordian–Kimmeridgian and Tithonian ages of the two formations.

Plate 5 (Page 113): Ammonites from the Badamu Formation, northern Lut Block and west Kerman, Central Iran. **(1a, b)** *Pleydellia* cf. *lugdunensis* Elmi, Gabilly, Mouterde, 1997. Upper Toarcian, Aalensis Zone (Seyed-Emami et al. 2004b, p. 84, pl. 1, fig. 8). **(2a, b)** *Peronoceras* sp. nov.?. Middle Toarcian, Bifrons Zone (Seyed-Emami et al. 2004b, p. 82, pl. 1, fig. 4). **(3a, b)** *Leioceras paucicostatum* Rieber, 1963. Lower Aalenian, Opalinum Zone (Seyed-Emami et al. 2004b, p. 85, pl. 1, fig. 11). **(4a, b)** *Graphoceras* sp. ex gr. *G. concavum* (Sowerby, 1815). Upper Aalenian, Concavum Zone (Seyed-Emami et al. 2004b, p. 87, pl. 2, fig. 8). **(5)** *Hildaites* sp. ex gr. *H. forte* (Buckman, 1921). Lower Toarcian, Serpentinum Zone (Seyed-Emami et al. 2004b, p. 84, pl. 1, fig. 7). **(6a, b)** *Leioceras costosum* (Quenstedt, 1886). Lower Aalenian, Opalinum Zone (Seyed-Emami et al. 2004b, p. 85, pl. 2, fig. 2). **(7a, b)** *Dactylioceras* (*Orthodactylites*) *semicelatum* (Simpson, 1843). Lower Toarcian, Tenuicostatum Zone (Seyed-Emami et al. 2004b, p. 81, pl. 1, fig. 1). **(8a, b)** *Harpoceras* cf. *falciferum* (Sowerby, 1820). Lower Toarcian, Falciferum Zone (Seyed-Emami et al. 2004b, p. 82, pl. 1, fig. 6). **(9a, b)** *Leioceras* aff. *comptum* (Reinecke, 1818). LowerAalenian, Opalinum Zone (Seyed-Emami et al. 2004b, p. 85, pl. 2, fig. 5). **(10a, b)** *Leioceras* aff. *lineatum* Buckman, 1899. Lower Aalenian, Opalinum Zone (Seyed-Emami et al. 2004b, p. 84, pl. 2, fig. 1). **(11a, b)** *Sonninia* cf. *propinquans* (Bayle, 1879). Lower Bajocian, Laeviuscula Zone (Seyed-Emami 1988b, p. 73, fig. 15). **(12a)** *Etropolia* aff. *renzi* Sapunov, 1971. Lower Bajocian, Laeviuscula Zone (Seyed-Emami 1988b, p. 79, fig. 29 a). **(12b)** *Lissoceras oolithicum* (d'Orbigny, 1854). Lower Bajocian, Laeviuscula Zone (Seyed-Emami 1988b, p. 78, fig. 27). **(13a, b)** *Pelekodites kermanensis* Seyed-Emami, 1988. Lower Bajocian, Laeviuscula Zone (Seyed-Emami 1988b, p. 73, fig. 16). **(14a, b)** *Strigoceras* cf. *languidum* (Buckman, 1924). Lower Bajocian, Laeviuscula Zone (Seyed-Emami 1988b, p. 76, fig. 23). **(15a, b)** *Witchellia platymorpha* Buckman, 1925. Lower Bajocian, laeviuscula Zone (Seyed-Emami et al. 2004b, p. 90, fig. 4). **(16a, b)** *Pelekodites nodosus* Seyed-Emami, 1988. Lower Bajocian, Laeviuscula Zone (Seyed-Emami 1988b, p. 74, fig. 18). **(17a, b)** *Etropolia sapunovi* Seyed-Emami, 1988. Lower Bajocian, Laeviuscula Zone (Seyed-Emami 1988b, p. 80, fig. 32a, c). **(18a, b)** *Lissoceras* (*Microlissoceras*) *badamui* Seyed-Emami, 1988. Lower Bajocian, Laeviuscula Zone (Seyed-Emami 2004b, p. 78, figs. 25a, b, 26a, b).

Plate 6 (Page 114): Ammonites from the Shemshak Group east of Shahmirzad, eastern Alborz, North Iran. **(1a, b; 3a, b)** *Pleydellia buckmani* Maubeuge, 1947. Upper Toarcian, Aalensis Zone (Seyed-Emami & Nabavi 1985, p. 265, fig. 28). **(2a, b)** *Pleydellia lotharingica* (Branco, 1879). Upper Toarcian, Aalensis Zone (Seyed-Emami & Nabavi 1985, p. 269, figs. 26, 29). **(4a, b)** *Pleydellia aalensis* (Zieten, 1830). Upper Toarcian, Aalensis Zone (Seyed-Emami & Nabavi 1985, p. 266, fig. 38). **(5a, b)** *Pleydellia mactra* Buckman, 1899. Upper Toarcian, Aalensis Zone (Seyed-Emami & Nabavi 1985, p. 260, fig. 22). **(6a, b)** *Dumortieria distans* (Buckman, 1890). Upper Toarcian, Aalensis Zone (Seyed-Emami & Nabavi 1985, p. 269, fig. 40). **(7a, b)** *Pleydellia subcompta* (Branco, 1879). Upper Toarcian, Aalensis Zone (Seyed-Emami & Nabavi 1985, p. 264, fig. 30). **(8a, b)** *Dumortieria levesquei* (d'Orbigny, 1844). Upper Toarcian, Pseudoradiosa Zone (Seyed-Emami & Nabavi 1985, p. 248, fig. 13). **(9a, b)** *Dumortieria bleicheri* Benecke, 1905. Upper Toarcian, Pseudoradiosa Zone (Seyed-Emami & Nabavi 1985, p. 252, fig. 11). **(10a, b)** *Paradumortieria aequicostata* (Seyed-Emami, 1985). Upper Toarcian, Pseudoradiosa Zone, Levesquei Subzone (Seyed-Emami & Nabavi 1985, p. 249, fig. 17). **(11a, b)** *Paradumortieria explanata* (Buckman, 1904). Upper Toarcian, Pseudoradiosa Zone (Seyed-Emami & Nabavi 1985, p. 252, fig. 19). **(12a, b)** *Dumortieria moorei* (Lycett, 1857). Upper Toarcian, Pseudoradiosa Zone (Seyed-Emami & Nabavi 1985, p. 255, fig. 9). **(13a, b)** *Paradumortieria* aff. *schaireri* Seyed-Emami, 1985. Upper Toarcian, Pseudoradiosa Zone, Levesquei Subzone (Seyed-Emami & Nabavi 1985, p. 259, fig. 6). **(14a, b)** *Dumortieria radiosa* (Seebach, 1864). Upper Toarcian, Pseudoradiosa Zone (Seyed-Emami & Nabavi 1985, p. 254, fig. 4).

Plate 7 (Page 115): Ammonites from the Shemshak Group, eastern Alborz, North Iran. **(1)** *Amaltheus stockesi* (Sowerby, 1818). Late Pliensbachian, Margaritatus Zone, Shahmirzad (Nabavi & Seyed-Emami 1977, p. 81, pl. 9, fig. 4). **(2, 3a, b, 4a–c)** *Paltechioceras* cf. *oosteri* (Dumortier, 1867). Upper Sinemurian, Raricostatum Zone, Shahmirzad (Nabavi & Seyed-Emami 1977, p. 82, pl. 9, figs. 1–3). **(5a, b)** *Podagrosites latescens* (Simpson, 1843). Upper Toarcian, Thouarsense Zone, Jajarm (Seyed-Emami et al. 2005, p. 357, fig. 5A). **(6a, b)** *Dumortieria striatulocostata* (Quenstedt, 1885). Upper Toarcian, Pseudoradiosa Zone, Jajarm (Seyed-Emami et al. 2005, p. 359, fig. 5G). **(7a, b)** *Dumortieria* aff. *levesquei* (d'Orbigny, 1844). Upper Toarcian, Pseudoradiosa Zone, Jajarm (Seyed-Emami et al. 2005, p. 359, fig. 5D). **(8a, b)** *Ptychophylloceras* (*Tatraphylloceras*) sp. aff. *tatricum* (Pusch, 1837). Upper Toarcian, thouarsense, Shahmirzad (Seyed-Emami et al. 2005, p. 354, fig. 4E).

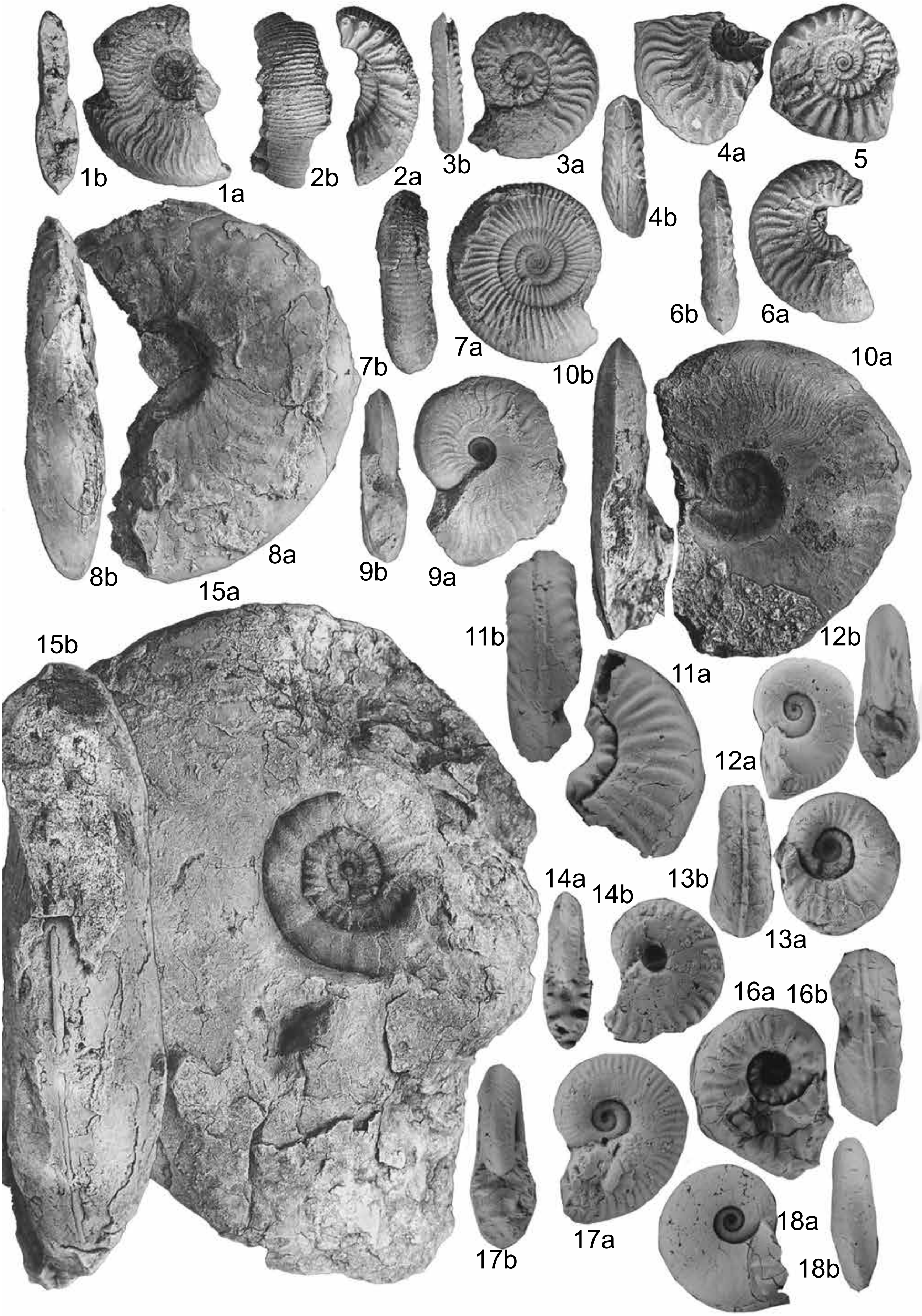
1b
1a
2b
2a
3b
3a
4a
5
4b
6b
6a
7b
7a
10b
10a
8b
8a
9b
9a
15a
15b
11b
11a
12b
12a
13b
13a
14a
14b
16a
16b
17b
17a
18a
18b

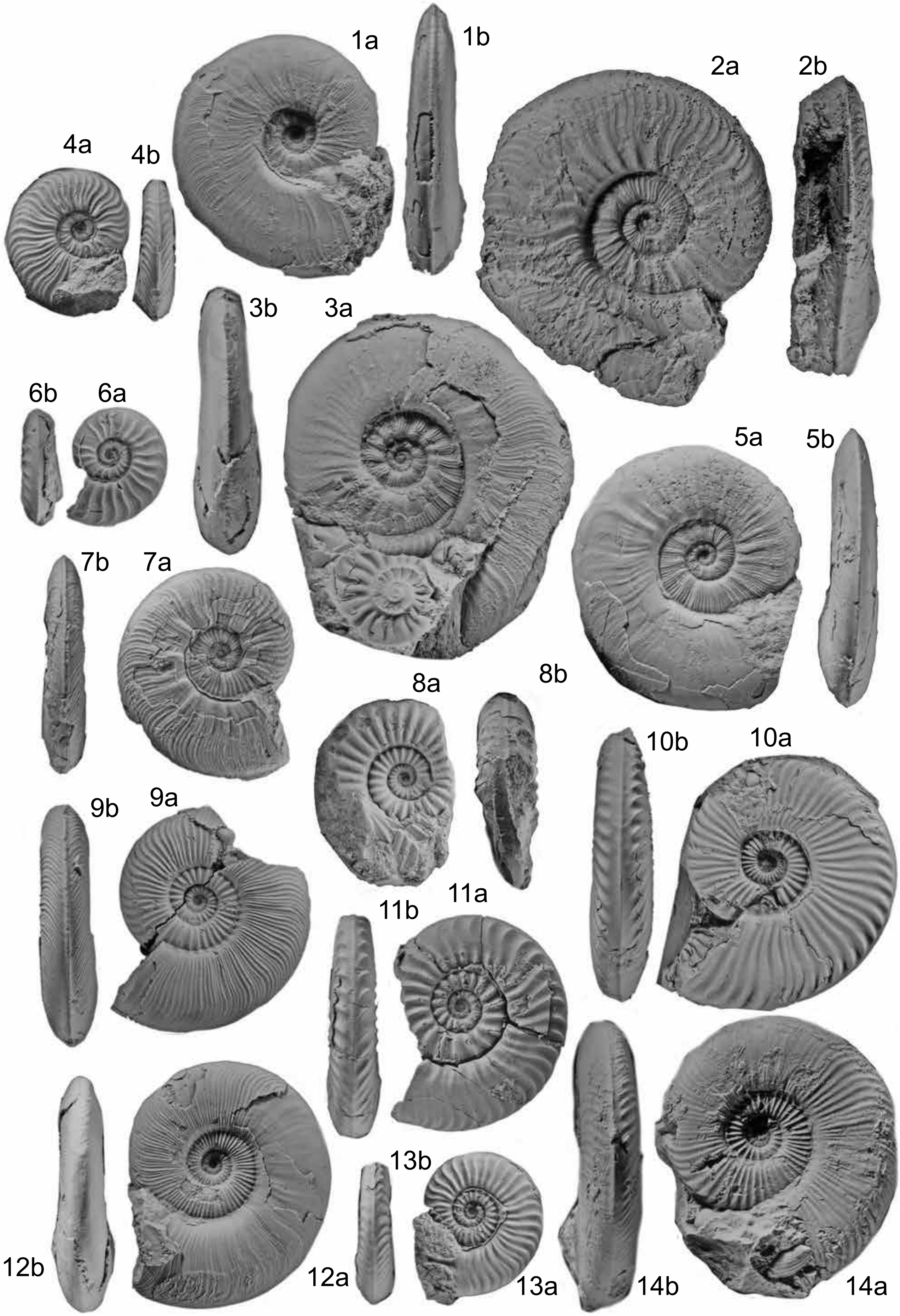
1a
1b
2a
2b
4a
4b
3b
3a
6b
6a
5a
5b
7b
7a
8a
8b
10b
10a
9b
9a
11a
11b
13b
12b
12a
13a
14b
14a

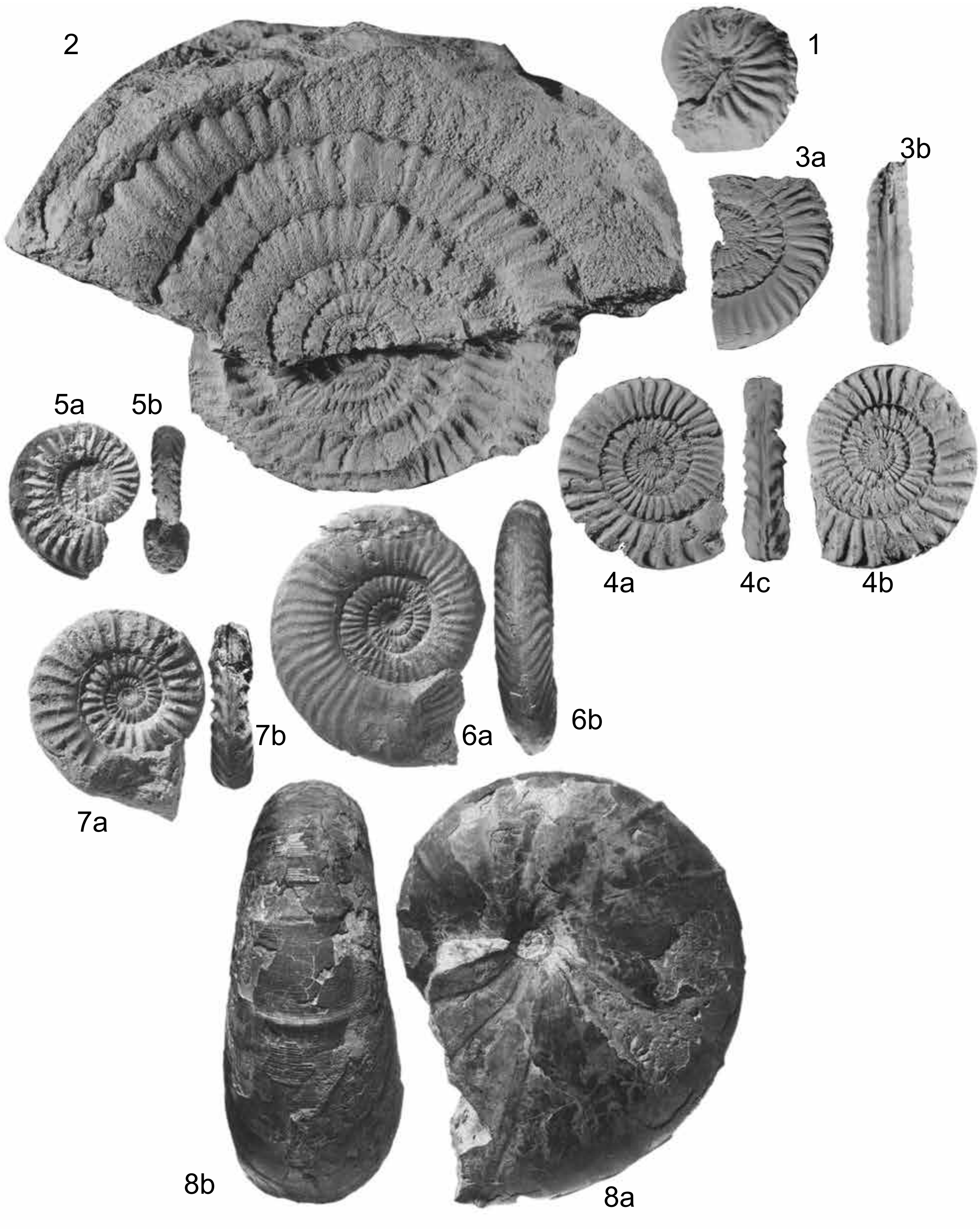
2
1
3a
3b
5a
5b
4a
4c
4b
6a
6b
7a
7b
8b
8a

Shal Formation—In the Talesh Mountains (northwestern Alborz) the Middle and Upper Jurassic strata consist of around 60–100 m of greyish-green, glauconitic sandstones and medium- to thick-bedded glauconitic limestones, called Shal Formation (Davies et al. 1972). The Shal Formation unconformably rests on the Shemshak Group; the boundary to the overlying cream-coloured, sub-lithographic, pelagic limestones and marls of the Kolur Formation (Neocomian) is transitional (Seyed-Emami 1975). In contrast to the central and southern Alborz, the Jurassic–Cretaceous boundary in the northern Alborz is continuous. The Shal Formation corresponds largely to the Dalichai and Lar formations.

The Shal Formation contains a fairly rich ammonite fauna with the following families: Phylloceratidae, Oppeliidae, Parkinsoniidae, Stephanoceratidae, Perisphinctidae, and Beriassellidae (Seyed-Emami 1975; Cecca et al. 2012). In the upper part, the formation yielded Tithonian and Berriasian Calpionellidae (Benzaggagh et al. 2012). The age of the Shal Formation is late Bajocian to early Berriasian.

Shurijeh Formation—In the Koppeh Dagh, the Mozduran Formation is followed by an up to 1000-m-thick succession of reddish to varicoloured siliciclastics with carbonate and evaporite intercalations, the Shurijeh Formation (Afshar Harb 1969, 1994; Zand-Moghadam et al 2016; Hosseinyar et al. 2019). The sedimentary environment of the Shurijeh Formation is mostly continental-arid with few marine ingressions (Moussavi-Harami & Brenner 1990; Moussavi-Harami et al. 2009). The age of the Shurijeh Formation is latest Jurassic to earliest Cretaceous.

3.2 East-Central Iran

In East-Central Iran, Jurassic strata occur in what has been termed Central-East Iranian Microcontinent (CEIM; Takin 1972). During the Late Triassic to early Middle Jurassic, the Iran Plate acted as a coherent structural unit and the rocks (Shemshak Group) are therefore widely similar. After the Mid-Cimmerian Tectonic Event, the CEIM broke up into three N-S oriented and differently acting structural units (blocks). These are from east to west the Lut, Tabas, and Yazd blocks (Fig. 1). Sedimentological and stratigraphic analyses indicate that the Jurassic seas mostly covered the Tabas and Lut blocks, whereas the Yazd Block remained emergent for most of the time (Wilmsen et al. 2009a). In contrast, Cretaceous strata are much reduced on the Lut and Tabas blocks, but extremely thick (up to 5,000 m) on the Yazd Block (Wilmsen et al. 2015).

3.2.1 Lower to lower Middle Jurassic strata (Ab-e-Haji Subgroup)

In Central Iran, similar to northern Iran, the Lower to lower Middle Jurassic rocks are largely siliciclastic and attain great thicknesses. The Ab-e-Haji Subgroup is subdivided from base to top into the following formations: Ab-e-Haji, Badamu, and Hojedk (Aghanabati 1977, 1998) (Fig.7).

Ab-e-Haji Formation—The Lower Jurassic to Aalenian Ab-e-Haji Formation (Aghanabati 1977, 1998) comformably overlies the Upper Triassic Nayband Formation. The formation strongly varies in thick-

Plate 8 (Page 117): Ammonites from the Shemshak Group east of Shahmirzad, eastern Alborz, North Iran. **(1a, b)** *Bredyia iranica* Seyed-Emami, 1987. Lower Aalenian, Opalinum Zone (Seyed-Emami 1987, p. 374, fig. 2(1)). **(2a, b)** *Accardia*(?) *shahmirzadense* Seyed-Emami, 1987. Lower Aalenian, Opalinum Zone (Seyed-Emami 1987, p. 377, fig. 3(1)). **(3)** *Gescyceras* aff. *tipperi* Seyed-Emami, 1967. Upper Toarcian, Levesquei Subzone (Seyed-Emami 1987, p. 372, fig. 4(5)). **(4a, b)** *Pseudaptetoceras klimakomphalum* (Vacek, 1886). Upper Aalenian (Seyed-Emami 1987, p. 379, fig. 4(1)). **(5a, b)** *Bredyia subinsignis* (Oppel, 1856). Lower Aalenian, Opalinum Zone (Seyed-Emami 1987, p. 377, fig. 3(3)).

Plate 9 (Page 118): Ammonites from the Shemshak Group, eastern Alborz, North Iran. **(1a, b)** *Paradumortieria tectiformis* Elmi & Caloo-Fortier, 1985. Upper Toarcian, Aalensis Zone, Tazareh (Seyed-Emami et al. 2006, p. 265, fig. 5(1a, b)). **(2)** *Leioceras comptum* (Reinecke, 1818). Lower Aalenian, Opalinum Zone, Jajarm (Seyed-Emami et al. 2005, p. 364, fig. 7D). **(3a, b)** *Pleydellia paucicostata* Buckman, 1904. Upper Torcian, Aalensis Zone, Jajarm (Seyed-Emami et al. 2005, p. 363, fig. 6H). **(4)** *Graphoceras decorum* Buckman, 1902. Upper Aalenian, Concavum Zone, Tazareh (Seyed-Emami et al. 2006, p. 265, fig. 5(1a, b)). (**5a, b**) *Accardia diadematoides* (Mayer, 1871). Middle Aalenian, Bradfordensis Zone, Tazareh (Seyed-Emami et al. 2006, p. 269, fig. 5(16a, b)). (**6, 8a, b**) *Shahrudites asseretoi* Seyed-Emami, 2006. Middle Aalenian, Bradfordensis Zone, Tazareh (Seyed-Emami et al. 2006, p. 270, fig. 6 (2a–c)). (**7a, b**) *Pleydellia subcompta* (Branco, 1879). Upper Toarcian, Aalensis Zone, Jajarm (Seyed-Emami et al. 2005, p. 360, fig. 6J). (**9a, b**) *Ceccaites* cf. *sieboldi* (Oppel, 1862). Aalenian, Ravar area, Central Iran (Seyed-Emami et al. 2006, p. 269, fig. 6(17)). (**10a, b**) *Shahrudites stoecklini* Seyed-Emami, 2006. Middle Aalenian, Bradfordensis Zone, Tazareh (Seyed-Emami et al. 2006, p. 271, fig. 6 (8a, b)).

Plate 10 (Page 119): Ammonites from the Shemshak Group east of Shahmirzad, eastern Alborz, North Iran. (**1a, b, 3a, b**) *Paradumortieria elmii* Seyed-Emami, 2008. Upper Toarcian, Pseudoradiosa Zone (Seyed-Emami et al. 2008, p. 251, fig. 5A, C). (**2a, b**) *Graphoceras* (*Ludwigella*) *cornu* Buckman, 1901. Upper Aalenian, Concavum Zone (Seyed-Emami et al. 2008, p. 254, fig. 6B). (**4a, b**) *Pleydellia aalensis* (Zieten, 1830). Upper Toarcian, Aalensis Zone (Seyed-Emami et al. 2008, p. 251, fig. 5E). **(5)** *Amaltheus margaritatus* de Montfort, 1808. Upper Pliensbachian, Margaritatus Zone (Seyed-Emami et al. 2008, p. 244, fig. 4C). (**6a, b**) *Amaltheus subnodosus* (Young & Bird, 1828). Upper Pliensbachian, Margaritatus Zone (Seyed-Emami et al. 2008, p. 246, fig. 4E). (**7a, b**) *Dactylioceras* (*Orthodactylites*) aff. *semicelatum* (Simpson, 1843). Lower Toarcian, Tenuicostatum Zone (Seyed-Emami et al. 2008, p. 247, fig. 4I). (**8a, b**) *Leioceras comptum* (Reinecke, 1818). Lower Aalenian, Opalinum Zone (Seyed-Emami et al. 2008, p. 254, fig. 6I). (**9a, b**) *Graphoceras decorum* Buckman, 1904. Upper Aalenian, Concavum Zone (Seyed-Emami et al. 2008, p. 254, fig. 6H). (**10 a, b**) *Pseudogrammoceras fallaciosum* (Bayle, 1878). Upper Toarcian, Thouarsense Zone (Seyed-Emami et al. 2008, p. 250, fig. 5N). (**11a, b**) *Erycites barodiscus* Gemmellaro, 1886. Lower Aalenian, Opalinum Zone (Seyed-Emami et al. 2008, p. 255, fig. 6L). (**12a, b**) *Dactylioceras* (*Eodactylites*?) *pseudocommune* Fucini, 1935. Lower Toarcian, Tenuicostatum Zone (Seyed-Emami et al. 2008, p. 246, fig. 4L). (**13a, b**) *Accardia diadematoides* Cresta, 1997. Upper Aalenian, Concavum Zone, Sharif-Abad (Seyed-Emami et al. 2008, p. 255, fig. 6N).

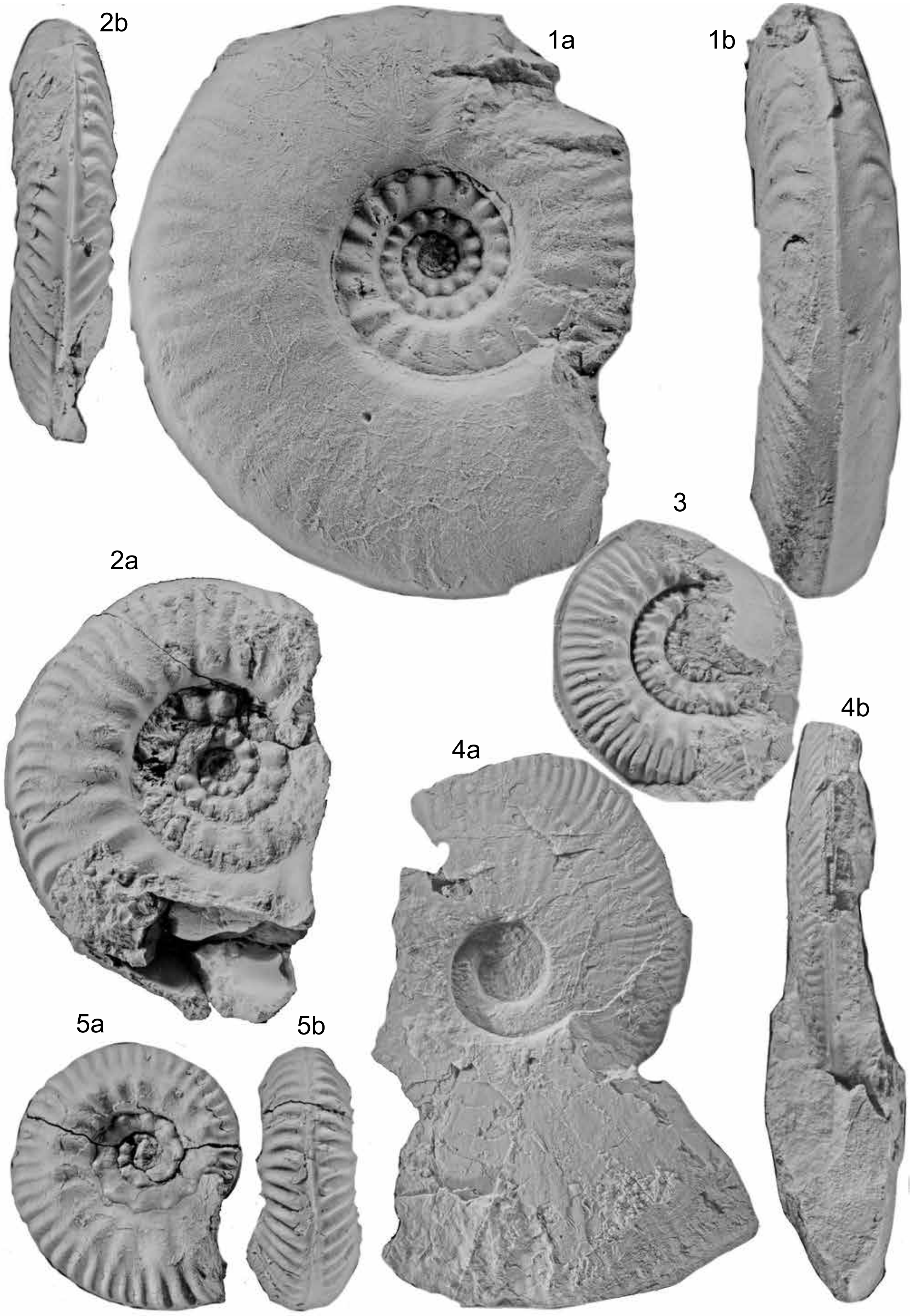
1a
1b
2a
2b
3
4a
4b
5a
5b

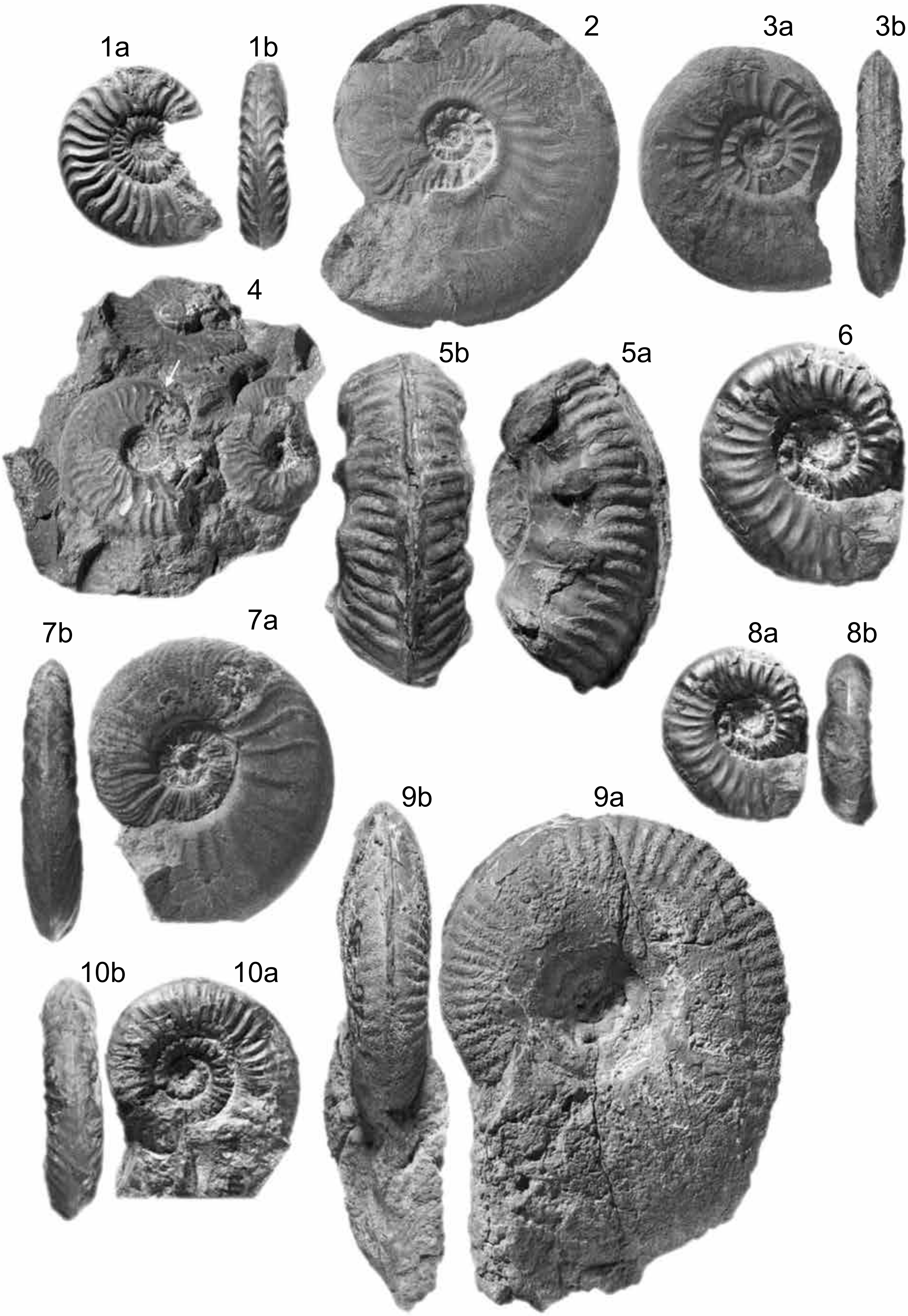
1a
1b
2
3a
3b
4
5b
5a
6
7b
7a
8a
8b
9b
9a
10b
10a

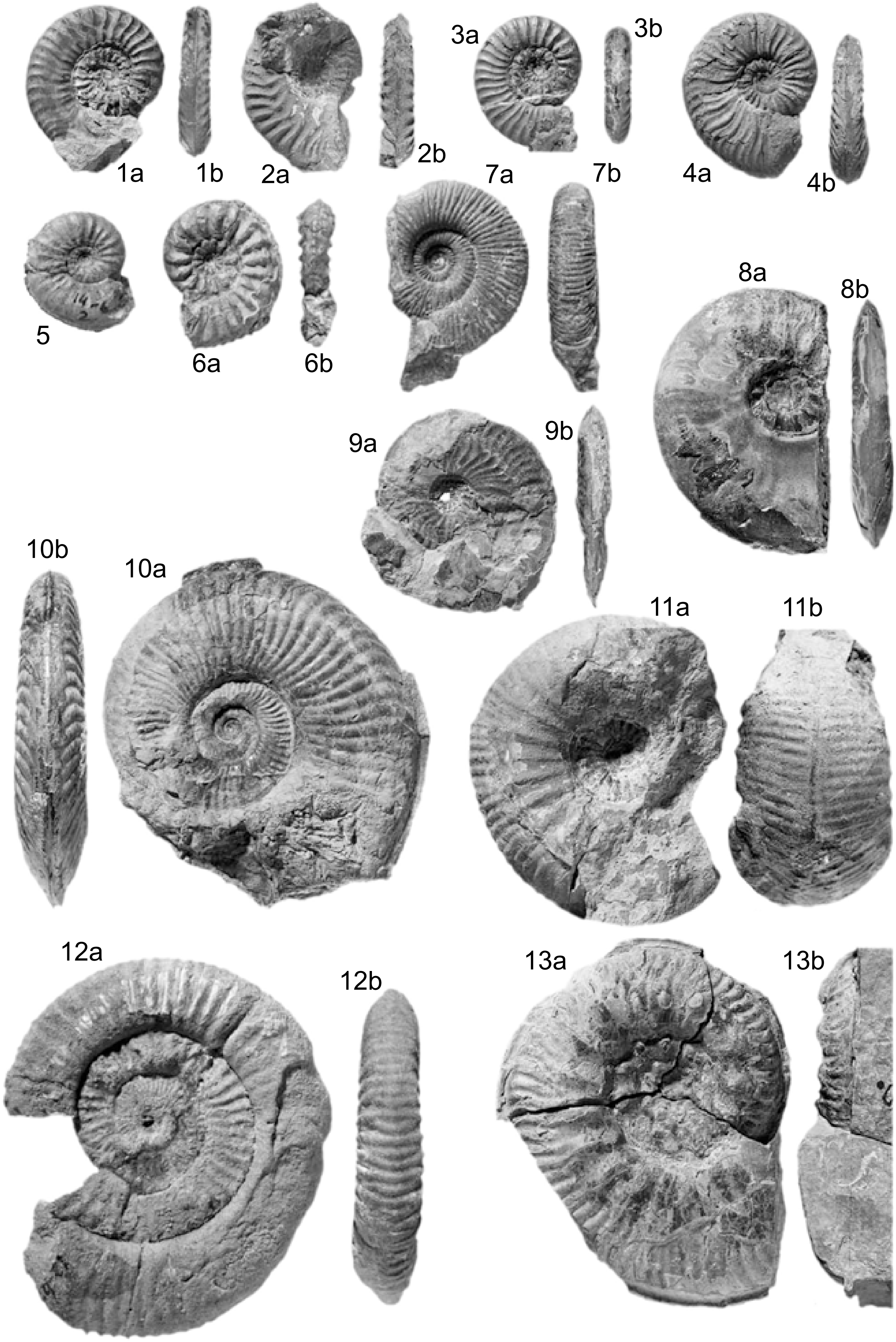
1a
1b
2a
2b
3a
3b
7a
7b
4a
4b
5
6a
6b
8a
8b
9a
9b
10a
10b
11a
11b
12a
12b
13a
13b

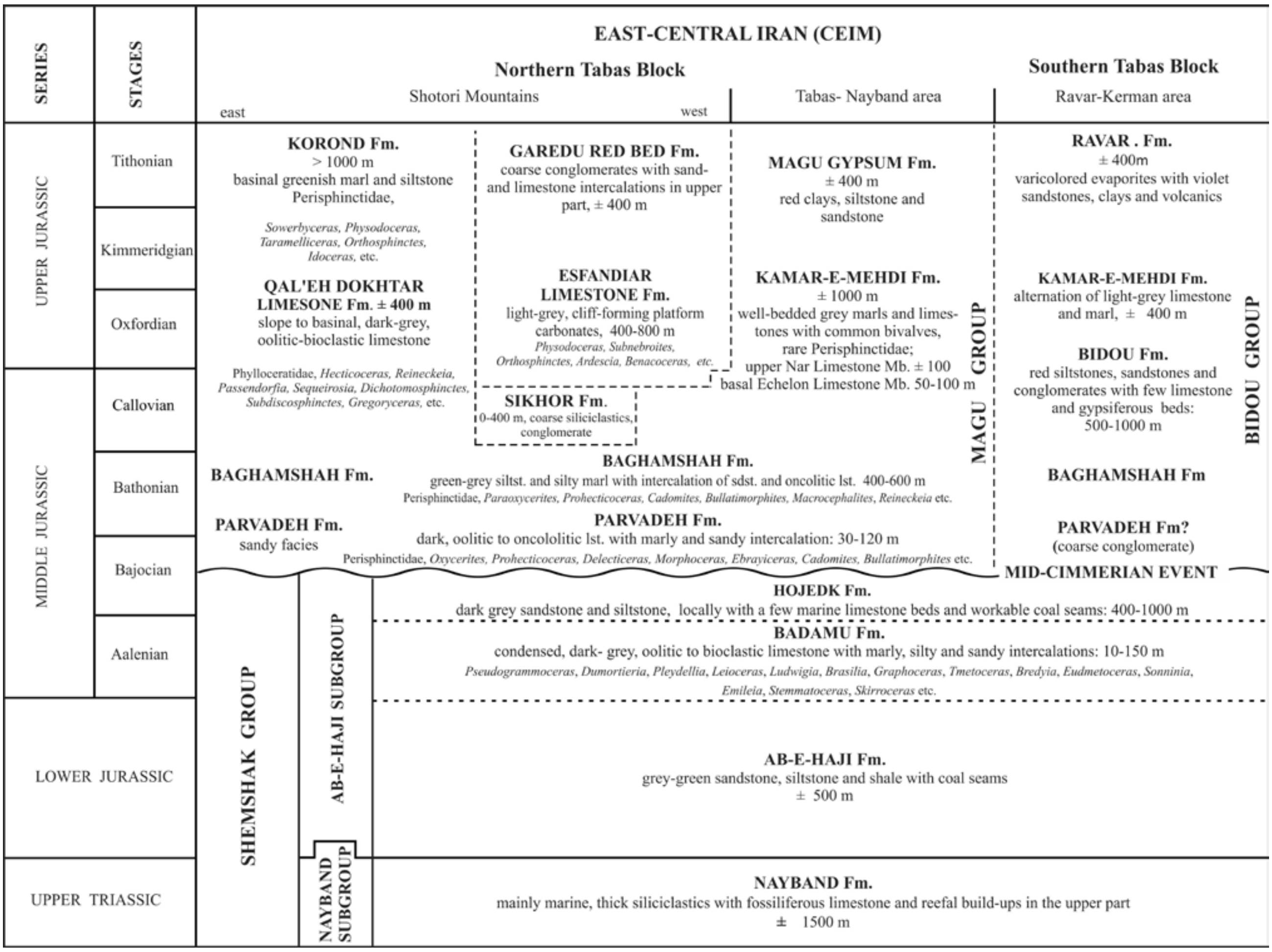

Figure 7. Generalized lithostratigraphic scheme of the Jurassic System in East-Central Iran.

Plate 11 (Page 121): Bajocian and Bathonian ammonites from the Dalichai Formation (Avaj area, SW Alborz) and the Baghamshah Formation (Tabas area, Central Iran). **(1)** *Procerites tmetelobus* Buckman, Buckman, 1923). Lower Bathonian (Seyed-Emami et al. 1985, p. 71, pl. 5, fig. 4). **(2)** *Vermisphinctes* aff. *vermiformis* (Buckman, 1920). Upper Bajocian (Seyed-Emami et al. 1985, p. 70, pl. 5, fig. 3). **(3)** *Delecticeras delectum* (Arkell, 1951). Middle-Upper Bathonian, Baghamshah Formation, Tabas area, Central Iran (Seyed-Emami et al. 1985, p. 65, pl. 1, fig. 11). **(4)** *Simirazkia procera* (Seebach, 1864). Lower Bathonian (Seyed-Emami et al. 1985, p. 72, pl. 5, fig. 1). **(5)** *Oecotraustes* (*Paroecotraustes*) *splendens* Arkell, 1951. Middle Bathonian, Baghamshah Formation, Tabas area, Central Iran (Seyed-Emami et al. 1985, p. 64, pl. 1, fig. 10). **(6)** *Morphoceras dehmi* Seyed-Emami, 1985. Lower Bathonian (Seyed-Emami et al. 1985, p. 69, pl. 4, fig. 8). **(7)** *Oecotraustes westermanni* Stephanov, 1966. Upper Bajocian (Seyed-Emami et al. 1985, p. 62, pl. 1, fig. 8). **(8)** *Parkinsonia parkinsoni* (Sowerby, 1823). Upper Bajocian, Parkinsoni Zone (Seyed-Emami et al. 1985, p. 67, pl. 3, fig. 1). **(9)** *Ebrayiceras filicostatum* Wetzel, 1937). Lower Bathonian, Zigzag Zone (Seyed-Emami et al. 1985, p. 70, pl. 3, fig. 6). **(10)** *Oxycerites seebachi* (Wetzel, 1950). Lower Bathonian (Seyed-Emami et al. 1985, p. 62, pl. 1, fig. 5). **(11a, b)** *Ebrayiceras sulcatum* (Zieten, 1830). Lower Bathonian, Zigzag Zone (Seyed-Emami et al. 1985, p. 69, pl. 3, fig. 9). **(12a, b)** *Parkinsonia dorni Arkell*, 1951. Upper Bajocian, Parkinsoni Zone (Seyed-Emami et al. 1985, p. 66, pl. 3, fig. 3). **(13a, b)** *Garantiana* (*Pseudogarantiana*) *dichotoma* Benz, 1928. Upper Bajocian, Garantiana Zone (Seyed-Emami et al. 1985, p. 66, pl. 2, fig. 8). **(14a, b)** *Oppelia pleurifer* (Buckman, 1924). Upper Bajocian, Parkinsoni Zone (Seyed-Emami et al. 1985, p. 62, pl. 1, fig. 3). **(15a, b)** *Parkinsonia radiata* Renz, 1904. Upper Bajocian, Parkinsoni Zone (Seyed-Emami et al. 1985, p. 66, pl. 3, fig. 2). **(16a, b)** *Polyplectites linguiferus* (Orbigny, 1845). Upper Bajocian (Seyed-Emami et al. 1985, p. 64, pl. 2, fig. 4).

Plate 12 (Page 122): Ammonites from the Lower Dalichai Formation north of Damghan, eastern Alborz, North Iran. **(1a, b)** *Parkinsonia rarecostata* (Buckman, 1818). Upper Bajocian, Parkinsoni Zone (Seyed-Emani et al. 2018, p. 192, fig. 4(1)). **(2a, b)** *Garantiana baculata* (Quenstedt, 1857). Upper Bajocian, Niortense-Garantiana Zone (Seyed-Emami et al. 2018, p. 194, fig. 4(2)). **(3a, b)** *Garantiana* cf. *wetzeli* Trauth, 1923. Upper Bajocian, Garantiana Zone (Seyed-Emami et al. 2018, p. 193, fig. 4(6)). **(4a, b)** *Parkinsonia* aff. *dorni* Arkell, 1951. Upper Bajocian (Seyed-Emami et al. 2018, p. 195, fig. 4(4)). **(5a, b)** *Parkinsonia* cf. *subarietis* Wetzel, 1911. Upper Bajocian (Seyed-Emami et al. 2018, p. 195, fig. 4(11)). **(6a, b, 10a, b)** *Polyplectites* aff. *zlatarskii* Stephanov, 1963. Lower Bathonian (Seyed-Emami et al. 2018, p. 192, fig. 3(9, 10)). **(7a, b)** *Parkinsonia* aff. *wetzeli* Schmidtill & Krumbeck, 1931. Upper Bajocian, Parkinsoni Zone (Seyed-Emami et al. 2018, p. 195, fig. 4(12)). **(8a, b)** *Oxycerites yeovilensis* Rollier, 1911. Lower Bathonian (Seyed-Emami et al. 2018, p. 188, fig. 3(1)). **(9a, b)** *Lissoceras psilodiscus* (Schloenbach, 1865). Lower Bathonian (Seyed-Emami et al. 2018, p. 186, fig. 3(4)).

Plate 13 (Page 123): Ammonites from the Lower Dalichai Formation north of Damghan, eastern Alborz, North Iran. **(1a, b)** *Morphoceras parvum* Wetzel, 1937. Lower Bathonian, Zigzag Zone (Seyed-Emami et al. 2018, p. 198, fig. 5(1)). **(2a, b)** *Morphoceras multiforme* Arkell, 1951. Lower Bathonian, Zigzag Zone (Seyed-Emami et al. 2018, p. 198, fig. 5(2)). **(3a, b)** *Prohecticoceras* aff. *dominjoni* Elmi, 1867. Lower–Middle Bathonian (Seyed-Emami et al. 2018, p. 189, fig. 5(3)). **(4a, b)** *Oecotraustes bomfordi* Arkell, 1951. Lower Bathonian, Zigzag Zone (Seyed-Emami et al. 2018, p. 189, fig. 5(7)). **(5a, b)** *Asphinctes* aff. *patrulii* Hahn, 1970. Lower Bathonian (Seyed-Emami et al. 2018, p. 196, fig. 5(5)). **(6a, b)** *Oxycerites* (*Alcidellus*) aff. *tenuistriatus* (Grossouvre, 1888). Middle–?Upper Bathonian (Seyed-Emami et al. 2018, p. 188, fig. 5(10)). **(7a, b)** *Morphoceras* aff. *thalmanni* Mangold, 1970. Lower Bathonian, Zigzag Zone (Seyed-Emami et al. 2018, p. 198, fig. 5(6)). **(8a, b)** *Prohecticoceras* cf. *mondegoense* Elmi, 1967. Upper Bathonian (Seyed-Emami et al. 2018, p. 190, fig. 3(2)).

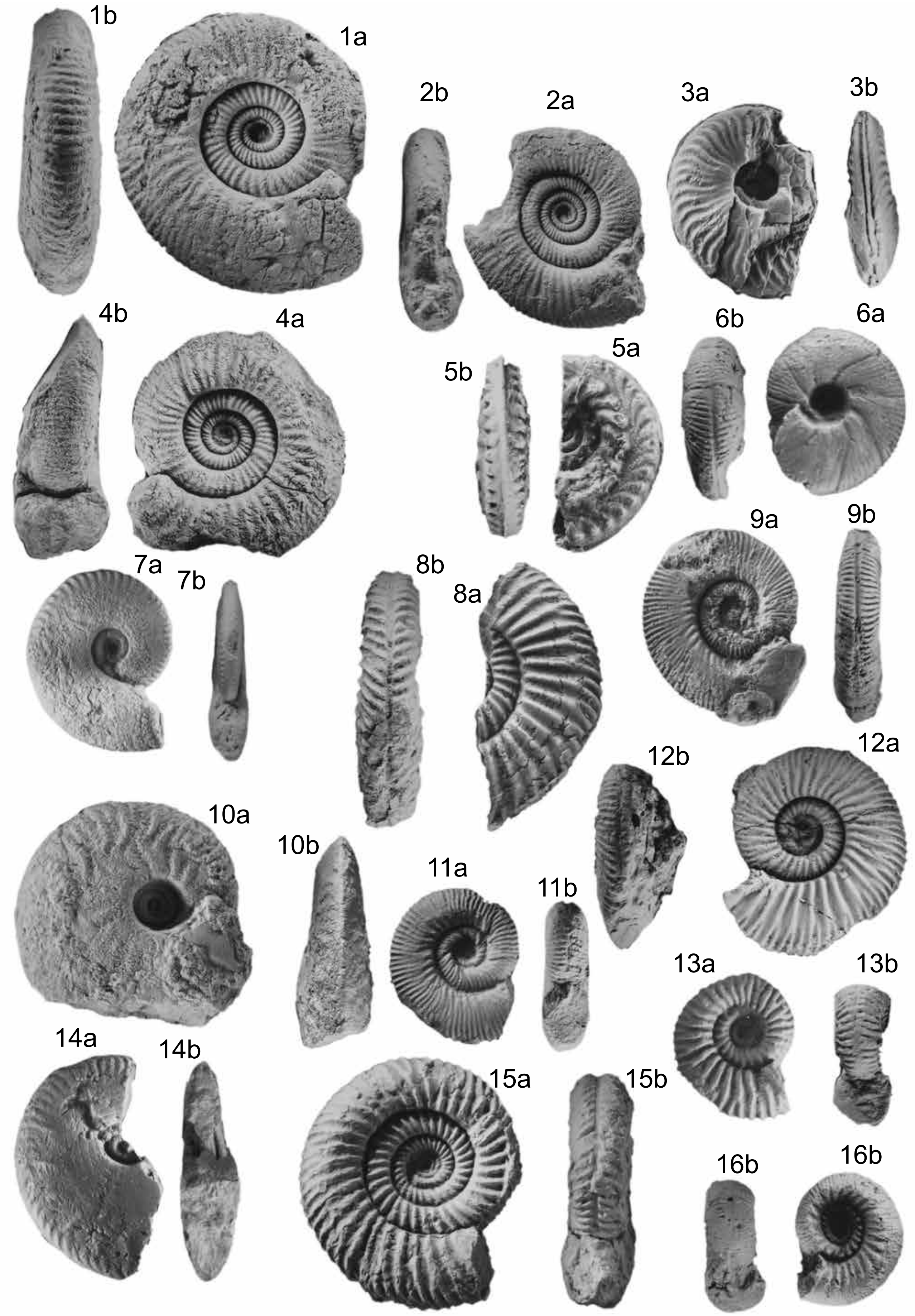
1a
1b
2a
2b
3a
3b
4a
4b
5a
5b
6a
6b
7a
7b
8a
8b
9a
9b
10a
10b
11a
11b
12a
12b
13a
13b
14a
14b
15a
15b
16b
16b

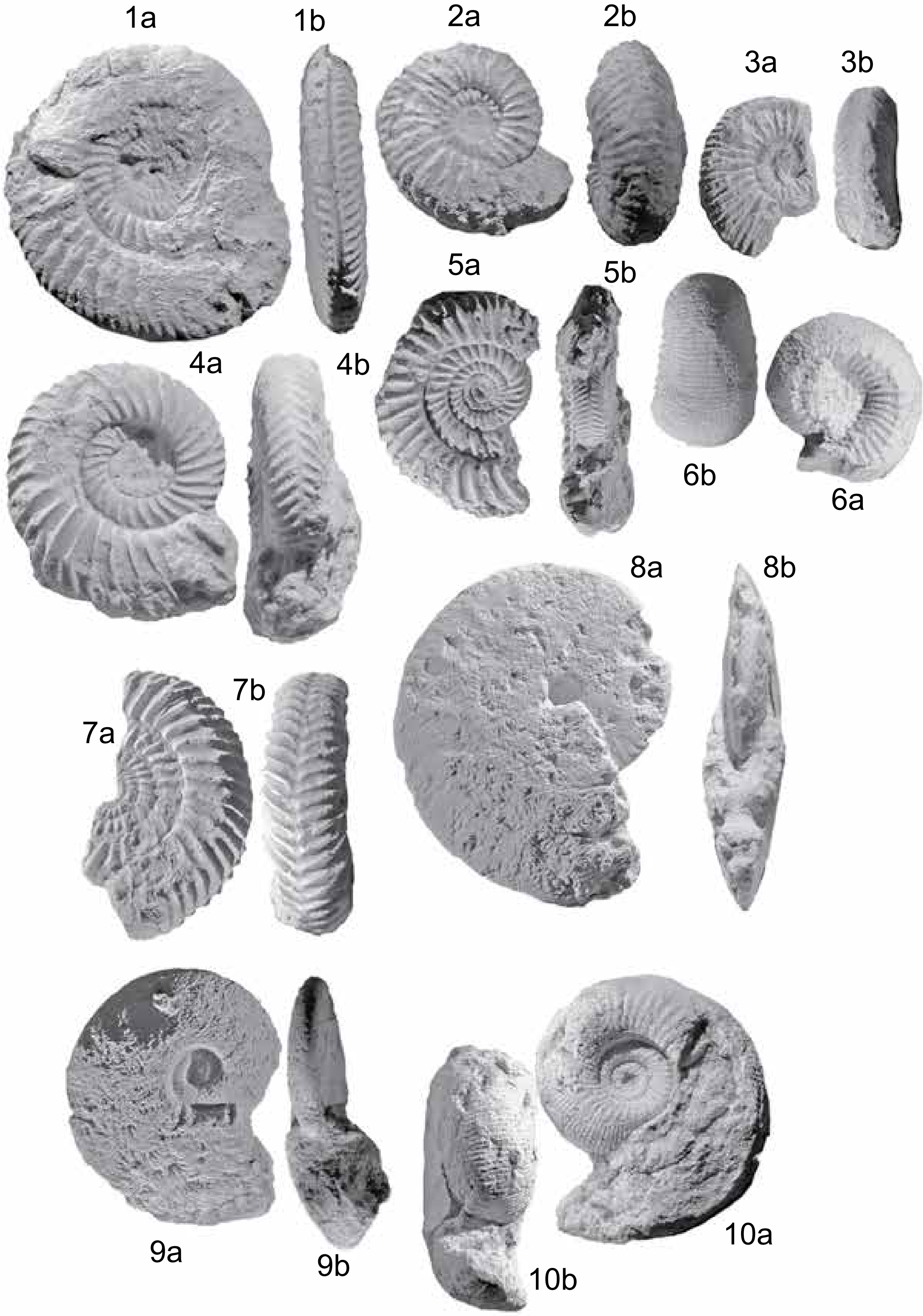
1a
1b
2a
2b
3a
3b
5a
5b
4a
4b
6b
6a
8a
8b
7b
7a
9a
9b
10b
10a

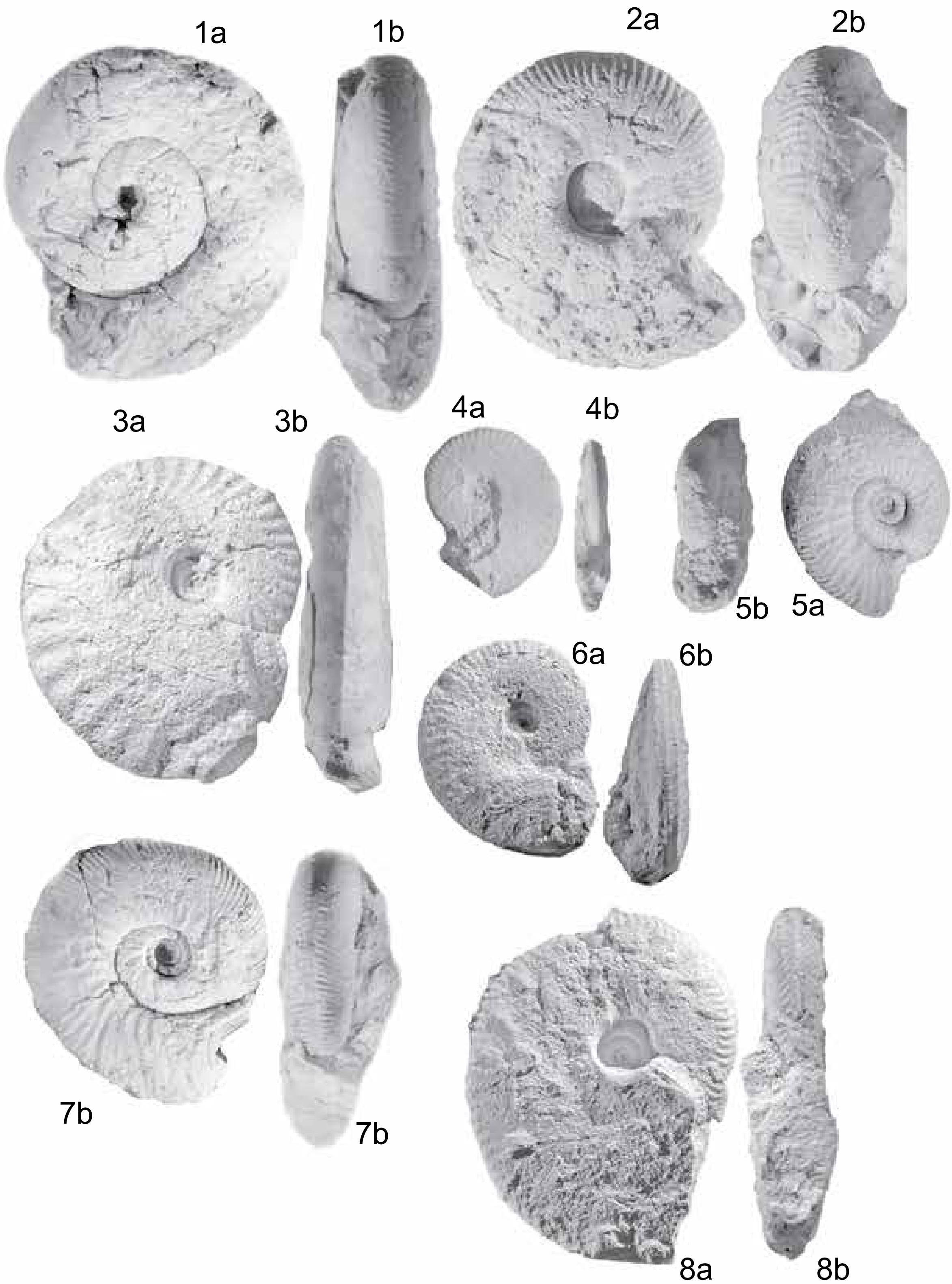
1a
1b
2a
2b
3a
3b
4a
4b
5b
5a
6a
6b
7b
7b
8a
8b

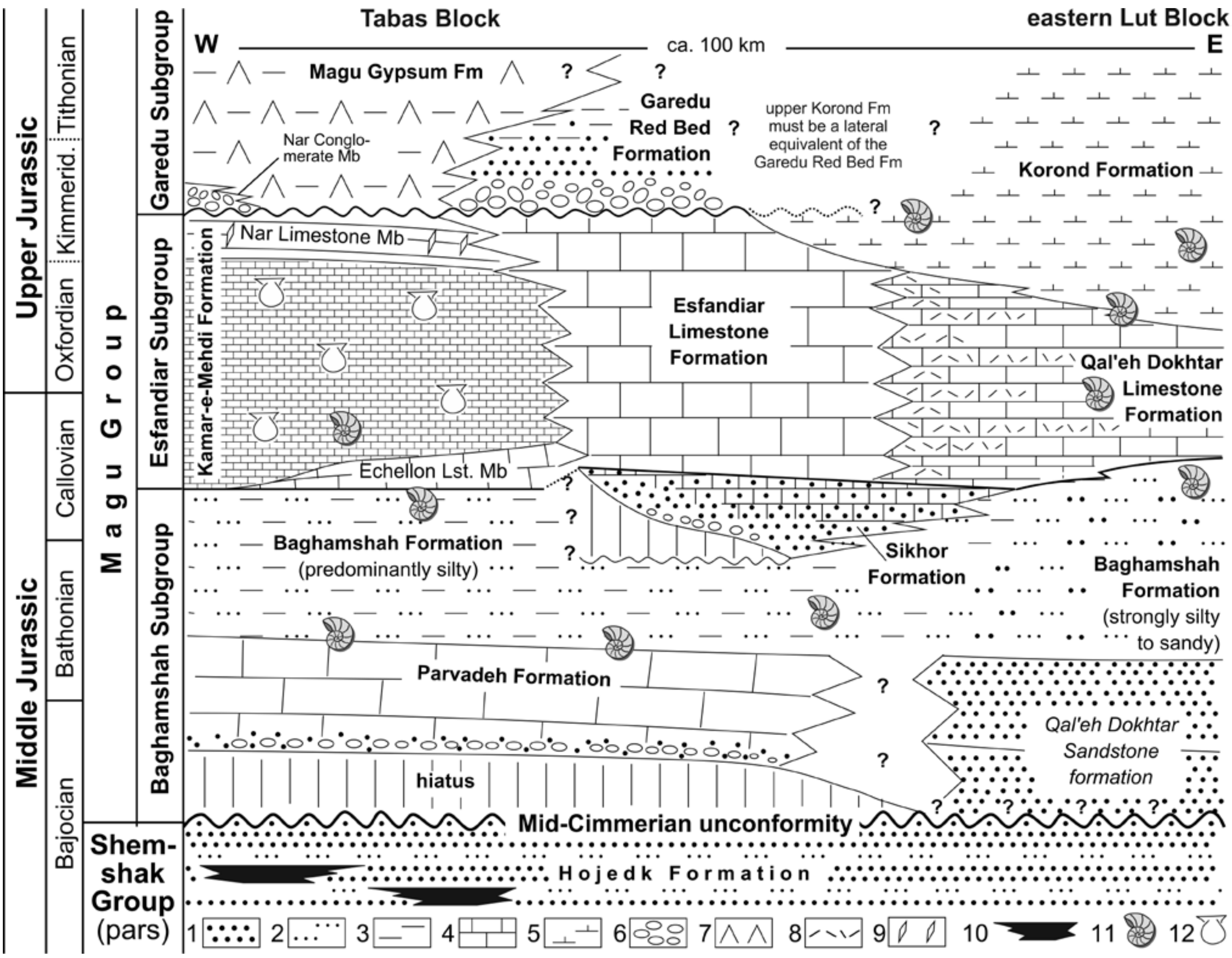

Figure. 8: Lithostratigraphic scheme of the Middle to Upper Jurassic Magu Group on the Tabas Block, East-Central Iran (modified after Wilmsen et al. 2003; bold: formal formations; italics: informal units; normal font: members). Key: 1, sandstone; 2, siltstone. 3, clay. 4, limestone. 5, marl. 6, conglomerate. 7, gypsum. 8, bioclasts. 9, gypsum pseudomorphs. 10, coal seams. 11, ammonites. 12, bivalves.

ness (0–700 m) and is mainly composed of greenish silt- to sand-sized siliciclastic rocks. Its base is comparatively coarse-grained and may contain workable coal seams. Most of the succession is non-marine and corresponds to fluvial and coastal plain environments, but also delta plain, delta front, prodelta, and shallow shelf environments are represented (Wilmsen et al. 2009a; Salehi et al. 2014, 2018). Deposition took place on large tilted fault blocks, and source areas were the Yazd Block in the west and the Shotori Swell at the eastern edge of the Tabas Block (Salehi et al. 2018). Generally, marine influences increase towards the east.

Badamu Formation—The Ab-e-Haji Formation is followed by several tens of metres up to 160 m of marine, comparatively condensed, dark-grey oolitic to bioclastic or nodular fossiliferous limestones with

Plate 14: Ammonites from the Dalichai Formation, Shahrud, eastern Alborz and Avaj area, southwestern Alborz. **(1a, b)** *Holcophylloceras zignodianum* (d'Orbigny, 1848). Upper Bajocian–Oxfordian, Shahrud (Seyed-Emami et al. 2013, p. 45, fig. 4a, b). **(2a, b)** *Sowerbyceras tortisulcatum* (d'Orbigny, 1841). Upper Callovian–Oxfordian, Shahrud (Seyed-Emami et al. 2013, p. 48, fig. 4c, d). **(3a)** *Hecticoceras* (*Rossiensiceras*) gr. *metomphalum* Bonarelli, 1894. Middle Callovian, Anceps-Lamberti zones, Shahrud (Seyed-Emami et al. 2013, p. 50, fig. 5f). **(4a, b)** *Hecticoceras* (*Lunuloceras*) *paulowi* Tsytovitch, 1911. Upper Callovian, Lamberti Zone, Shahrud (Seyed-Emami et al. 2013, p. 50, fig. 5c, d). **(5a, b)** *Alborzites binaludensis* Seyed-Emami, 1912). Middle Callovian, Shahrud (Seyed-Emami et al. 2013, p. 57, fig. 8n, o). **(6a, b)** *Morrisiceras morrisi* (Oppel, 1857). Middle Bathonian, Morrisi Zone, Shahrud (Seyed-Emami et al. 2013, p. 51, fig. 6c, d). **(7a, b)** *Morphoceras multiforme* Arkell, 1951. Lower Bathonian, Zigzag Zone, Avaj, southwest Alborz (Seyed-Emami et al. 1985, p. 67, pl. 4, fig. 7). **(8a, b)** *Morphoceras dehmi* Seyed-Emami, 1985. Lower Bathonian, Zigzag Zone, Avaj, southwest Alborz (Seyed-Emami et al. 1985, p. 69, pl. 4, fig. 8). **(9a, b)** *Rehmannia* (*Loczyceras*) aff. *reissi* (Steinmann, 1881). Middle Callovian, Shahrud (Seyed-Emami et al. 2013, p. 59, fig. 8i, j). **(10a, b)** *Morphoceras macrescens* (Buckman, 1923). Lower Bathonian, Zigzag Zone, Avaj, southwest Alborz (Seyed-Emami et al. 1985, p. 68, pl. 4, fig. 4). **(11a, b)** *Morphocers thalmanni* Mangold, 1970. Lower Bathonian, Zigzag Zone, Avaj, southwest Alborz (Seyed-Emami et al. 1985, p. 68, pl. 4, fig. 1). **(12a, b)** *Morphoceras parvum* Wetzel, 1937. Lower Bathonian, Avaj, southwest Alborz (Seyed-Emami et al. 1985, p. 68, pl. 4, fig. 2).

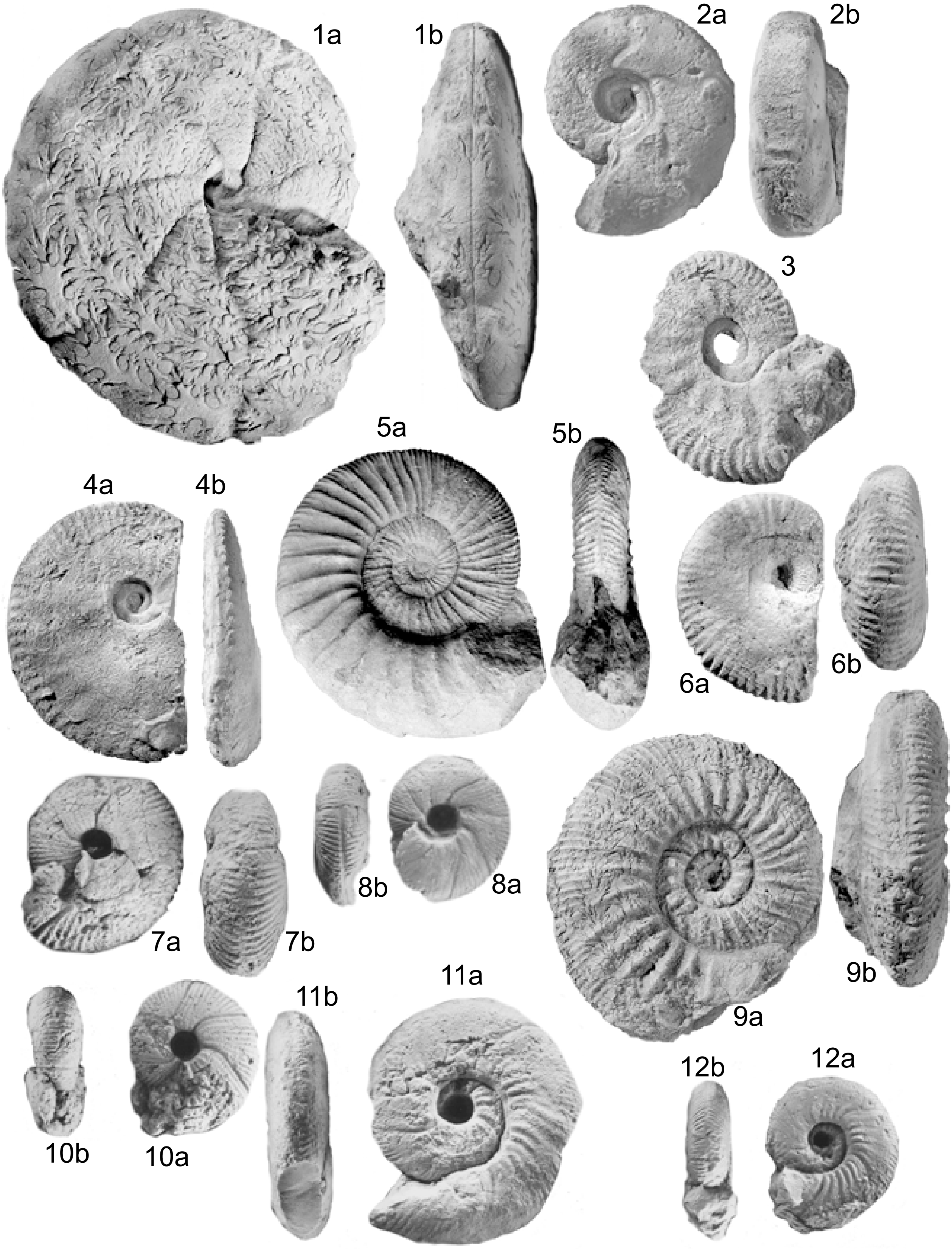
1a
1b
2a
2b
3
4a
4b
5a
5b
6a
6b
7a
7b
8a
8b
9a
9b
10a
10b
11a
11b
12a
12b

marl as well as silt- and sandstone intercalations, the Badamu Formation (Huckriede et al. 1962; Seyed-Emami 1967, 1971). The formation records the most prominent marine transgression within the Ab-e-Haji Subgroup and is a key-unit between two coal-bearing, siliciclastic units, i.e., the Ab-e-Haji and Hojedk formations. The Badamu Formation contains a rich benthic macrofauna (e.g., bivalves, corals, gastropods) and an ammonite fauna comprising the following families: Dactylioceratidae, Hildoceratidae, Graphoceratidae, Tmetoceratidae, Hammatoceratidae, Erycitidae, Stephanoceratidae, Sonniniidae, etc., indicating a late Toarcian to Early Bajocian age (Seyed-Emami 1971, 1988, 1993, 2000, 2004b; Seyed-Emami et al. 2000).

Hojedk Formation—The Badamu Formation is followed conformably by a thick, greyish siliciclastic succession called Hojedk Formation (Stöcklin 1972). The thickness of the Hojedk Formation varies within short distances and may reach up to 1000 m. On the northern Tabas Block, the Hojedk Formation is partly fluvial and lacustrine and partly shallow marine. On the western and southern Tabas Block, the formation consists of marginally marine to non-marine sandstones and carbonaceous siltstones. It contains the most workable coal seams of the Tabas Block. The marine influence increases towards the east, especially on the Lut Block (Seyed-Emami et al. 2004b; Wilmsen et al. 2009b). The age of the Hojedk Formation is, based on the ammonite record of the under- and overlying formations (Badamu and Parvadeh, respectively) late Early Bajocian to earliest late Bajocian.

3.2.2 Middle and Upper Jurassic strata

After the Mid-Cimmerian Event, the Tabas Block broke up into several areas with different sedimentary histories. Lithostratigraphically, the sedimentary succession of the northern and central Tabas Block has been accommodated in the Magu Group (Aghanabati 1977; Wilmsen et al. 2003, 2009b), which is composed of the Baghamshah (Upper Bajocian-Lower Callovian), Esfandiar (Callovian to Lower Kimmeridgian), and Garedu (Kimmeridgian-Tithonian) subgroups (Fig. 8). Equivalent strata in the southern Tabas Block have been accommodated in the Bidou Group. The strong lithological variability reflects increased activity of synsedimentary block faulting (Fürsich et al. 2003a; Seyed-Emami et al. 2004a; Wilmsen et al. 2009a). The Baghamshah

---

Plate 15 (Page 127): Ammonites from the Lower Dalichai Formation east of Semnan, eastern Alborz, North Iran. **(1a, b)** *Wagnericeras* sp. Lower Bathonian (Seyed-Emami et al. 1989, p. 87, pl. 3, fig. 5). **(2a, b, 7a, b)** *Polyplectites* aff. *zlatarskii* (Stephanov, 1963). Lower Bathonian (Seyed-Emami et al. 1989, p. 83, pl. 2, figs. 1, 3). **(3a–c)** *Pseudodimorphinites komsi* Seyed-Emami, 1989. Lower Bathonian, Zigzag Zone, Yeovilensis Subzone (Seyed-Emami et al. 1989, p. 85, pl. 1, fig. 15). **(4a, b)** *Procerites* (*Siemiradzkia*) *procerus* (Seebach, 1864). Lower Bathonian (Seyed-Emami et al. 1989, p. 86, pl. 3, fig. 3). **(5a, b)** *Morphoceras* aff. *jactatum* (Buckman, 1920). Lower Bathonian, Zigzag Zone (Seyed-Emami et al. 1989, p. 84, pl. 1, fig. 9). **(6a, b)** *Ebrayiceras* aff. *sulcatum* (Zieten, 1830). Lower Bathonian, Zigzag Zone (Seyed-Emami et al. 1989, p. 85, pl. 1, fig. 12). **(8a, b)** *Pseudodimorphinites foersteri* Seyed-Emami, 1989. Lower Bathonian, Zigzag Zone, Yeovilensis Subzone (Seyed-Emami et al. 1989, p. 85, pl. 1, fig. 14). **(9a, b)** *Procerites* (*Procerite*s) aff. *progracilis* Cox & Arkell, 1950. Lower Bathonian, Progracilis Zone (Seyed-Emami et al. 1989, p. 86, pl. 3, fig. 7c, d). **(10a, b)** *Oxycerites seebachi* (Wetzel, 1950, 1950). Lower Bathonian (Seyed-Emami et al. 1989, p. 83, pl. 1, fig. 4). **(11a, b)** *Lissoceras* cf. *psilodiscus* (Schloenbach, 1865). Bathonian (Seyed-Emami et al. 1989, p. 82, pl. 2, fig. 11). **(12 a, b)** *Oxycerites yeovilensis* (Rollier, 1911). Lower Bathonian, Zigzag Zone, Yeovilensis Subzone (Seyed-Emami et al. 1989, p. 82, pl. 1, fig. 1).

Plate 16 (Page 128): Ammonites from the Dalichai Formation east of Semnan, eastern Alborz, North Iran. **(1)** *Hecticoceras* (*Lunuloceras*) cf. *lunuloides* (Kilian, 1899). Middle Callovian, Jason Zone (Schairer et al. 1991, p. 51, pl. 1, fig. 4). **(2a, b)** *Indosphinctes* (*Indosphinctes*) aff. *pseudopatina* (Parona & Bonarelli, 1895). Lower–Middle Callovian (Schairer et al. 1991, p. 59, pl. 3, fig. 3). **(3a–c)** *Pseudopeltoceras* sp. Middle Callovian, Athleta Zone (Schairer et al. 1991, p. 61, pl. 3, fig. 4). **(4a–c)** *Hecticoceras* (*Putealiceras*) aff. *lugeoni* Tsytovitch, 1911. Middle Callovian (Schairer et al. 1991, p. 54, pl. 1, fig. 5). **(5a, b)** *Hecticoceras* (*Lunuloceras*) aff. *pseudopunctatum* (Lahusen, 1883). Middle–Upper Callovian (Schairer et al. 1991, p. 52, pl. 1, fig. 3). **(6a)** *Rehmannia* (*Loczyceras*) aff. *discrepans* (Bourqin, 1967–68). Middle Callovian (Schairer et al. 1991, p. 55, pl. 2, fig. 2). **(7a, b)** *Binatisphinctes* sp. Middle–Upper Callovian (Schairer et al. 1991, p. 60, pl. 3, fig. 2).

Plate 17 (Page 129): Bathonian ammonites from the Parvadeh and Baghamshah formations, Tabas area, Central Iran. **(1a, b)** *Homoeoplanulites* (*Parachoffatia*) sp. Bathonian (Seyed-Emami et al. 1991, p. 77, pl. 7, fig. 3). **(2a, b)** *Oecotraustes bradleyi* Arkell, 1951. Lower Bathonian (Seyed-Emami et al. 1991, p. 70, pl. 2, fig. 8). **(3a, b)** *Polyplectites tabasi* Seyed-Emami 1991. Middle–Upper Bathonian (Seyed-Emami et al. 1991, p. 71, pl. 2, fig. 15). **(4a, b)** *Treptoceras* aff. *uhligi* (Popovici-Hatzeg, 1905). Middle–Upper Bathonian (Seyed-Emami et al. 1991, pl. 2, fig. 16). **(5a, b)** *Paroecotraustes formosus* (Arkell, 1951). Lower–Upper Bathonian (Seyed-Emami et al. 1991, p. 70, pl. 2, fig. 6). **(6a, b)** *Ebrayiceras sulcatum* (Zieten, 1830). Lower Bathonian, Zigzag Zone (Seyed-Emami et al. 1991, p. 73, pl. 4, fig. 3). **(7a, b)** *Homoeoplanulites* (*Homoeoplanulites*) *rambertensis* Mangold, 1970. Upper Bathonian, Blanazense Zone (Seyed-Emami et al. 1991, p. 76, pl. 6, fig. 6). **(8a, b)** *Wagnericeras* aff. *bathonicum* Arkell, 1958. ?Middle Bathonian (Seyed-Emami et al. 1991, p. 76, pl. 6, fig.2). **(9a, b)** *Prohecticoceras haugi* (Popovivi-Hatzeg, 1905). Middle–Upper Bathonian, Hodsoni Zone (Seyed-Emami et al. 1991, p. 71, pl. 2, fig. 12). **(10a, b)** *Ebrayiceras filicostatum* Wetzel, 1937. Lower Bathonian (Seyed-Emami et al., 1991 p. 73, pl. 4, fig. 9). **(11)** *Polysphinctes* cf. *polysphinctus* Buckman, 1922. Lower Bathonian (Seyed-Emami et al. 1991, p. 74, pl. 4, fig. 14). **(12a, b)** *Procerites* (*Siemiradzkia*) *pseudorjazanensis* (Lissajous, 1923). Middle–Upper Bathonian (Seyed-Emami et al. 1991, p. 75, pl. 5, fig. 2). **(13a, b)** *Pseudodimorphinites pinguis* (Grossouvre, 1919). Lower Bathonian, Zigzag Zone (Seyed-Emami et al. 1991, p. 73, pl. 4, fig. 11). **(14a, b)** *Lissoceras psilodiscus* (Schloenbach, 1865). Lower Bathonian (Seyed-Emami et al. 1991, p. 69, pl. 1, fig. 10). **(15a, b)** *Oxycerites yeovilensis* (Rollier, 1911). Lower Bathonian, Zigzag Zone, Yeovilensis Subzone (Seyed-Emami et al. 1991, p. 69, pl. 1, fig. 12). **(16a, b)** *Morphoceras macrescens* (Buckman, 1923). Lower Bathonian, Zigzag Zone, Macrescens Subzone (Seyed-Emami et al. 1991, p. 73, pl. 4, fig. 6). **(17a, b)** *Oxycerites oxus* (Buckman, 1926). Lower Bathonian (Seyed-Emami et al. 1991, p. 69, pl. 2, fig. 4).

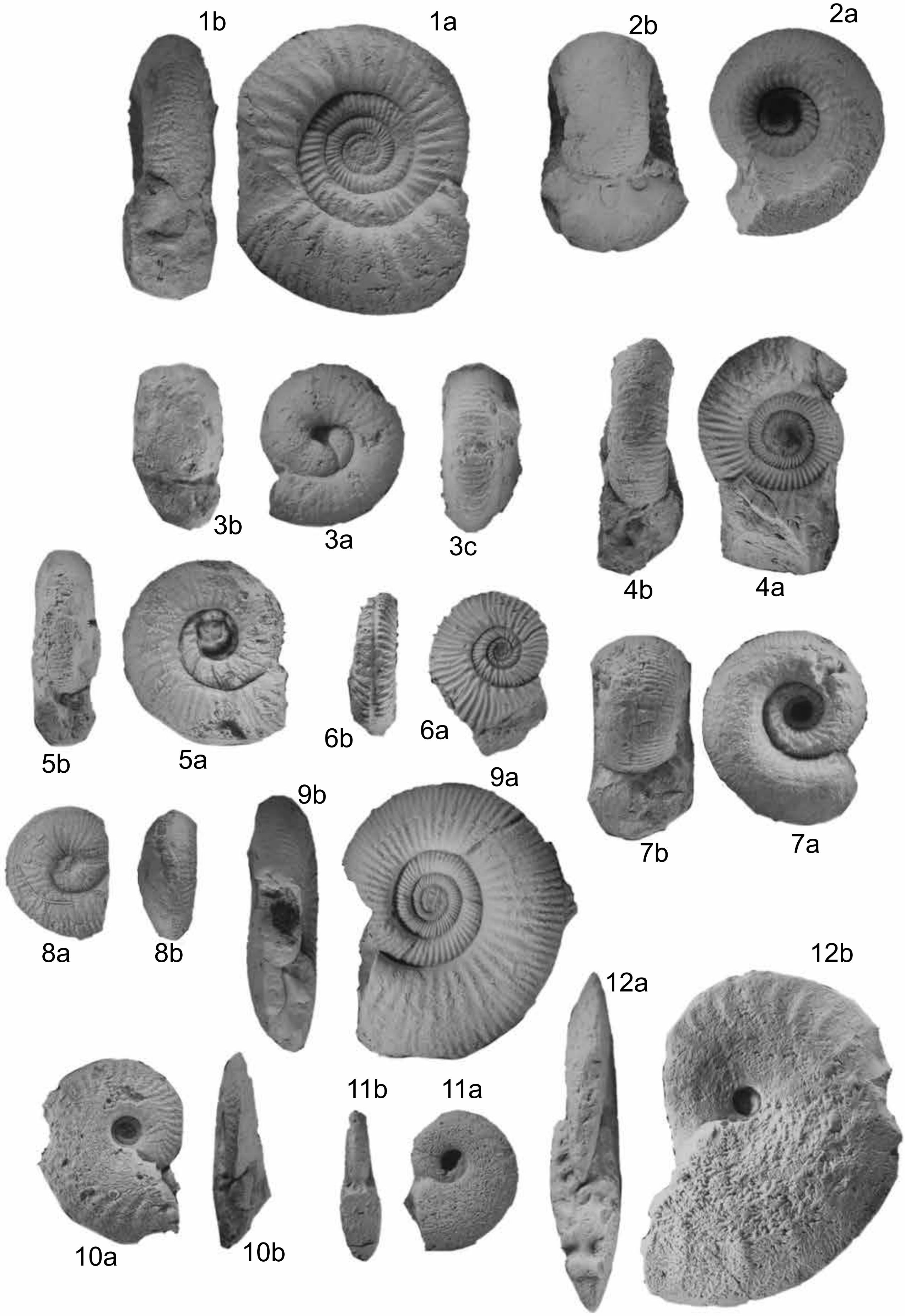
1b
1a
2b
2a
3b
3a
3c
4b
4a
5b
5a
6b
6a
7b
7a
9b
9a
8a
8b
12a
12b
11b
11a
10a
10b

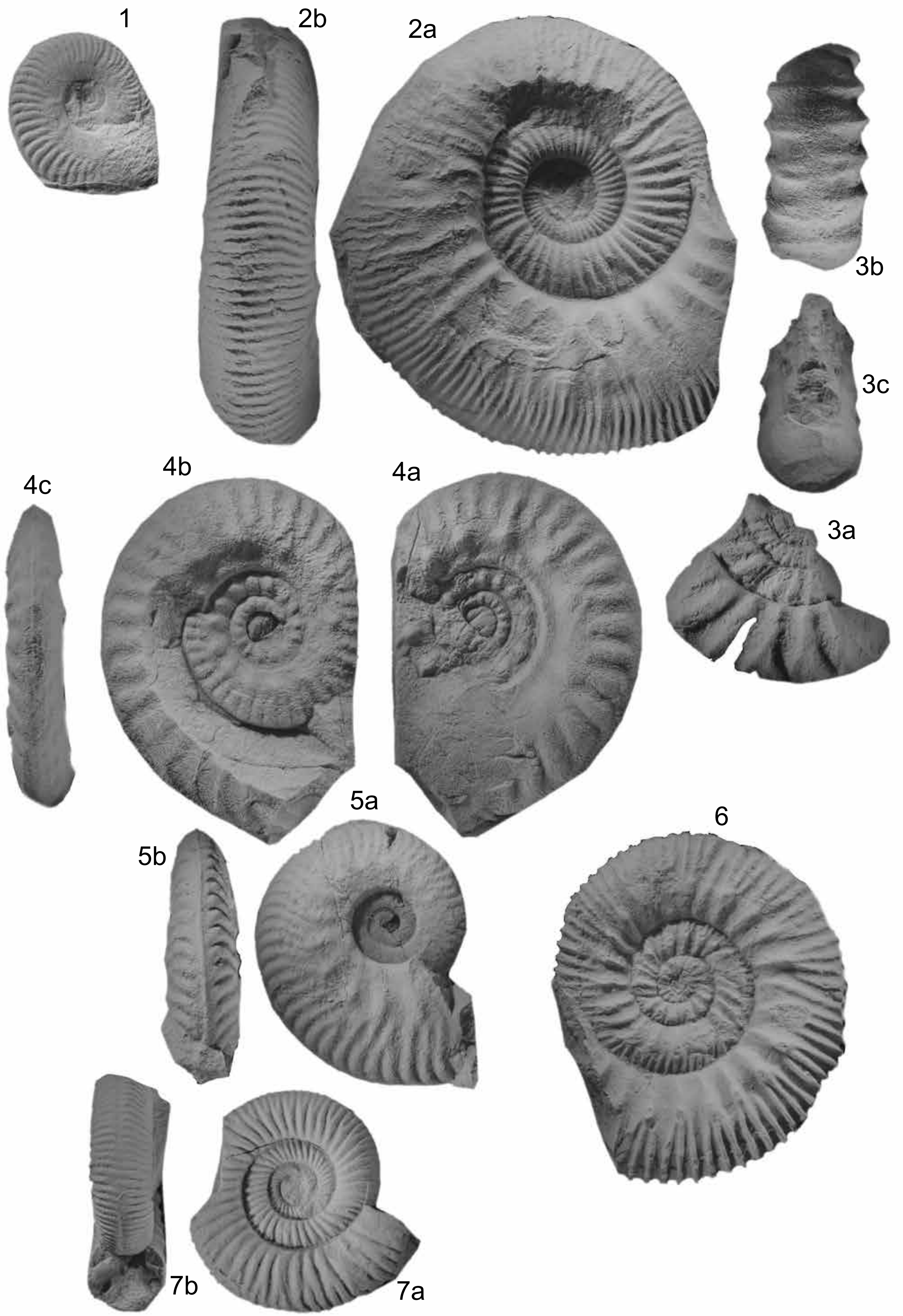
1
2b
2a
3b
3c
4c
4b
4a
3a
5a
5b
6
7b
7a

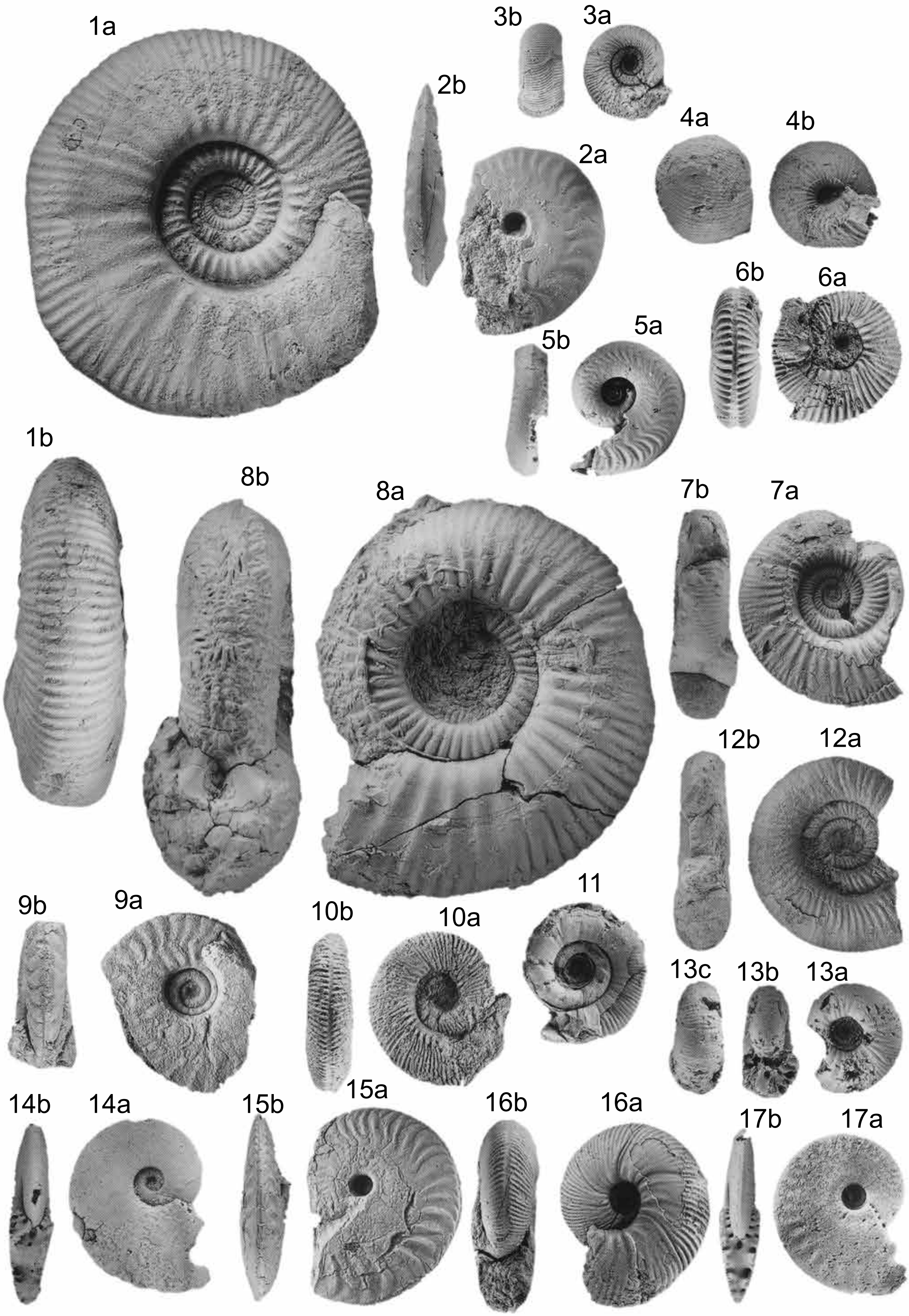
1a
3b
3a
2b
4a
4b
2a
6b
6a
5a
5b
1b
8b
8a
7b
7a
12b
12a
11
9b
9a
10b
10a
13c
13b
13a
14b
14a
15b
15a
16b
16a
17b
17a

Subgroup comprises, from base to top, the Parvadeh, Baghamshah, and the Sikhor Formation and the informal Qal-eh-Dokhtar Sandstone formation; the Esfandiar Subgroup the Esfandiar, Qal'eh Dokhtar, Korond, and the Kamar-e-Mehdi Formation; and the Garedu Subgroup the Garedu Red Bed and Magu Gypsum Formation (Fig. 8). The Bidou Group is, in ascending order, composed of the Bidou, Kamar-e-Mehdi, and the Ravar Formation.

Parvadeh Formation—The Parvadeh Formation (Aghanabati 1996) is a comparatively condensed unit (30–150 m in thickness), documenting the extensive Late Bajocian transgression that followed the Mid-Cimmerian Tectonic Event on the Tabas Block (Fürsich et al. 2009b). Its sharp, often erosional base unconformably rests on the Hodjedk Formation or even older strata, and is followed by a decimetre- to metre-thick conglomerate, composed of milk quartz, quartzite and sandstone pebbles. The thin lower siliciclastic part of the formation is followed by bedded oncolitic-microbial limestones with some marl intercalations. The formation documents a gradual but pronounced deepening. Macrobenthic fossils are common, in particular bivalves, sponges, gastropods, and brachiopods. In addition, it contains a rich ammonite fauna of the following families: Phylloceratidae, Haploceratidae, Oppeliidae, Stephanoceratidae, Sphaeroceratidae, Morphoceratidae, and Perisphinctidae (Seyed-Emami et al. 1991; 1998a, b), indicating a Late Bajocian to Early–Middle Bathonian age.

Qal'eh Dokhtar Sandstone formation—The informal formation is restricted to the easternmost part of the Tabas Block. It consists of 186 m of cross-bedded sandstones intercalated between the Hojedk and Baghamshah formations and represents high-energy shallow-marine environments. From its stratigraphic setting it corresponds partially or completely to the Parvadeh Formation of other areas.

Baghamshah Formation—The Baghamshah Formation (Stöcklin et al. 1965) consists mostly of soft, greenish, marly silts with minor intercalations of fine-grained sandstones and limestones, deposited in a deeper shelf setting. Its thickness reaches several hundred meters (usually between 400 and 600 m), but towards the south, in the Lakar Kuh area, its thickness increases up to 1000 m and more. There, huge slumped turbidite sequences point to a rapidly subsiding, still deeper depositional environment (Kluyver et al. 1983a, b). In general, the formation was deposited in open shelf environments below the fair-weather wave-base down to basinal settings. Due to shallowing towards the top of the formation the carbonate content (e.g., documented by intercalated oncoid layers and a generally more marly sediment) increased and so did the abundance of benthic macrofauna such as bivalves, gastropods, crinoids, and sponges. Towards the Lut Block, the source area of the siliciclastic material, intercalations of thin, sharp-based sandstones are more common. Due to local uplift around the Bathonian–Callovian boundary, the Baghamshah Formation has been partially or fully eroded in parts of the Shotori Mountains. The formation contains a poor ammonite fauna consisting of members of the families Clydoniceratidae, Sphaeroceratidae, Morphoceratidae, Macrocephalitidae, and Perisphinctidae (Seyed-Emami et al. 1997, 1998 a, 1998 b, 2015) indicating a Late Bathonian to Early Callovian time interval, but locally it may extend to the Middle Callovian (Seyed-Emami et al. 2002).

Sikhor Formation—Underlying the Esfandiar Limestone Formation at the eastern margin of the Tabas Block (Shotori Swell) there exists a partly reddish, fluvio-deltaic siliciclastic succession of conglomerates, sandstones, and siltstones with a thickness of up to 400 m, the Sikhor Formation (Fürsich et al. 2003a). It comprises a clastic wedge, which decreases in thickness (and finally disappears) towards the west, north, and east. A lower siliciclastic Kuh-e-Neygu Member represents floodplain silts with caliche nodules and calcrete layers as well as fluvial channel sandstones, which laterally grade into cross-bedded delta-front sandstones. The mixed carbonate-siliciclastic sediments of the upper Majid Member have been deposited on a carbonate ramp. The Sikhor Formation reflects synsedimentary faulting and erosional processes at the eastern margin of the Tabas Block, i.e., within the central part of the Shotori Mountains, around the Bathonian–Callovian boundary and may rest on erosional remnants of the Baghamshah Formation or even onlap on Permian strata. This tectonic event is well known on the Tabas Block (Seyed-Emami et al. 2004a) and has been called "Tabasian" by Aghanabati (1977). Considering its stratigraphic position, the age of the Sikhor Formation is Early Callovian.

Esfandiar Limestone Formation—Together with the Qal'e Dokhtar, Kamar-e-Mehdi, and Korond formations the Esfandiar Limestone Formation (Stöcklin et al. 1965) composes the carbonate-dominated Esfandiar Subgroup (Wilmsen et al. 2003). The Esfandiar Limestone Formation represents an extensive carbonate platform at the raised eastern margin of

Plate 18: Bathonian ammonites from the Parvadeh and Baghamshah formations, Tabas area, Central Iran. **(1a, b)** *Kheraiceras* aff. *bullatum* (d'Orbigny, 1846). Lower–Middle Bathonian (Seyed-Emami et al. 1991, p. 72, pl. 4, fig. 1). **(2a, b)** *Choffatia* (*Subgrossouvria*) aff. *kranaiformis* Arkell, 1958. Upper Bathonian (Seyed-Emami et al. 1991, p. 78, pl. 8, fig. 6). **(3a, b)** *Bullatimorphites* aff. *ymir* (Oppel, 1862). Middle Bathonian (Seyed-Emami et al. 1991, p. 72, pl. 3, fig. 2).

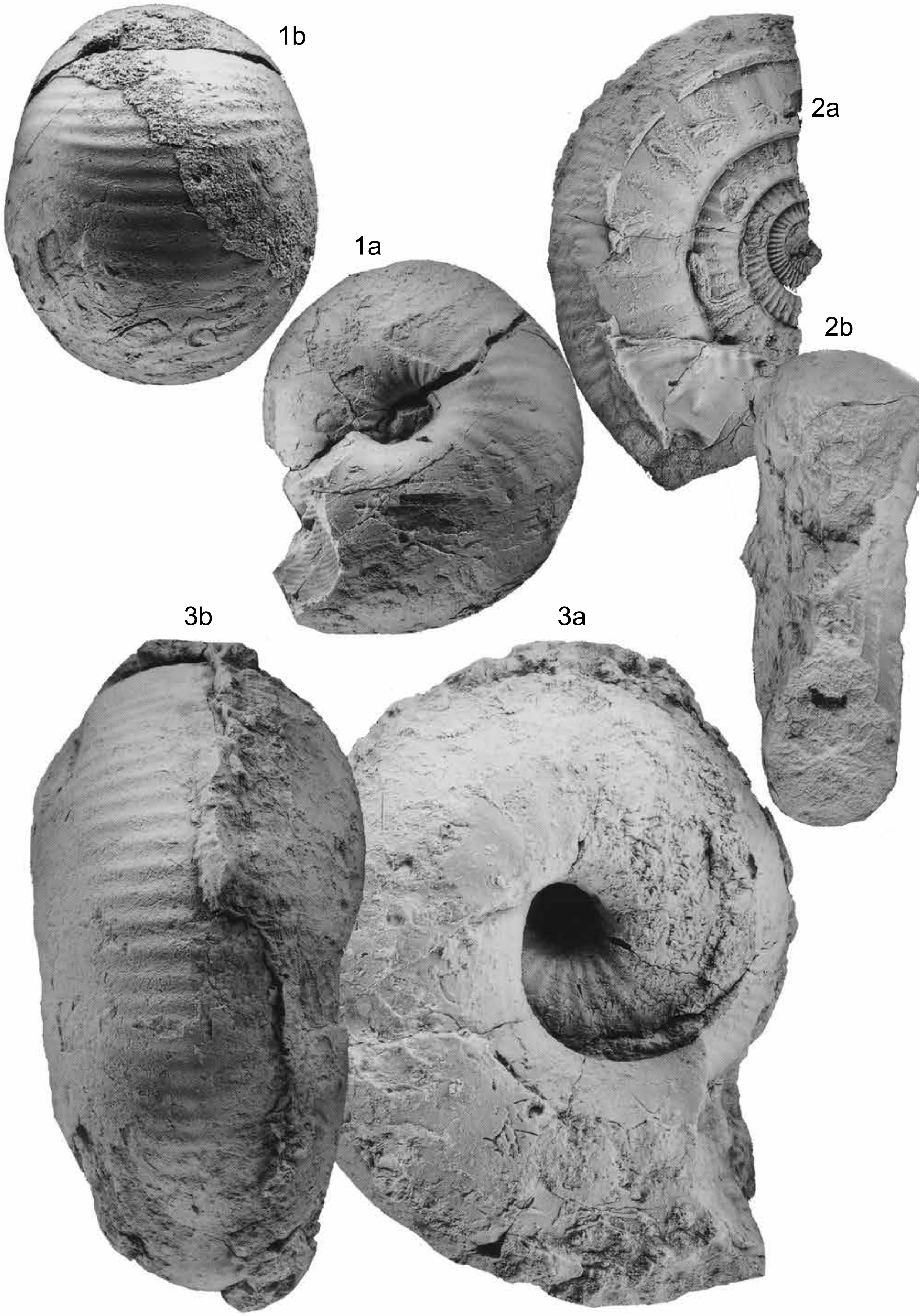
1b
1a
2a
2b
3b
3a

the Tabas Block and consists of light yellowish-grey, partly dolomitized, medium-bedded to massive carbonates, which were deposited in shallow, warm waters (Fürsich et al. 2003b). Characteristic facies types of the platform interior are carbonate mudstones, bioclastic wackestones, peloid pack- and grainstones and *Neuropora* floatstones, documenting a predominantly low-energy environment, in which diceratid bivalves and sponges (chaetetids, *Neuropora*) thrived. The high-energy platform margin, in contrast, was characterized by ooid grainstones, bioconglomerates, shell concentrations, and rare small patch reefs composed of corals and calcareous sponges. The Esfandiar platform developed gradually from the underlying Baghamshah or Sikhor Formation. The upper contact of the formation is usually sharp, and the formation may be overlain by formations of different ages. The Esfandiar Limestone Formation has a thickness of 760 m at the type locality at Kuh-e-Esfandiar in the southern Shotori Mountains, where it is unconformably overlain by the uppermost Cretaceous Kerman Conglomerate of Huckriede et al. (1962). Occasionally it contains a few ammonites of the family Perisphinctidae, which indicate a (?Early) Callovian to (?Early) Kimmeridgian age.

Qal'eh Dokhtar Limestone Formation—The up to 400-m-thick Qal'eh Dokhtar Limestone Formation, as defined by Wilmsen et al. (2003), is the slope facies of the Esfandiar carbonate platform at the eastern margin of the Tabas Block, restricted to the central and northern Shotori Mountains (Stöcklin et al. 1965). It consists of partly autochthonous, partly allochthonous carbonate sediments (Fürsich et al. 2003b). The former include oncolitic float- and rudstones of the upper slope, sponge microbialites that formed small buildups on the upper to middle slope, and thinly bedded spiculitic wackestones, bedded mudstones and marly mudstones of the lower slope. Intercalated between these predominantly low-energy sediments are dm- to m-thickdark-grey sharp-based and commonly graded bioclastic grain- and rudstones, occasionally associated with slumping structures (Fürsich et al. 2003b; Wilmsen et al. 2009a). Their components consist of debris of *Neuropora*, crinoids, brachiopods, *Tubiphytes*, corals, and ooids which are clearly derived from the carbonate platform. These allochthonous sediments represent partly debris flows, partly proximal turbidites. Where the slope of the carbonate platform was steeper olistostromes occur. These features do not support the interpretation of the formation as a ramp, as proposed by Sabbagh Bajestani et al. (2017). The Qaleh Dokhtar Formation contains a sparse ammonite fauna of the families Phylloceratidae, Lytoceratidae, Hecticoceratidae, Haploceratidae, Reineckeiidae, Aspidoceratidae, and Perisphinctidae, indicating a Callovian to Oxfordian age (Schairer et al. 2000, 2003; Seyed-Emami et al. 2002).

Korond Formation—The Korond Formation (Schairer et al. 2003) is a thick (>1000 m), monotonous succession bordering the eastern margin of the northern Tabas Block. It is composed chiefly of light-green, silty marls, subordinately of fine-grained sandstone beds, and in the lower part of sporadically intercalated allochthonous biorudstones derived from the Esfandiar carbonate platform. In earlier publications the Korond Formation, due to its lithological similarity, usually was erroneously identified and mapped as Baghamshah Formation (Stöcklin et al. 1965; Ruttner et al. 1968).

The Korond Formation conformably overlies either the Qal'eh Dokhtar Limestone or onlaps the Esfandiar Limestone Formation; its lower boundary is diachronous and its upper boundary is not known. The Korond Formation was deposited in a deeper, open marine basinal environment, which shallowed to a depth above the storm wave-base with time. Benthic macroinvertebrates are partly autochtho-

Plate 19 (Page 133): Ammonites from the Baghamshah Formation, Tabas area, Central Iran. **(1a, b)** *Prohecticoceras retrocostatum* (Grossouvre, 1888). Upper Bathonian, Retrocostatum Zone (Seyed-Emami et al. 1998a, p. 116, pl. 1, fig. 1). **(2a, b)** *Alcidellus* aff. *tenuistriatus* (Grossouvre, 1888). Upper Bathonian (Seyed-Emami et al. 1998b, p. 128, pl. 1, fig. 1). **(3a, b)** *Prohecticoceras haugi* (Popovici-Hatzeg, 1905). Upper Bathonian, Retrocostatum Zone (Seyed-Emami et al. 1998b, p. 128, pl. 1, fig. 2). **(4a, b)** *Cadomites* (*Polyplectites*) *claromontanus* Kopik, 1974. Upper Bathonian, Retrocostatum Zone (Seyed-Emami et al. 1998a, p. 115, pl. 1, fig. 9). **(5a, b)** *Cadomites* (*Polyplectites*) *bozorgniai* Seyed-Emami, 1998. Upper Bathonian, Retrocostatum Zone (Seyed-Emami et al. 1998a, p. 114, pl. 1, fig. 3). (6a, b) *Choffatia euryptycha* (Neumayr, 1871). Lower Callovian (Seyed-Emami et al. 1997, p. 33, pl. 2, fig. 3). **(7a, b)** *Macrocephallites* cf. *caucasicus* Djanalidze, 1929. Lower Callovian, Bullatum Zone (Seyed-Emami et al. 1997, p. 33, pl. 3, fig. 2). **(8a, b)** *Oxycerites* (*Paroxycerites*) *subdiscus* (d'Orbigny, 1846). Upper Bathonian–?Lower Callovian (Seyed-Emami et al. 1997, p. 29, pl. 2, fig. 1).

Plate 20 (Page 134): Ammonites from the Kashafrud Formation, Upper Bajocian east of Mashhad. **(1a, b, c)** *Sphaeroceras brongniarti* (Sowerby, 1818). Upper Bajocian (Seyed-Emami et al. 1994, p. 149, pl. 1, fig. 2). **(2a, b)** *Garantiana* (*Orthgarantiana*) *conjugata* (Quenstedt, 1887). Upper Bajocian (Seyed-Emami et al. 1996, p. 95, pl. 1, fig. 5). **(3)** *Parkinsonia* (*Parkinsonia*) aff. *rarecostata* (Buckman, 1881). Upper Bajocian, Parkinsoni Zone (Seyed-Emami et al. 1996, p. 96, pl. 3, fig. 3). **(4)** *Parkinsonia* (*Parkinsonia*) aff. *parkinsoni* (Sowerby, 1821). Upper Bajocian, Parkinsoni Zone (Seyed-Emami et al. 1996, p. 96, pl. 2, fig. 4). **(5)** *Leptosphinctes* (*Leptosphinctes*) *kitiae* (Kakhadze & Zesashvili, 1956). Upper Bajocian, Niortense Zone (Seyed-Emami et al. 1996, p. 97, pl. 3, fig. 2).

Plate 21 (Page 135). Ammonites from the Dalichai Formation north of Damghan, East Alborz, North Iran. **(1a, b)** *Adabofoloceras* aff. *adabofolense* Collignon, 1958. Middle Callovian (Seyed-Emami & Raoufian 2017, p. 254, pl. 1, fig. 1). **(2a, b, 4a, b, 5)** *Hecticoceras* gr. *metomphalum* Bonarelli, 1894. Lower Middle Callovian, Anceps Zone (Seyed-Emami & Raoufian 2017, p. 258, pl. 1, figs. 3, 4, 5). **(3a, b)** *Bullatimorphites* (*Bomburites*) aff. suevicus (Roemer, 1911). Upper Bathonian, Retrocostatum Zone (Seyed-Emami & Raoufian 2017 p. 264, pl. 2, fig. 7). **(6a, b)** *Lytoceras* sp. Lower–Middle Callovian. (Seyed-Emami & Raoufian 2017, p. 258, pl. 1, fig. 2).

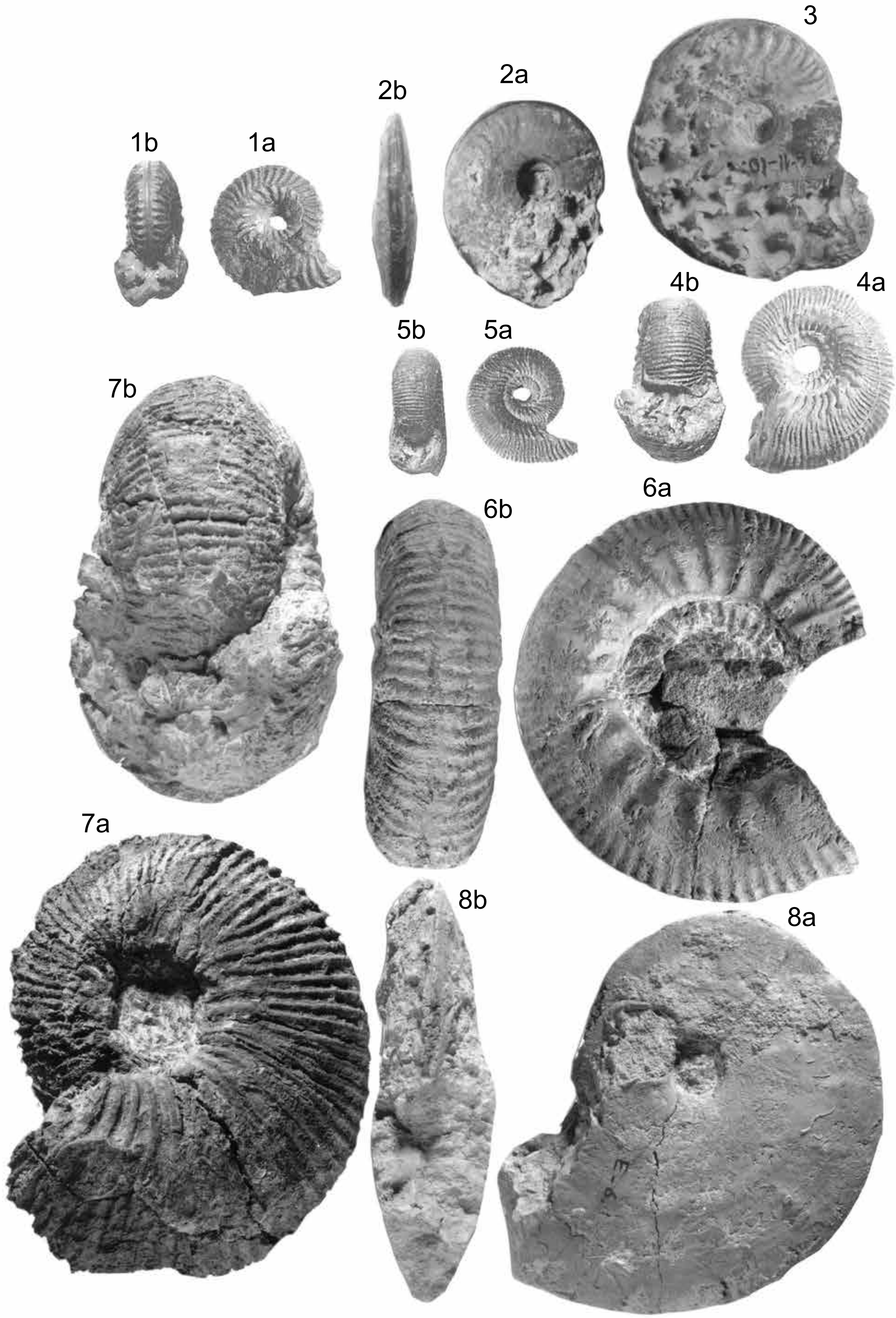
1b
1a
2b
2a
3
4b
4a
5b
5a
6a
6b
7b
7a
8b
8a

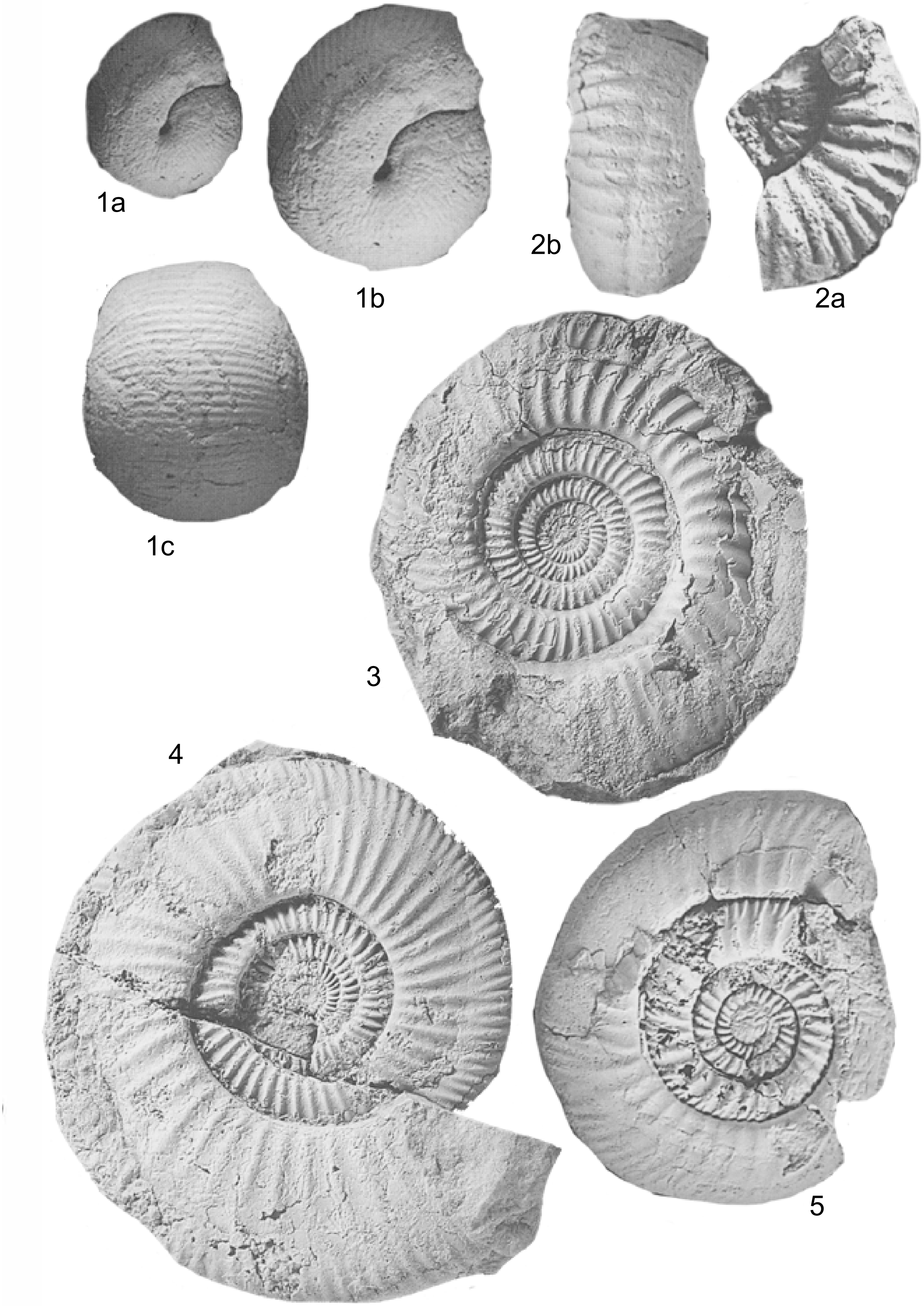
1a
1b
2b
2a
1c
3
4
5

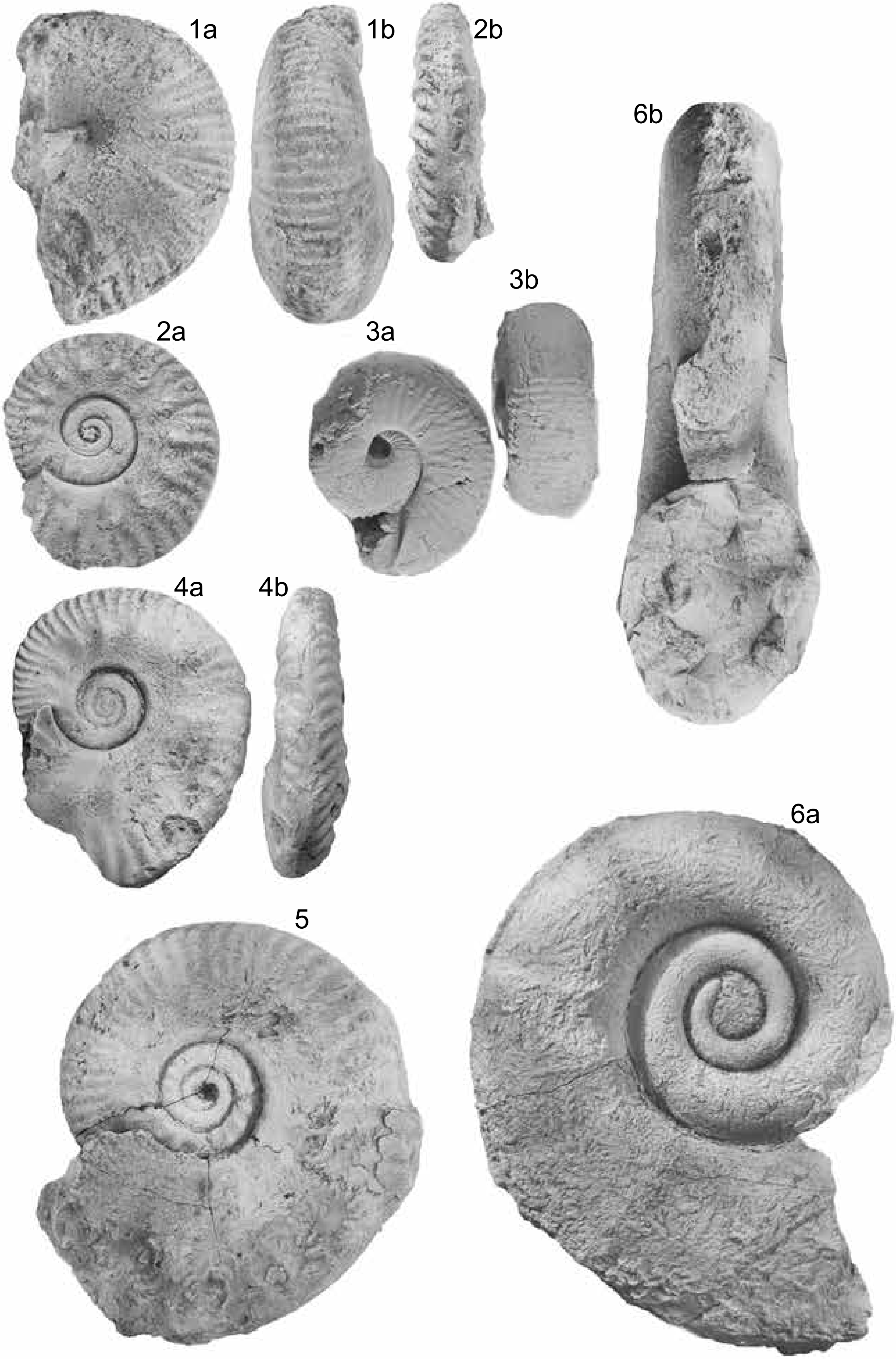
1a
1b
2b
6b
3b
2a
3a
4a
4b
6a
5

nous (mainly bivalves and irregular echinoids), partly derived from the carbonate platform (e.g., bivalves, sponges, crinoids, brachiopods, cidaroid spines). In addition, the formation contains few phylloceratid and perisphictid ammonites, which indicate an Oxfordian to Kimmeridgian age (Schairer et al. 2003). However, unpublished Sr isotope data from calcitic shells (*Rostroperna* sp.) suggest a Tithonian age for the upper part of the formation and that it may even range into the Cretaceous.

Kamar-e-Mehdi Formation—The Kamar-e-Mehdi Formation (Wilmsen et al. 2003, 2010) is an up to 1300-m-thick succession of greyish marl, marly limestones and micritic limestones with a basal Echellon Limestone Member and a capping, cliff-forming Nar Limestone Member It is restricted to the western part of the Tabas Block, extending from north of Tabas southward to the Kerman area. The up to 200-m-thick Echelon Limestone Member is characterized by microbialites, marly oncolites, marls, bio-floatstones and small microbial coral-sponge patch reefs. The Nar Limestone Member is 90–150 m thick and composed of bedded carbonate mudstones, commonly with pseudomorphs after gypsum, and peloid wacke- to packstones. The bulk of the formation consists of metre-scale asymmetric thickening-upward cycles, which start with marl and end in shelly micritic floatstones. In the upper part of the formation pseudomorphs after gypsum are common in well-bedded micrites, and two decametre-thick intercalations of gypsum occur in the west-central Tabas Block. Sporadic intercalations of thin parallel-laminated and ripple-bedded silt- and sandstones were derived from the Lut Block in the west, whereas the carbonate mud was derived from the Esfandiar carbonate platform in the east. The abundant but low- to moderate-diverse benthic macrofauna was dominated by bivalves, in particular pectinids, whereas gastropods and brachiopods are rare. Small microbial calcareous sponge-coral and oyster patch reefs occur at several levels in the lower part of the formation (Fürsich et al. 2016).

The Kamar-e-Mehdi Formation has been deposited in an extensive shelf lagoon on the western side of the Esfandiar carbonate platform (Wilmsen et al. 2010). Fully marine conditions prevailed for most of the time but became increasingly restricted towards the top of the formation, which is indicated by the increasing presence of evaporitic sediments and the decreasing faunal diversity. The formation rests conformably on the Baghamshah Formation and is overlain sharply by the evaporitic Magu Gypsum Formation. Due to the prominent large pectinid bivalves, the Kamar-e-Mehdi Formation had been named Pectinidenkalk-Gips-Fazies by Huckriede et al. (1962) and Calcaires à pectens by Aghanabati (1977). Its age is Callovian to Kimmeridgian based on very rare perisphinctid ammonites and benthic agglutinated foraminifera (Wilmsen et al. 2010).

Garedu Red Bed Formation—The Garedu Red Bed Formation (Ruttner et al. 1968) forms, together with the Magu Gypsum Formation, the Garedu Subgroup (Wilmsen et al. 2003). It is locally developed in the northern and central part of the Tabas Block. However, a lithologically and stratigraphically very similar conglomerate unconformably resting on the Qal-eh-Dokhtar and Esfandiar Limestone formations at Kuh-e-Birg, 80 km east of the Shotori Mountains on the Lut Block, indicates a much wider distribution of the unit. On the northwestern flank of the Shotori Mountains, it consists of reddish limestone conglomerates with a mixed carbonate-siliciclastic matrix and fine to coarse siliciclastics that unconformably overlie the Esfandiar Limestone Formation. On the northeastern flank of the Shotori Mountains, it rests, with a more gradual contact, on the Qal'eh Dokhtar Limestone Formation. Its thickness strongly varies, from a few metres to more than 400 m. Similarly, the facies changes within short lateral distances. These features point to a fault-controlled deposition. Occasional intercalations of limestones, oyster fragments, and microbialites in the lower part point to a shallow, probably often marginal marine setting, whereas in the upper part reddish silt with pebbly sandstone intercalations indicate fluvial and floodplain environments. The age of the Garedu Red Bed Formation, considering its stratigraphic position above the Esfandiar Limestone and Qal'eh Dokhtar Limestone formations, is post-Early Kimmeridgian.

Magu Gypsum Formation—The Magu Gypsum Formation (Aghanabati 1977) is a succession of red, soft-weathering, fine-grained sandstones, siltstones and clays, with decametre-thick gypsum intercalations and sporadic thin limestone (oo- and intra-grainstones and -rudstones) and dolostone beds, in the western part of the Tabas Block. It overlies with sharp contact the Nar Limestone of the Kamar-e-Mehdi Formation. Its thickness is about 600 m at the type section (Aghanabati 1977). The sediments have been deposited in a sabkha environment with episodic marine ingressions (Wilmsen et al. 2009b; Zamani Pedram 2011). In the northern part of the Tabas Block near Echellon, a several-metres-thick conglomerate composed of large limestone pebbles (Nar Conglomerate Member) at the base of the formation can be followed for several kilometres and indicates tectonic activity following the deposition of the Kamar-e-Mehdi Formation. Considering its stratigraphic position, the age of the Magu Gypsum Formation is probably post-Early Kimmeridgian to Early Cretaceous (Late Kimmeridgian to Berriasian – Valanginian according to Zamani Pedram 2011).

The following two formations compose the Bidou Group (Aghanabati 1977, 1998), restricted to the southern Tabas Block (see Wilmsen et al. 2009b for a synopsis). The group is equivalent to the Baghamshah, Esfandiar, and Magu subgroups of the central and northern Tabas Block.

Bidou Formation—The Bidou Formation (Bidou-Schichten of Huber & Stöcklin 1954; Bidou-Fazies of Huckriede et al 1962; Seyed-Emami 1999; Seyed-Emami et al. 2001) is a thick (up to 1000 m) sequence of varicoloured conglomerates, sandstones, shales with intercalation of gypsiferous marls and limestones. Common sedimentary structures are cross-stratification, ripple marks and mud cracks. Together with the evaporate layers they indicate a coastal plain to very shallow marginal marine setting. The formation rests discontinuously and occasionally with a basal coarse conglomerate (the expression of the Mid-Cimmerian Tectonic Event) on the Hojedk Formation. The Bidou Formation corresponds in part to the Parvadeh, in parts to the Baghamshah Formation of the northern Tabas Block. Its age is probably Late Bajocian to Callovian.

Ravar Formation—The Ravar Formation ("Ravar series" *sensu* Huckriede et al. 1962, *non* Stöcklin 1961) is a mixture of varicoloured siliciclastics, evaporites and dark volcanics, occasionally forming small salt plugs in the southern part of the Tabas Block (Seyed-Emami 1999; Wilmsen et al. 2009b). It overlies, with gradual contact, the Kamar-e-Mehdi Formation and is overlain unconformably by the Late Barremian–Albian *Orbitolina* Limestone. Its thickness is around 400 m but may be more. The Ravar Formation is equivalent to the Magu Gypsum Formation of the northern Tabas Block and like the latter also represents a sabkha environment. The occurrence of lavas may be due to synsedimentary tectonic movements. The age of the formation is Late Jurassic to ?Early Cretaceous.

4 Biostratigraphic classification of the ammonite faunas

Ammonites often occur in connection with transgressive phases and are sometimes concentrated in condensed beds, where taxa of several biozones are mixed. The ammonite faunas are illustrated in Plates 1–30; for biozonation, see Tables 1–3.

4.1 Lower Jurassic (Table 1)

4.1.1 Hettangian

So far, no record, neither from North nor Central Iran.

4.1.2 Sinemurian

Only few, scattered specimens of the subfamily Echioceratinae have been reported from the Upper Sinemurian (Raricostatum Zone) of the Alborz Mountains (North Iran): *Paltechioceras* cf. *oosteri* (Pl. 7, Figs. 2, 3a, b; 4a, c).

Table 1: Northwest European standard ammonite biozones for the Lower Jurassic Series and their documentation in northern (NI) and Central Iran (CI).

Series	Stage	Biozone	NI	CI
LOWER JURASSIC	Toarcian	Aalensis	x	x
		Pseudoradiosa	x	x
		Dispansum	x	x
		Thouarsense	x	x
		Variabilis	x	x
		Bifrons	x	x
		Serpentinum	x	x
		Tenuicostatum	x	x
	Pliensbachian	Spinatum		
		Margaritatus	x	
		Davoei		
		Ibex		
		Jamesoni		
	Sinemurian	Raricostatum	x	
		Oxynotum		
		Obtusum		
		Turneri		
		Semicostatum		
		Bucklandi		
	Hettangian	Angulata		
		Liasicus		
		Tabulata		

4.1.3 Pliensbachian

North Iran: Only few Upper Pliensbachian (Domerian) Amaltheidae and Harpoceratinae are known from the Margaritatus Zone: *Amaltheus stockesi* (Pl. 7, Fig. 1), *A. margaritatus* (Pl. 10, Fig. 5), *A. subnodosus* (Pl. 10, Fig. 6a, b), and *Protogrammoceras* (*P.*) cf. *celebratum*.

Central Iran: So far, no record.

4.1.4 Toarcian

The Toarcian stage coincides with the most extensive transgression within the Lower to lower Middle Jurassic Ab-e-Haji Subgroup of the Shemshak Group. Ammonites from this stage, especially from the Upper Toarcian, are commonly present in North and Central Iran.

Lower Toarcian (Tenuicostatum/Serpentinum zones): Some taxa of the subfamilies Dactylioceratinae, Hildoceratinae, and Harpoceratinae are present locally in North and Central Iran (Pls. 5, 7, 10): *Dactylioceras* (*Orthodactylites*) *semicelatum* (Pl. 5, Fig. 7a, b), *D.* (*Orthodactylites*) aff. *semicelatum* (Pl. 10, Fig. 7a, b), *D.* (*Eodactylites*?) *pseudocommune* (Pl. 10, Fig. 12a, b), *Hildaites* sp. ex gr. *H. forte* (Pl. 5, Fig. 5), and *Harpoceras* cf. *falciferum* (Pl. 5, Fig. 8a, b).

Midddle Toarcian (Bifrons/Variabilis zones): Members of the subfamilies Dactylioceratinae, Protogrammoceratinae, and Arieticeratinae (Pls. 4, 7) are locally present, i.e. *Hildoceras bifrons* (Pl. 4: Fig. 2a, b), *Peronoceras* sp. nov.? (Pl. 7, Fig. 6a, b), and *Catacoeloceras* cf. *requiniatum*.

Table 2: Northwest European standard ammonite biozones for the Middle Jurassic Series and their documentation in northern (NI) and Central Iran (CI).

Series	Stage	Biozone	NI	CI
MIDDLE JURASSIC	Callovian	Lamberti	x	
		Athleta	x	
		Coronatum		
		Anceps/Jason	x	
		Gracilis/Calloviense/Koenigi		
		Bullatus/Herveyi	x	x
	Bathonian	Discus	x	x
		Retrocostatum/Orbis	x	x
		Bremeri/Hodsoni	x	x
		Morrisi	x	x
		Subcontractus	x	
		Progracilis	x	x
		Aurigerus/Tenuiplicatus	x	x
		Zigzag	x	
	Bajocian	Parkinsoni	x	
		Garantiana	x	
		Niortense	x	
		Humphresianum		x
		Propinquans		x
		Laeviuscula (Sauzei)		x
		Discites		x
	Aalenian	Concavum	x	x
		Murchisonae	x	x
		Opalinum	x	x

Upper Toarcian: All standard Northwest European ammonite biozones are present in North and Central Iran (Pls. 6, 7, 9, 10).

Thouarsense/Dispansum zones: *Pseudogrammoceras fallaciosum* (Pl. 10, Fig. 10) and *Podagrosites latescens* (Pl. 7, Fig. 5).). In Iran, the Pseudogrammoceras fallaciosum Zone is widely distributed and corresponds approximately to the Thouarsense/Dispansum zones.

Pseudoradiosa/Aalensis zones: *Dumortieria moorei* (Pl. 1, Fig. 6, Pl. 6, Fig. 12), *D. distans* (Pl. 6, Fig. 6), *D. levesquei* (Pl.6, Fig. 8), *D. radiosa* (Pl. 6, Fig. 14), *D. bleicheri* (Pl. 6, Fig. 9), *D. striatulocostata* (Pl. 7, Fig. 7), *Paradumortieria explanata* (Pl. 6, Fig. 11), *P. aequicostata* (Pl. 6, Fig. 10), *Pleydellia aalensis* (Pl. 6, Fig. 4; Pl. 10, Fig. 4), *Pl. buckmani* (Pl. 6, Fig. 3), *Pl. lotharingica* (Pl. 6, Fig. 2), *Pl. subcompta* (Pl. 6, Fig. 7; Pl. 9, Fig. 7), *Pl. paucicostata* (Pl. 9, Fig. 3), *Geczyceras tipperi* (Pl. 2, Fig. 3), etc.

4.2 Middle Jurassic (Table 2)

4.2.1 Aalenian

All standard Northwest European Ammonite biozones are present in North and Central Iran.

Opalinum Zone:

North Iran: *Leioceras comptum* (Pl. 9, Fig. 2), *Erycites barodiscus* (Pl. 10, Fig. 11), *Bredyia iranica* (Pl. 8, Fig. 1), *B. subinsignis* (Pl. 8, Fig. 5), *Accardia*(?) *shahmirzadense* (Pl. 8, Fig. 2).

Central Iran: *Leioceras comptum* (Pl. 1, Fig. 4), *L. crassicostatum* (Pl. 1, Fig. 5), *L. paucicostatum* (Pl. 5, Fig. 3), *L. costosum* (Pl. 5, Fig. 6), *Tmetoceras scissum* (Pl. 1, Fig. 7), *Bredyia brancoi* (Pl. 2, Fig. 1).

Murchisonae Zone

North Iran: *Accardia diadematoides* (Pl. 9, Fig. 5), *Shahrudites asseretoi* (Pl. 9, Fig. 6), *S. stoecklini* (Pl. 9, Fig. 8), *Ceccaites* cf. *sieboldi* (Pl. 9, Fig. 9).

Central Iran: *Ludwigia murchisonae* (Pl. 1, Fig. 3), *Brasilia bradfordensis* (Pl. 1, Fig. 1), *Abbasitoides modestum* (Pl. 2, Fig. 11), *Ceccaites* cf. *sieboldi* (Pl. 9, Fig. 9).

Concavum Zone

North Iran: *Graphoceras decorum* (Pl. 9, Fig. 4; Pl. 10, Fig. 9), *G.* (*Ludwigella*) *cornu* (Pl. 10, Fig. 2), *Pseudaptetoceras klimakomphalum* (Pl. 8, Fig. 4), *Accardia diadematoides* (Pl. 10, Fig. 13).

Central Iran: *Graphoceras* (*Ludwigella*) *arcitenens* (Pl. 1, Fig. 2), *G.* sp. ex gr. *G. concavum* (Pl. 5, Fig. 4), *Pseuaptetoceras amplectens* (Pl. 2, Fig. 7), *P. amaltheiforme* (Pl. 3, Fig 9; Pl. 4, Fig. 4).

4.2.2 Bajocian

Lower Bajocian

Discites/Laeviuscula/Propinquans zones:

North Iran: So far, no record.

Central Iran: *Lissoceras oolithicum* (Pl. 5, Fig. 12), *L.* (*Microlissoceras*) *badamui* (Pl. 5, Fig. 18), *Strigoceras* cf. *languidum* (Pl. 5, Fig. 14), *Bradfordia inclusa* (Pl. 4, Fig. 4), *Malladaites kermanensis* (Pl. 2, Fig. 5), *Haplopleuroceras subspinatum* (Pl. 2, Fig. 6), *Witchellia laeviuscula* (Pl. 2, Fig. 7), *W. connata* (P. 3, Fig. 2), *W. platymorpha* (Pl. 3, Fig. 5), *Pelekodites macer* (Pl. 2, Fig. 8), *P. varicosa* (Pl. 2, Fig. 9), *P. kermanensis* (Pl. 5, Fig. 13), *P. nodosus* (Pl. 5, Fig. 16), *Etropolia* aff. *renzi* (Pl. 5, Fig. 12), *E. sapunovi* (Pl. 5, Fig. 17), *Sonninia* (*Euhoploceras*) *adicra* (Pl. 2, Fig. 10), *Sonninia* cf. *propinquans* (Pl. 5, Fig. 11), *Parsemileites liebi* (Pl. 2, Fig. 2), *Otoites* cf. *sauzei* (Pl. 3, Fig. 1), *O. contractus* (Pl. 3, Fig. 8), *Kumatostephanus kumaterus persicus* (Pl. 4, Fig. 2), *Emileia quenstedti* (Pl. 4, Fig. 3), *E.* cf. *polyschides* (Pl. 4, Fig. 5), etc.

Plate 22: Lower Callovian Macrocephalitinae from North and Central Iran. **(1a, b)** *Macrocephalites* (*Tmetokephalites*) *verus* Buckman, 1920. Dalichai Formation, East Alborz, Lower Callovian, Bullatus Zone (Seyed-Emami et al. 2015, p. 266, fig. 6(1a, b)). **(2a, b)** *Macrocephalites* (*Platystomatoceras*) *pila* Nikitin, 1885. Dalichai Formation, East Alborz, Lower Callovian, Bullatus Zone (Seyed-Emami et al. 2015, p. 267, fig. 7(3a, b)). **(3a, b)** *Macrocephalites* (*Pleurocephalites*) sp. Baghamshah Formation, Kuh-e-Echellon, Tabas area, Central Iran, Lower Callovian (Seyed-Emami et al. 2015, p. 267, fig. 11(1a, b)). **(4a, b)** *Macrocephalites* (*Dolikephalites*) *hoyeri* Mönnig, 1995. Dalichai Formation, East Alborz, Lower Callovian, Bullatus Zone (Seyed-Emami et al. 2015, p. 270, fig. 9(3a, b)).

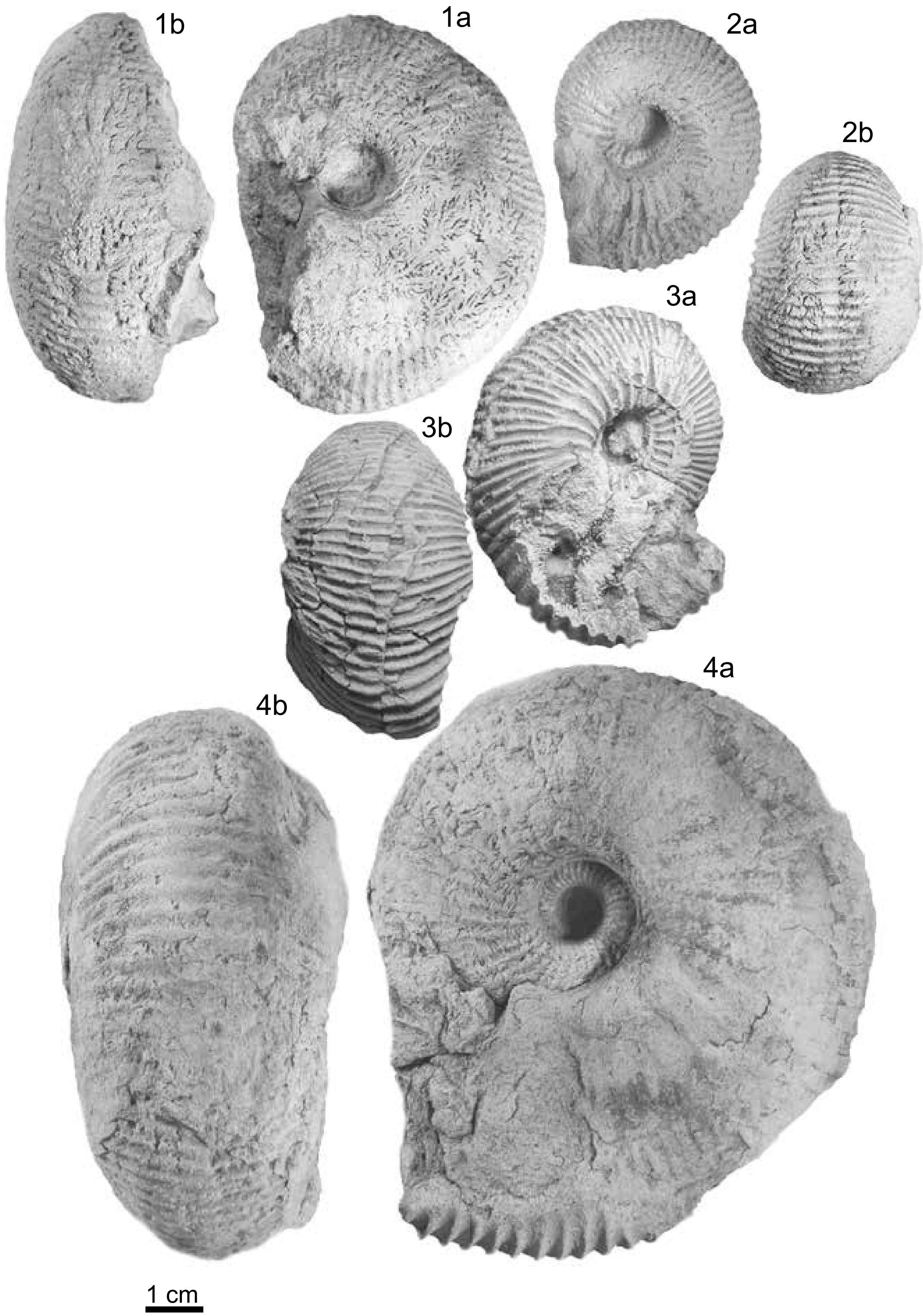
1b
1a
2a
2b
3a
3b
4b
4a
1 cm

Humphriesianum Zone

North Iran: So far, no record.

Central Iran: *Stephanoceras* sp., *Skirroceras* sp. (pers. obs.).

Uppper Bajocian

Niortense/Garantiana zones

North Iran: *Strenoceras* sp., *Garantiana* (*Pseudogarantiana*) *dichotoma* (Pl. 11, Fig. 13), *G. baculata* (Pl. 12, Fig. 2), *G.* cf. *wetzeli* (Pl. 12, Fig. 3), *Polyplectites linguiferus* (Pl. 11, Fig. 16).

Central Iran: So far, no record.

Parkinsoni Zone

North Iran: *Oppelia pleurifer* (Pl. 11, Fig. 14), *Oecotraustes westermanni* (Pl. 11, Fig. 7), *Parkinsonia parkinsoni* (Pl. 11, Fig. 8), *P. dorni* (Pl. 11, Fig. 12), *P. radiata* (Pl. 11, Fig. 15), *P.* rarecostata (Pl. 12, Fig. 1), *P.* cf. *subarietis* (Pl. 12, Fig. 5), *Vermisphinctes* aff. *vermiformis* (Pl. 11, Fig. 2), etc.

Central Iran: So far, no record.

4.2.3 Bathonian

Lower Bathonian

Zigzag/Tenuiplicatus zones

North Iran: *Lissoceras psilodiscus* (Pl. 12, Fig. 9), *Oxycerites yeovilensis* (Pl. 12, Fig. 8; Pl. 15, Fig. 12), *O. seebachi* (Pl. 15, Fig. 10), *Oecotraustes bomfordi* (Pl. 13, Fig. 4), *Polyplectites* aff. *zlatarskii* (Pl. 12, Fig. 6; pl. 14, Fig. 2, 7), *Asphinctes* aff. *patrulii* (Pl. 13, Fig. 5), *Pseudodimorphinites pinguis* (Pl. 17, Fig. 13), *P. komsi* (Pl. 15, Fig. 3), *P. foersteri* (Pl. 15, Fig. 8), *Morphoceras multiforme* (Pl. 13, Fig. 2), *M. parvum* (Pl. 13, Fig. 1), *M.* aff. *thalmanni* (Pl. 13, Fig. 7), *M. thalmanni* (Pl. 14, Fig. 11), *M. macrescens* (Pl. 14, Fig. 10), *M. dehmi* (Pl. 11, Fig. 6), *M.* aff. *jactatum* (Pl. 15, Fig. 5), *Ebrayiceras* aff. *sulcatum* (Pl. 15, Fig. 6), *Procerites tmetelobus* (Pl. 11, Fig. 1), *Siemirazkia procera* (Pl. 11, Fig. 4), *Procerites* (*Procerite*s) aff. *progracilis* (Pl. 15, Fig. 9), *Wagnericeras* sp. (Pl. 15, Fig. 1), etc.

Central Iran: *Lissoceras psilodiscus* (Pl. 17, Fig. 14) *Oxycerites yeovilensis* (Pl. 17, Fig. 15), *O. oxus* (Pl. 17, Fig. 17), *O. seebachi* (Pl. 11, Fig. 10), *Ebrayiceras filicostatum* (Pl. 11, Fig. 9), *E. sulcatum* (Pl. 11, Fig. 11), *Simirazkia procera* (Pl. 11, Fig. 4), etc.

Middle Bathonian

Progracilis/Subcontractus/Morrisi zones

North Iran: *Prohecticoceras* aff. *dominjoni* (Pl. 13, Fig. 3), *P.* cf. *mondegoense* (Pl. 13, Fig. 8), *Oxycerites* (*Alcidellus*) aff. *tenuistriatus* (Pl. 13, Fig. 6), *Morrisiceras morrisi* (Pl. 14, Fig. 6), etc.

Central Iran (Tabas area): *Oecotraustes* (*Paroecotraustes*) *splendens* (Pl. 11, Fig. 5), *Kheraiceras* aff. *bullatum* (Pl. 18, Fig. 1), *Bullatimorphites* aff. *ymir* (Pl. 18, Fig. 3), *Procerites* (*Siemiradzkia*) *pseudorjazanensis* (Pl. 17, Fig. 12).

Plate 23 (Page 141): Ammonites from the Dalichai Formation north of Damghan, East Alborz, North Iran. **(1a, b)** *Alborzites binaludensis* Seyed-Emami, 2013. Lower Middle Callovian, Anceps Zone (Seyed-Emami & Raoufian 2017, p. 267, pl. 4, fig. 3). **(2a, b)** *Reineckeia* (*Reineckeia*) gr. *stuebeli* (Steinmann, 1881). Lower Middle Callovian, Anceps Zone (Seyed-Emami & Raoufian 2017, p. 264, pl. 4, fig. 4). **(3a, b)** *Reineckeia* (*Reineckeia*) gr. *anceps* (Reinecke, 1818). Lower Middle Callovian, Anceps Zone (Seyed-Emami & Raoufian 2017, p. 266, pl. 4, fig. 1). **(4a, b)** *Cadomites bremeri* Tsereteli, 1968. Upper Bathonian, Bremeri Zone (Seyed-Emami & Raoufian 2017, p. 261, pl. 3, fig. 2). **(5a, b)** *Bullatimorphites* (*Bomburites*) *microstoma* (d'Orrbigny, 1846). Lower Callovian, Bullatus Zone (Seyed-Emami & Raoufian 2017, p. 262, pl. 2, fig. 5).

Plate 24 (Page 142): Upper Jurassic ammonites from Alborz, Binalud and Koppeh Dagh, North Iran. **(1a, b)** *Ochetoceras* (*Granulochetoceras*) *cristatum* Dietrich, 1940. Upper Oxfordian, Planulata Zone, Lar Formation, Central Alborz (Seyed-Emami et al. 1998c p. 99, pl. 1, fig. 2). **(2a, b)** *Lingulaticeras nudatum* (Oppel, 1858). Upper Oxfordian, Bimmamatum/Planulata zones, Dalichai/Chaman Bid Formation, eastern Binalud, west Mashhad (Seyed-Emami & Schairer 2011b, p. 375, fig. 3(F)). **(3)** *Sutneria eumela* (d'Orbigny, 1847). Middle Kimmeridgian, Lar Formation, east Semnan, Alborz, North Iran (Seyed-Emami et al. 1998c, p. 104, pl. 1, fig. 8). **(4a, b)** *Taramelliceras* (*Taramelliceras*) *costatum* (Quenstedt, 1849). Upper Oxfordian, Bimmamatum/Planulata zones, Lar Formation, Central Alborz (Seyed-Emami et al. 1998c, p. 100, pl. 1, fig. 3). **(5)** *Taramelliceras* (*Taramelliceras*) cf. *trachinotum* (Oppel, 1857). Early Middle Kimmeridgian, Lar Formation, east Semnan, Alborz, North Iran (Seyed-Emami et al. 1998c, p. 102, pl. 1, fig. 4). **(6)** *Orthosphinctes* (*Ardescia*) aff. *schaireri* Atrops, 1982. Lower Kimmeridgian, Platynota Zone, Mozduran Formation, northwest Mashhad, east Koppeh Dagh (Seyed-Emami et al. 1998c, p. 105, pl. 2, fig. 3). **(7a, b)** *Hecticoceras* (*Rossiensiceras*) aff. *metomphalum* Bonarelli, 1894. Middle Callovian, Anceps Zone, Dalichai/Chaman Bid Formation, eastern Binalud, west Mashhad, northeast Iran (Seyed-Emami & Schairer 2011b, p. 376, fig. 3(A)). **(8a, b)** *Cymaceras*? sp. Lower Kimmeridgian, Mozduran Formation, Koppeh Dagh, northeast Mashhad (Seyed-Emami et al. 1998c, p. 99, pl. 1, fig. 1). **(9)** *Taramelliceras* (*Strebliticeras*) *externnodatum* (Dorn, 1931). Upper Oxfordian, Bimmamatum Zone, Mozduran Formation, Koppeh Dagh, northwest Mashhad, northeast Iran (Seyed-Emami et al. 1998c, p. 102, pl. 1, fig. 5). **(10a, b)** *Euaspidoceras* aff. *douvillei* (Collot, 1917). Lower Oxfordian, Cordatum Zone, Lar/Mozduran Formation, eastern Binalud, west Mashhad, northeast Iran (Seyed-Emami & Schairer 2011b, p. 377, fig. 3(E)). **(11)** *Euaspidoceras douvillei* (Collot, 1917). Lower Oxfordian, Cordatum Zone, Lar Formation, east Semnan, Alborz, North Iran (Seyed-Emami et al. 1998c, p. 104, pl. 2, fig. 1). **(12)** *Horioceras* sp. Lower–Middle Callovian, Dalichai/Chaman Bid Formation, eastern Binalud, west Mashhad, northeast Iran (Seyed-Emami & Schairer 2011b, p. 376, fig. 3(D)).

Plate 25 (Page 143): Middle/ and Upper Jurassic ammonites from the Dalichai Formation, Shahrud area, eastern Alborz. **(1a, b)** *Peltoceratoides* (*Parawedekindia*) aff. *arduennensis* (d'Orbigny, 1948). Lower Oxfordian, Mariae/Costatum Zone (Seyed-Emami et al. 2013, p. 61, fig. 9a, b). **(2a, b)** *Binatisphinctes binatus* (Leckenby, 1859). Upper Callovian, Athleta/Lamberti Zone (Seyed-Emami et al. 2013, p. 53, fig. 7a, b). **(3a, b)** *Peltoceras* (*Peltoceras*) aff. *breckhemmeri* Prieser, 1937. Upper Callovian (Seyed-Emami et al. 2013, p. 59, fig. 9e, f). **(4)** *Passendorfia* (*Enayites*) *rozaki* Meléndez, 1989. Upper Oxfordian, Bimmamatum Zone (Seyed-Emami et al. 2013, p. 55, fig. 7g). **(5a, b)** *Peltoceratoides* (*Parawedekindia*) *arduennensis* (d'Orbigny, 1948). Lower Oxfordian, Mariae/Costatum Zone (Seyed-Emami et al. 2013, p. 60, fig. 9k, l). **(6a, b)** *Lissoceras voultense* (Oppel, 1865). Lower–Middle Callovian (Seyed-Emami et al. 2013, p. 48, fig. 4g, h). **(7a, b)** *Peltoceras* sp. ex gr. *athleta* (Phillips, 1829). Upper Callovian, Athleta Zone (Seyed-Emami et al. 2013, p. 59, fig. 5k–m).

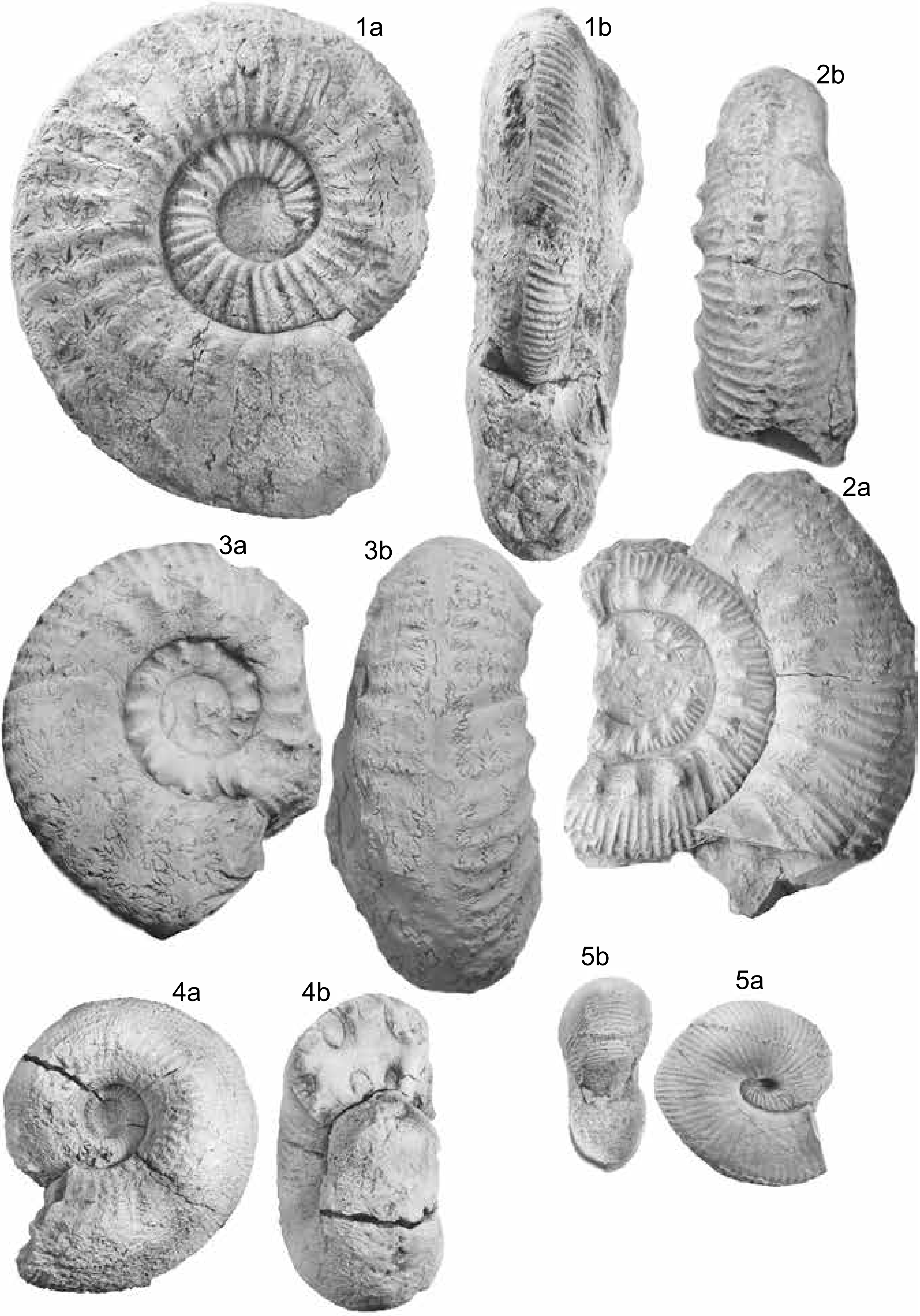
1a
1b
2b
2a
3a
3b
4a
4b
5b
5a

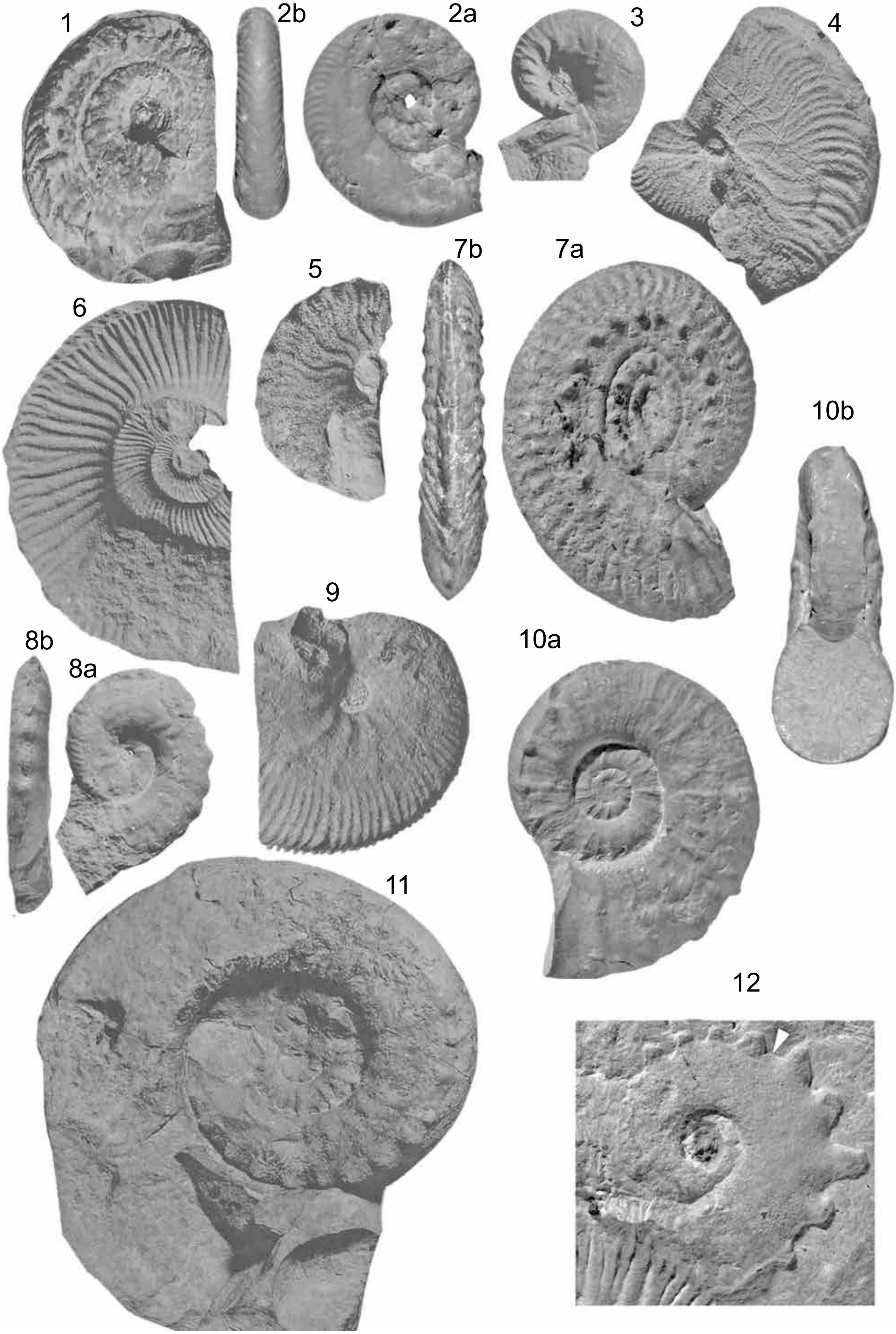
1
2b
2a
3
4
5
6
7b
7a
8b
8a
9
10a
10b
11
12

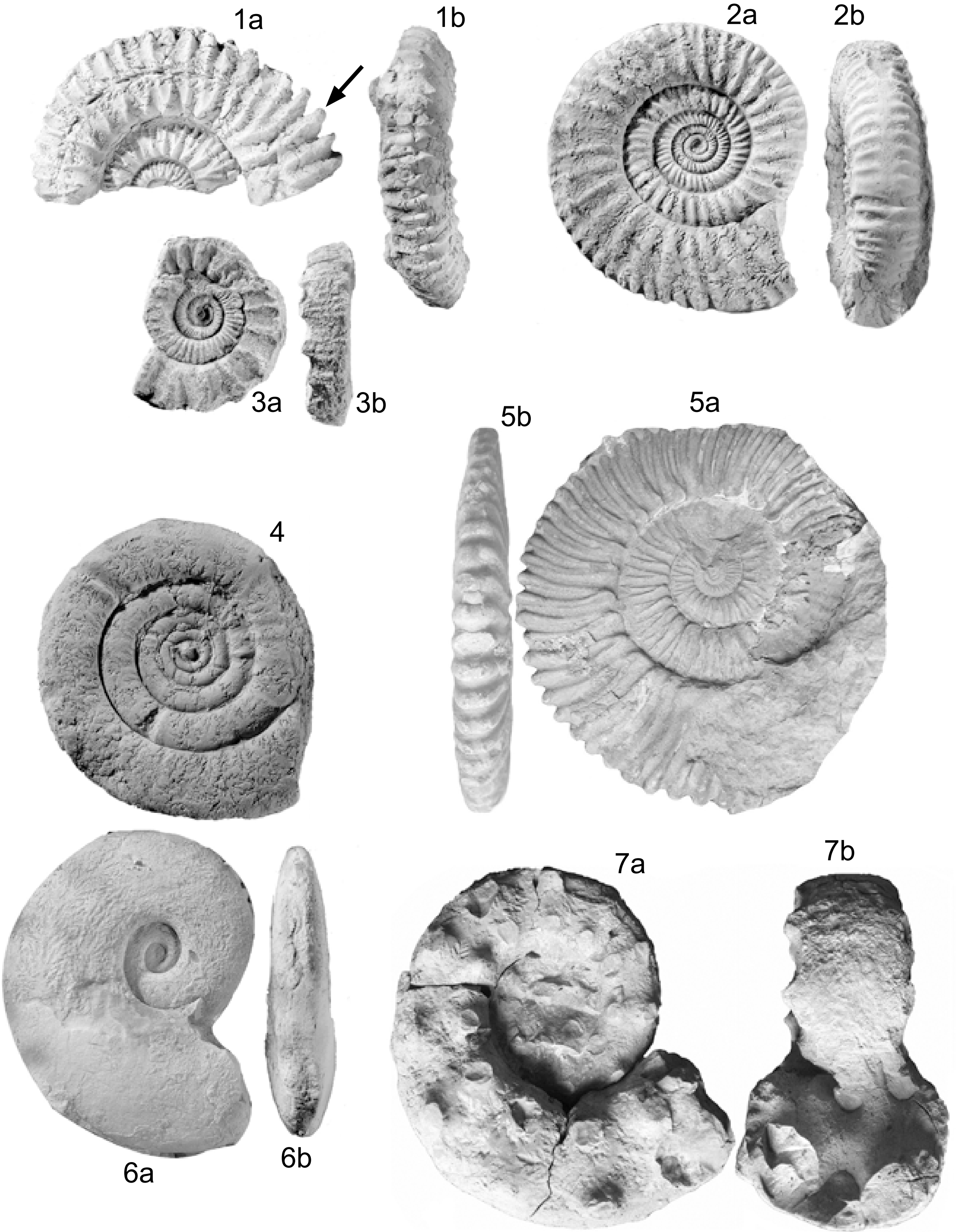
1a
1b
2a
2b
3a
3b
4
5a
5b
6a
6b
7a
7b

Upper Bathonian

Retrocostatum/Discus zones

North Iran: *Bullatimorphites* (*Bomburites*) aff. *suevicus* (Pl. 23, Fig. 3), *Cadomites bremeri* (Pl. 24, Fig. 4), etc.

Central Iran (Tabas area): *Prohecticoceras retrocostatum* (Pl. 19, Fig. 1), *P. haugi* (Pl. 17, Fig.9; Pl. 19, Fig. 3), *Alcidellus* aff. *tenuistriatus* (Pl. 19, Fig. 2), *Delecticeras delectum* (Pl. 11, Fig. 3), *Cadomites* (*Polyplectites*) *claromontanus* (Pl. 19, Fig. 4), *C.* (*Polyplectites*) *bozorgniai* (Pl. 19, Fig. 5), *C.* (*Polyplectites*) *tabasi* (Pl. 17, Fig. 3), *Treptoceras* aff. *uhligi* (Pl. 17, Fig. 4), *Choffatia* (*Subgrossouvria*) aff. *kranaiformis* (Pl. 18, Fig. 2), *Homoeoplanulites* (*Homoeoplanulites*) *rambertensis* (Pl. 17, Fig. 7), etc.

4.2.4 Callovian

Lower Callovian

Bullatus/Gracilis zones

North Iran: *Oxycerites* (*Paroxycerites*) *subdiscus* (Pl. 19, Fig. 8), *Bullatimorphites* (*Bomburites*) *microstoma* (Pl. 24, Fig. 5), *Macrocephalites* (*Tmetokephalites*) *verus* (Pl. 22, Fig. 1), *M.* (*Platystomaceras*) *pila* (Pl. 22, Fig. 2), *M.* (*Dolikephalites*) *hoyeri* (Pl. 22, Fig. 4), etc.

Central Iran: *Lissoceras voultense* (Pl. 25, Fig. 6), *Macrocephalites* (*Pleurocephalites*) sp. (Pl. 21, Fig. 3), *Choffatia euryptycha* (Pl. 19, Fig. 6), etc.

Middle Callovian

Anceps/Coronatum zones

North Iran: *Hecticoceras* (*Rossiesiceras*) gr. *metomphalum* (Pl. 14, Fig. 3; Pl. 23, Figs. 2, 5; Pl. 24, Fig. 7), *Hecticoceras* (*Lunuloceras*) *paulowi* (Pl. 14, Fig. 4), *H.* (*Lunuloceras*) *pseudopunctatum* (Pl. 26, Fig. 4). *Horioceras* sp. (Pl. 24, Fig. 12), *Reineckeia* (*Reineckeia*) gr. *stuebeli* (Pl. 23, Fig. 2), *R.* (*Reineckeia*) gr. *anceps* (Pl. 23, Fig. 3), *Alborzites binaludensis* (Pl. 14, Fig. 5; Pl. 24, Fig. 1), *Rehmannia* (*Loczyceras*) aff. *reissi* (Pl. 14, Fig. 9).

Central Iran: So far, no record.

Upper Callovian

Athleta/Lamberti zones

North Iran: *Quenstedtoceras* ex gr. *lamberti* (Pl. 26, Fig. 7), *Peltoceras* sp. ex gr. *athleta* (Pl. 26, Fig. 7), *P.* (*Peltoceras*) aff. *breckhemmeri* (Pl. 26, Fig. 3), *Binatisphinctes binatus* (Pl. 25, Fig. 2), etc.

Central Iran: So far, no record.

4.3 Upper Jurassic (Table 3)

4.3.1 Oxfordian

Lower Oxfordian

Mariae/Cordatum zones

North Iran: *Creniceras renggeri* (Pl. 26, Fig. 5), *Cardioceras* (*Scarburgiceras*) *praecordatum* (Pl. 26, Fig. 2), *Euaspidoceras* aff. *douvillei* (Pl. 24, Fig. 11), *Peltoceratoides* (*Parawedekindia*) aff. *arduennensis* (Pl. 25, Fig. 5), etc.

Central Iran: So far, no record.

Middle Oxfordian

Plicatilis/Transversariumzones

Plate 26 (Page 145): Upper Jurassic ammonites from North Iran. **(1, 6a, b)** *Phanerostephanus subsenex* Spath, 1950. Lower Tithonian, Chaman Bid Formation, Koppeh Dagh, northeast Iran (Majidifard 2003, p. 156, pl. 18, figs. 6, 8). **(2a, b)** *Cardioceras* (*Scarburgiceras*) *praecordatum* (Douville, 1912). Lower Oxfordian, Chaman Bid Formation, Tooy (Majidifard 2003, p. 106, pl. 6, fig. 3). **(3a, b)** *Mirosphinctes* aff. *niedzwiedzkii* (Siemiradzki, 1891). Lower–Midlle Oxfordian, Cordatum/Plicatilis Zone, Dalichai Formation, Central Alborz, North Iran (Seyed-Emami et al. 1995, p. 45, pl. 1, fig. 7). **(4a, b)** *Hecticoceras* (*Lunuloceras*) *pseudopunctatum* (Lahusen, 1883). ?Middle Callovian, Dalichai Formation, Central Alborz, North Iran (Seyed-Emami et al. 1995, p. 41, pl. 1, fig. 4). **(5a, b)** *Creniceras renggeri* (Oppel, 1863). Lower Oxfordian, Mariae Zone, Lar Formation, Central Alborz, North Iran (Seyed-Emami et al. 1995, p. 42, pl. 1, fig. 9). **(7a, b)** *Quenstedtoceras* ex gr. *lamberti* (Sowerby, 1821). Upper Callovian, Lamberti Zone, Dalichai Formation, Central Alborz, North Iran (Seyed-Emami et al. 1995, p. 43, pl. 1, fig. 1).

Plate 27 (Page 146): Ammonites from the Upper Jurassic Lar Formation, Jajarm, eastern Alborz, north Iran. **(1a, b)** *Euaspidoceras* sp. Upper Oxfordan, Bimammatum Zone (Seyed-Emami & Schairer 2010, p. 277, fig. 7d). **(2)** *Taramelliceras* (*Taramelliceras*) *costatum* (Quenstedt, 1849). Upper Oxfordan, Bimammatum Zone (Seyed-Emami & Schairer 2010, p. 271, fig. 6d). **(3a–c, 5)** *Epipeltoceras bimammatum* (Quenstedt, 1857). Upper Oxfordan, Bimammatum Zone (Seyed-Emami & Schairer 2010, p. 277, fig. 7a1–a3; 7b). **(4)** *Orthosphinctes* sp. Upper Oxfordan, Bimammatum Zone (Seyed-Emami & Schairer 2010, p. 275, fig. 8a). **(6)** *Ochetoceras* aff. *marantianum* (d'Orbigny, 1850). Upper Oxfordan, Bimammatum Zone (Seyed-Emami & Schairer 2010, p. 273, fig. 6g). **(7)** *Orthosphinctes* aff. *tiziani* (Oppel, 1863). Upper Oxfordan, Bimammatum Zone (Seyed-Emami & Schairer 2010, p. 273, fig. 8e).

Plate 28 (Page 147): Ammonites from the Qal'eh Dokhtar and Korond formations, eastern Tabas Block, East-Central Iran. **(1, 7)** *Passendorfia* (*Enayites*) sp. Middle Oxfordian, Transversarium Zone, Qal'eh Dokhtar Formation, east of Korond, northeast Tabas (Schairer et al. 2000, p. 205, fig. 8 (7, 9)). **(2)** *Sowerbyceras loryi* (Munier-Chalmas in Hébert, 1875). Lower Kimmeridgian, Herbichi Zone, Korond Formation, northeast Tabas (Schairer et al. 2003, p. 214, fig. 11(1)). **(3, 6)** *Idoceras* sp. Lower Kimmerigdian, Korond Formation, northeast Tabas (Schairer et al. 2003, p. 218, fig. 11(5, 20)). **(4a–c)** *Gregoryceras* (*Gregoryceras*) cf. *fouquei* (Kilian, 1889). Middle–Upper Oxfordian, Qal'eh Dokhtar Formation, east of Korond, northeast Tabas (Schairer et al. 2000, p. 209, fig. 8(3–5)). **(5)** *Orthosphinctes* aff. *laufensis* (Siemiradzki, 1898). Middle–Upper Oxfordian, Qal'eh Dokhtar Formation, south of Korond, northeast Tabas (Schairer et al. 2003, p. 211, fig. 9(8)). **(7)** *Subdiscosphinctes* (*Subdiscosphinctes*) sp. Middle Oxfordian, Transversarium Zone, Qal'eh Dokhtar Formation, east of Korond, northeast Tabas (Schairer et al. 2003, p. 209, fig. 8(9)). **(8)** *Subdiscosphinctes* (*Subdiscosphinctes*) cf. *kreutzi* (Siemiradzki, 1891). Middle Oxfordian, Transversarium Zone, Qal'eh Dokhtar Formation, east of Korond, northeast Tabas (Schairer et al. 2003, p. 209, fig. 8(12)). **(9)** *Perisphinctes* (*Dichotomoshinctes*) aff. *marnesiae* (de Loriol, 1903). Middle Oxfordian, Transversarium Zone, Qal'eh Dokhtar Formation, east of Korond, northeast Tabas (Schairer et al. 2003, p. 207, fig. 9(1)). **(10)** *Sequeirosia* (*Gemmelarites*) cf. *trichoploca* (Gemmellaro, 1875). Middle Oxfordian, Transversarium Zone, Qal'eh Dokhtar Formation, east of Korond, northeast Tabas (Schairer et al. 2003, p. 207, fig. 8(6)).

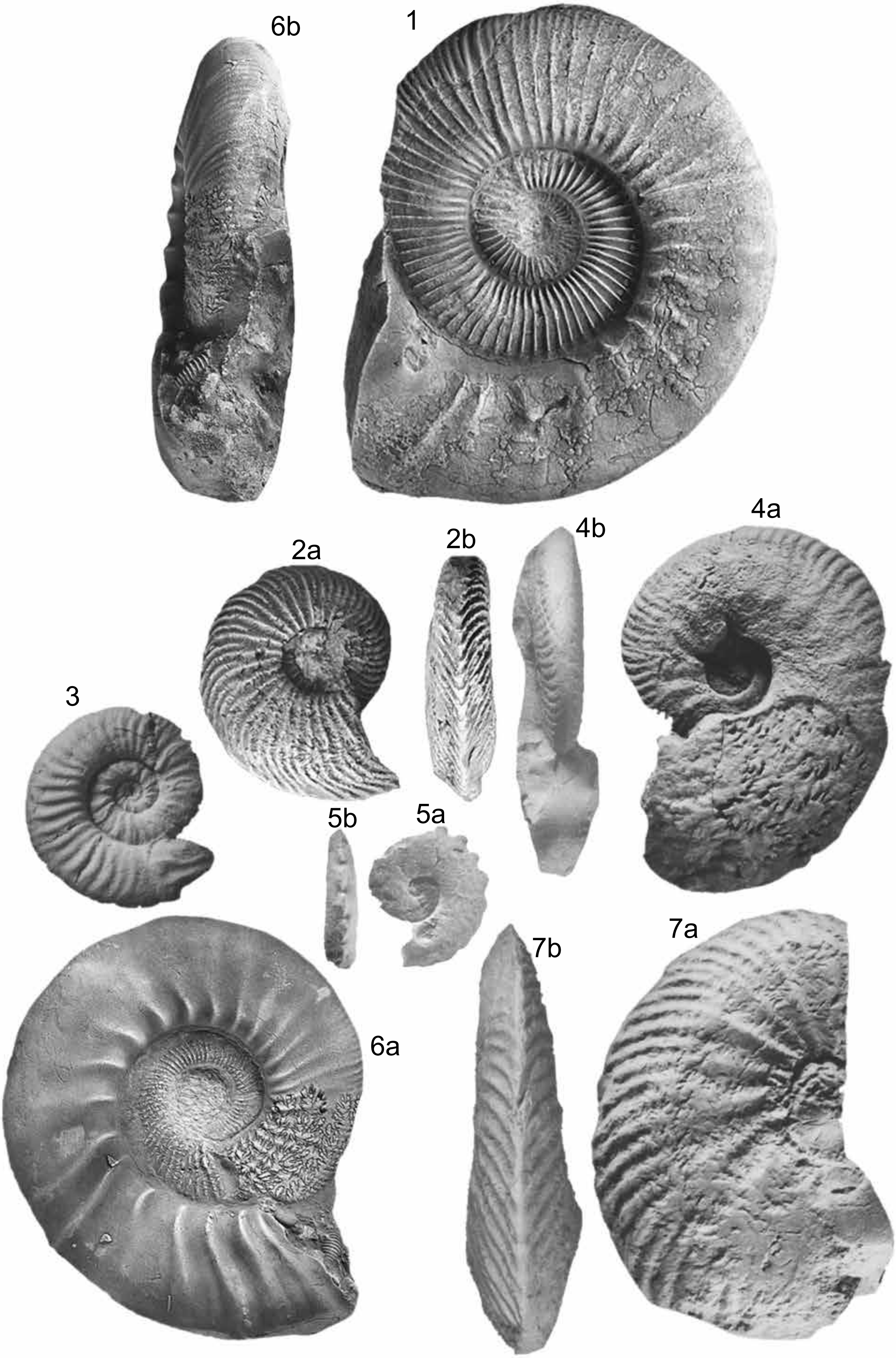
6b
1
2a
2b
4b
4a
3
5b
5a
7b
7a
6a

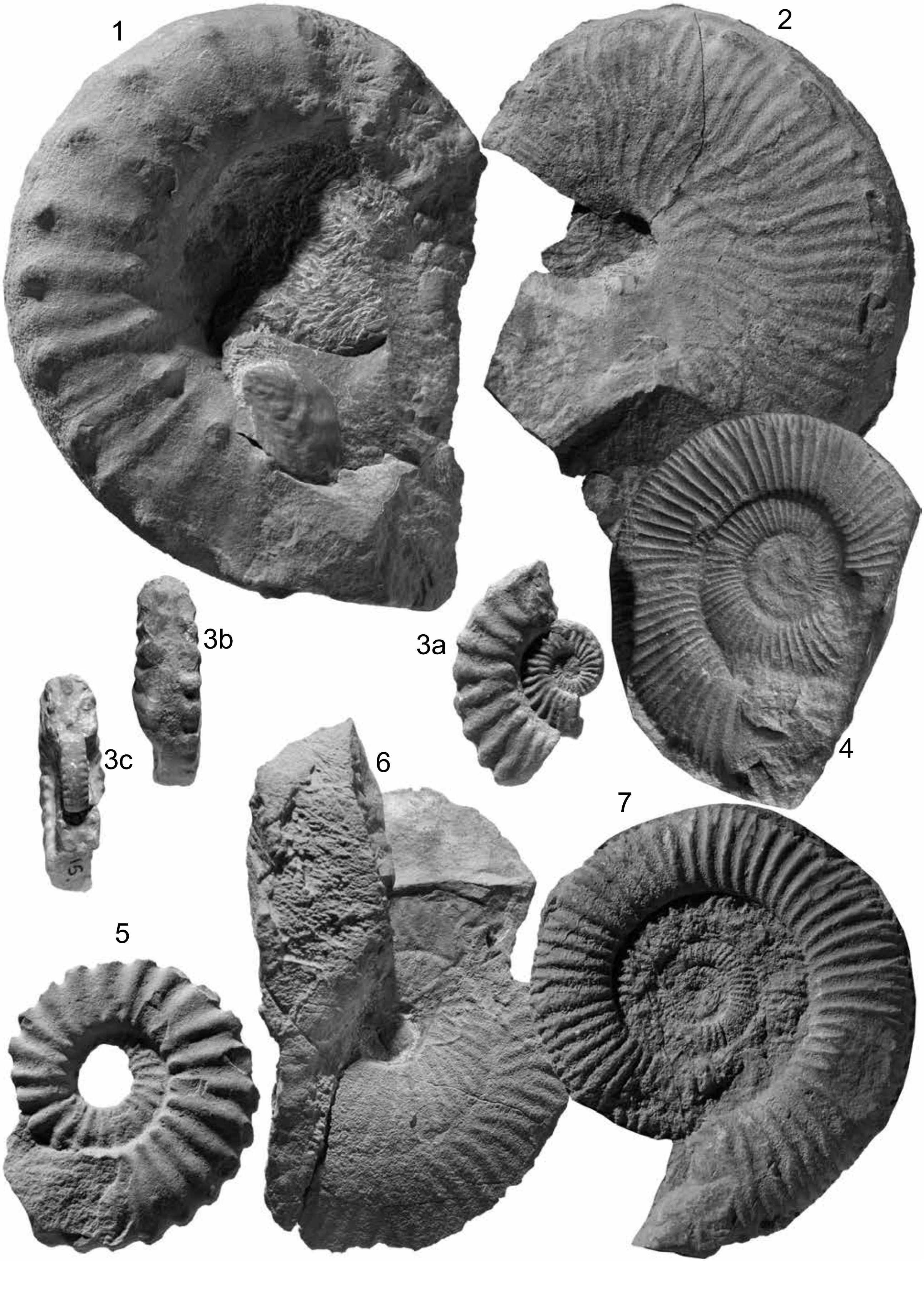
1
2
3b
3a
3c
4
6
7
5

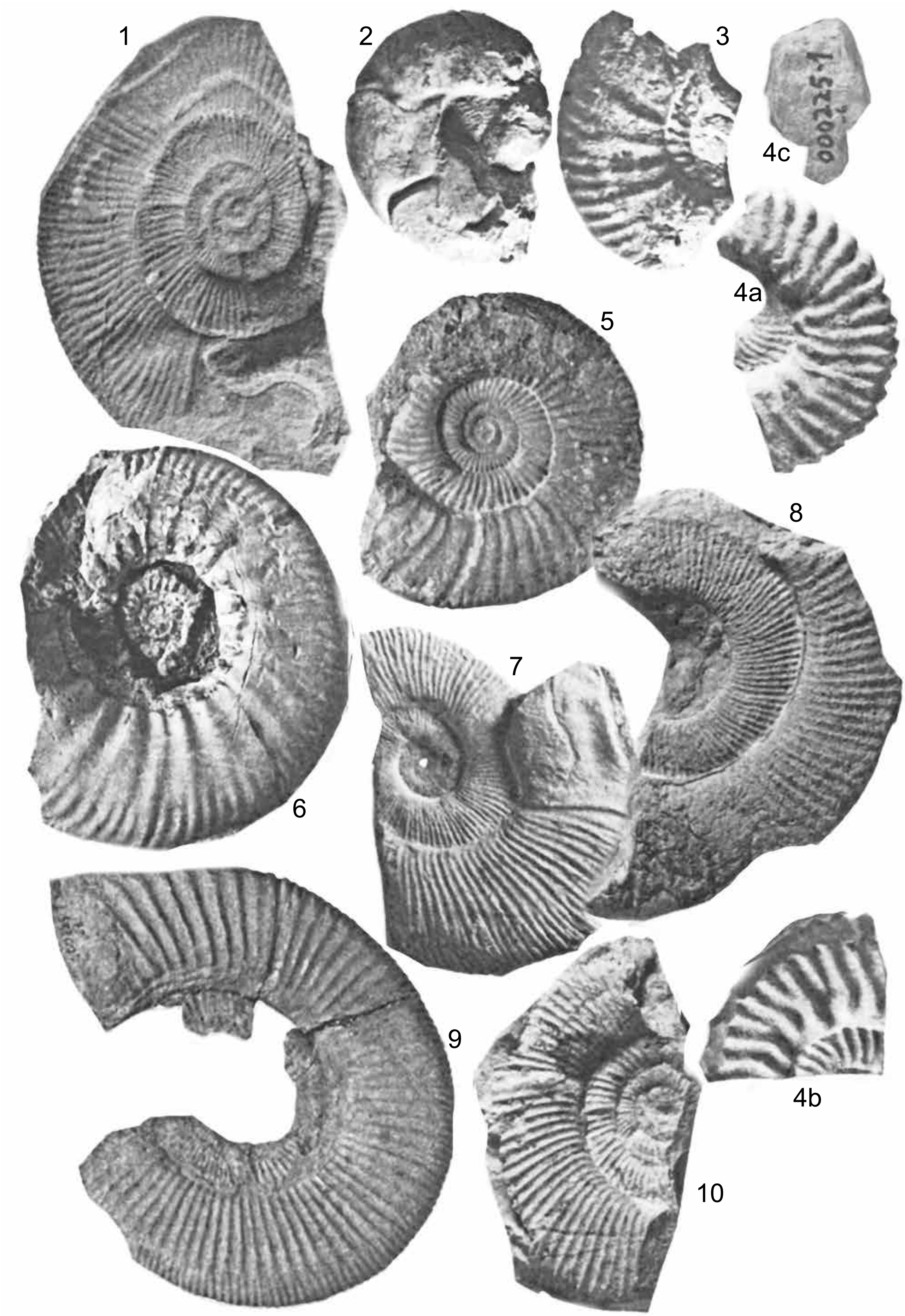
1
2
3
4c
4a
5
8
7
6
9
4b
10

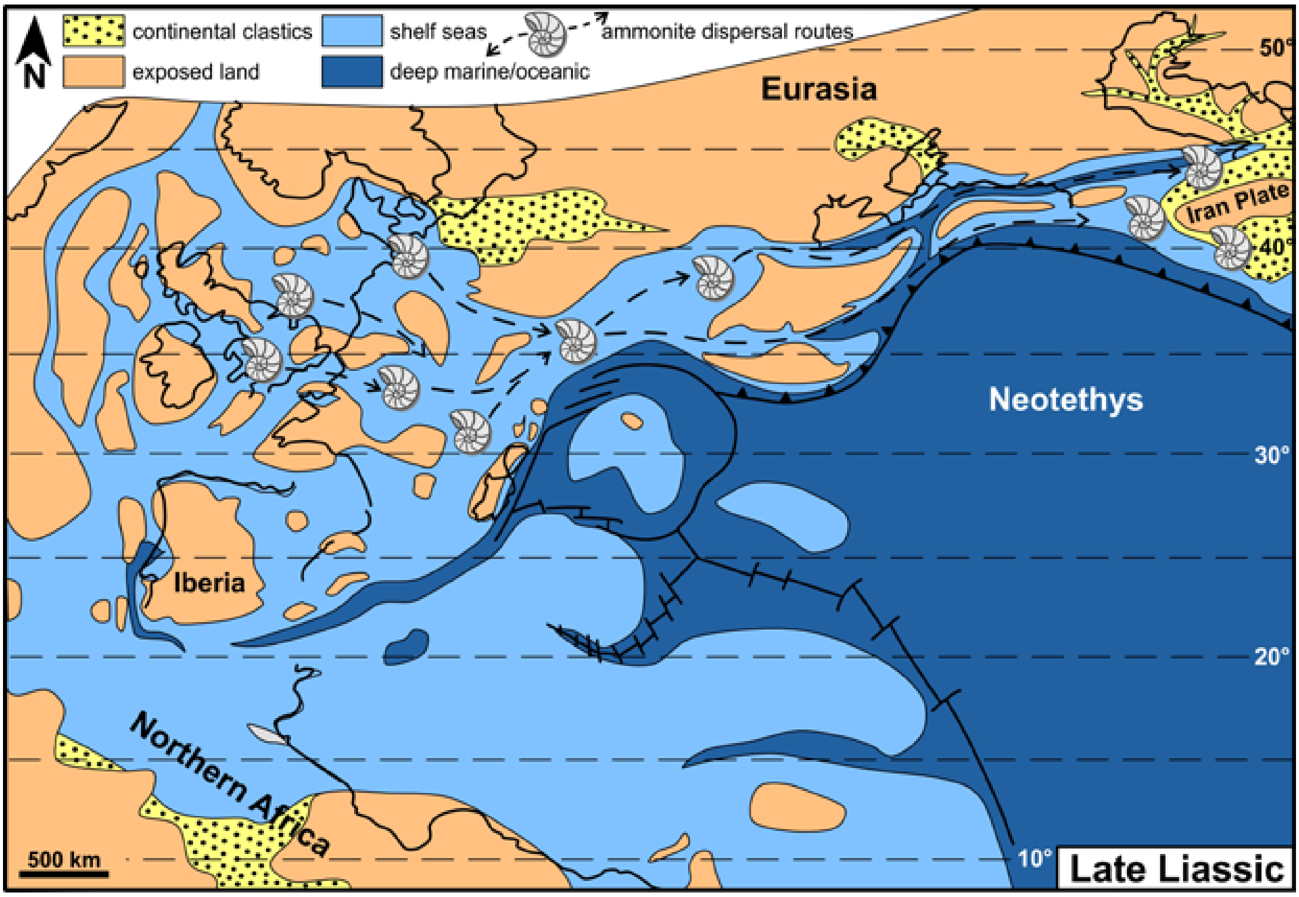

Figure 9: Late Early Jurassic palaeogeographic map of the western Tethys showing the inferred ammonite dispersal routes between Europe and Iran (modified after Seyed-Emami et al. 2008, base map revised from Dercourt et al. 2000).

Table 3. Northwest European standard ammonite biozones for the Upper Jurassic Series and their documentation in northern (NI) and Central Iran (CI).

Series	Stage	Biozone	NI	CI
UPPER JURASSIC	Tithonian	Durangites		
		Microcanthum		
		Ponti		
		Fallauxi	x	
		Semiforme		
		Darwini		
		Hybonotum		
	Kimmeridgian	Beckeri		?
		Cavouri		
		Acanthicum		x
		Divisum/Herbichi	x	
		Strombecki/Hypseocyclum		
		Platynota	x	x
	Oxfordian	Planulata	x	
		Bimmamatum	x	x
		Bifurcatus	?	
		Transversarium	?	x
		Plicatilis	?	
		Cordatum	x	
		Mariae	x	

North Iran: So far, no record.

Central Iran: *Orthosphinctes* aff. *laufensis* (Pl. 28, Fig. 5), *Subdiscosphinctes* (*Subdiscosphinctes*) cf. *kreutzi* (Pl. 28, Fig. 8), *Perisphinctes* (*Dichotomosphinctes*) aff. *marnesiae* (Pl. 28, Fig. 9), *Sequeirosia* (*Gemmelarites*) cf. *trichoploca* (Pl. 28, Fig. 10), etc.

Upper Oxfordian

Bifurcatus/Bimammatum/Planula zones

North Iran: *Ochetoceras* aff. *marantianum* (Pl. 27, Fig. 6), *Ochetoceras* (*Granulochetoceras*) *cristatum* (Pl. 24, Fig. 1), *Lingulaticeras nudatum* (Pl. 24, Fig. 2), *Taramelliceras* (*Taramelliceras*) *costatum* (Pl. 24, Fig. 4), *T.* (*Taramelliceras*) *costatum* (Pl. 27, Fig. 2), *T.* (*Strebliticeras*) *externnodatum* (Pl. 24, Fig. 9), *Epipeltoceras bimammatum* (Pl. 27, Figs. 3, 5), *Euaspidoceras* sp. (Pl. 27, Fig. 1; Pl. 30, Fig. 1), *Orthosphinctes* (*Orthosphinctes*) cf. *polygyratus* (Pl. 30, Fig. 2), *O.* (*Pseudorthosphinctes*) aff. *suevicus* (Pl. 30, Fig. 3), *O.* aff. *tiziani* (Pl. 27, Fig. 7), *Mirosphinctes* aff. *niedzwiedzkii* (Pl. 26, Fig. 3), *Passendorfia* (*Enayites*) *rozaki* (Pl. 25. Fig. 4), etc.

Central Iran: *Gregoryceras* (*Gregoryceras*) cf. *fouquei* (Pl. 28, Fig. 4), *Passendorfia* (*Enayites*) sp. (Pl. 28, Figs. 1, 7), *Subnebrodites* cf. *proteron* (Pl. 29, Fig. 4), *Orthosphinctes* (*Orthosphinctes*) *tiziani* (Pl. 29, Fig. 5).

4.3.2 Kimmeridgian

Lower Kimmeridgian

Platynota/Strombecki zones

North Iran: *Orthosphinctes* (*Ardescia*) aff. *schaireri* (Pl. 24, Fig. 6).

Central Iran: *Sowerbyceras loryi* (Pl. 28, Fig. 2), *Idoceras* sp. (Pl. 28, Figs. 3, 6), *Orthosphinctes* (*Ardescia*) sp. (Pl. 29, Fig. 1), *Benacoceras* sp. (Pl. 29, Fig. 2).

Middle Kimmeridgian
Divisum/Acanthicum
Norh Iran: *Taramelliceras* (*Taramelliceras*) cf. *trachinotum* (Pl. 24, Fig. 5), *Sutneria eumela* (Pl. 24, Fig. 3).
Central Iran: *Physodoceras insulatum* (Pl. 29, Fig. 3).

Upper Kimmeridgian
Not yet proved in North or Central Iran.

4.3.3 Tithonian

Lower/Middle Tithonian
North Iran: *Phanerostephanus subsenex* (Pl. 26, Figs. 1, 6), *Richterella richteri* (Pl. 30, Figs. 4–6), *Sublithacoceras* sp. (Pl. 30, Fig. 7).
Central Iran: So far, no record.
Upper Tithonian
The Upper Tithonian Substage in the northern Alborz has been documented by microfauna. In the northwestern Alborz (Talesh area), besides Tithonian calpionellids (Benzaggagh et al. 2012), also ammonites (Himalayitinae, Berriasellinae etc.) occur (Seyed-Emami 1971).
Central Iran: So far, no record.

5 Jurassic-Cretaceous boundary

The Jurassic–Cretaceous boundary within the Iran Plate is marked by a long-ranging hiatus caused by the Late Cimmerian tectonic movements. Near the boundary, the occurrence of red siliciclastic sediments with evaporates and volcanic rocks indicates the beginning of the Late Cimmerian tectonic movements, which persist into the Early Cretaceous. Locally in the central Alborz Mountains, there is a succession of red siliciclastic sediments intermingled with gypsum and basic volcanic rocks (“Gypsum and Melaphyr” Formation of Steiger 1966). Towards the northeast, in the Koppeh Dagh Basin, the red, siliciclastic-gypsiferous sediments attain a great thickness, up to 1000 m and more (Shurijeh Formation; Afshar-Harb 1994). As shown above, red siliciclastic-gypsiferous formations are also widely distributed across the Tabas Block in East- Central Iran.

In the northern Alborz Mountains, contrary to the former regions, the Jurassic–Cretaceous boundary is mostly continuous. The most complete continuous marine section, with nannoconids, calpionellids, and ammonites exists in the Talesh area in the northwestern Alborz Mountains (Davies et al. 1972; Seyed-Emami 1975; Benzaggagh et al. 2012).

6 Palaeogeography and palaeobiogeography

The ammonite fauna of the Jurassic Ab-e-Haji Subgroup (Lower to lower Middle Jurassic) is closely related, even at the species level, to northwestern European (Subboreal) ammonite faunas, allowing a similar biozonation. Remarkable is the low percentage of Phylloceratidae (<1%) and the total absence of Lytoceratidae.

Of special palaeobiogeographic importance is the presence of Amaltheidae (Pourmotamed & Motamed 1976; Nabavi & Seyed-Emami 1977; Seyed-Emami et al. 2008), a strictly Boreal group (Smith et al. 2001). A Boreal influence of the ammonite fauna is again indicated during the “Middle” Cretaceous (Albian and Cenomanian stages) in some parts of North and Central Iran (Koppeh Dagh and Yazd Block) by the presence of Leymeriellidae, Hoplitidae, and Schloenbachiidae (e.g., Seyed-Emami 1988b; Immel et al. 1997; Mosavinia et al. 2014; Seyed-Emami & Wilmsen 2016). The faunal migration route during the Early and early Middle Jurassic followed probably the epicontinental platforms at the southern margin of the Eurasian landmass (Fig. 9).

Following the Mid-Cimmerian Tectonic Event around the Early/Late Bajocian boundary and the subsequent Late Bajocian transgression, there is an abrupt change from siliciclastic sediments of the Shemshak Group (Ab-e-Haji Subgroup) to marls and limestones of deeper marine environments (Dalichai and Lar formations in the Alborz, also documented in

Plate 29 (Page 150): Ammonites from the Esfandiar and Korond formations, eastern Tabas Block, East-Central Iran. **(1)** *Orthosphinctes* (*Ardescia*) sp. Lower Kimmeridgian, Korond Formation, west of Qassem-Abad, northeast Tabas (Schairer et al. 2003, p. 217, fig. 13(2)). **(2)** *Benacoceras* sp. Lower Kimmeridgian, top of Esfandiar Formation, south of Korond, northeast Tabas (Schairer et al. 2003, p. 213, fig. 10(7)). **(3a, b)** *Physodoceras insulatum* (Gemmellaro, 1875). Upper Korond Formation, west of Qassem-Abad, northeast Tabas (Schairer et al. 2003, p. 215, fig. 12). **(4a, b)** *Subnebrodites* cf. *proteron* Nitzopoulos, 1974. Upper Oxfordian, upper Esfandiar Formation, south of Korond, northeast Tabas (Schairer et al. 2003, p. 212, fig. 10(5, 6)). **(5)** *Orthosphinctes* (*Orthosphinctes*) *tiziani* (Oppel, 1863). Upper Oxfordian, Bimammatum Zone, top of Esfandiar Formation, south of Korond, northeast Tabas (Schairer et al. 2003, p. 210, fig. 10(1)).

Plate 30 (Page 151): Upper Jurassic ammonites from the Lar and Chaman Bid formations, North Iran. **(1)** *Euaspidoceras* sp. Upper Oxfordian, ?Bimammatum Zone, Lar Formation, Kuhe-Sharaf, northeast Semnan, east Alborz (not yet published). **(2)** *Orthosphinctes* (*Orthosphinctes*) cf. *polygyratus* (Reinecke, 1818). Upper Oxfordian, ?Bimammatum Zone, Lar Formation, Kuhe-Sharaf, northeast Semnan, east Alborz (not yet published). **(3)** *Orthosphinctes* (*Pseudorthosphinctes*) aff. *suevicus* (Siemiradzki, 1898). Upper Oxfordian, Bimammatum Zone, Lar Formation, Kuhe-Sharaf, northeast Semnan, east Alborz (not yet published). **(4–6)** *Richterella richteri* (Oppel, 1865). Middle Tithonian, Fallauxi Zone, Chaman Bid Formation, Kuhe-Kurkhud, north Bash-Kalateh, Koppeh Dagh, northeast Iran (Schairer et al. 1999, p. 27, pl. 2, figs. 3–5). **(7)** *Sublithacoceras* sp. Lower Tithonian, Fallauxi Zone, Chaman Bid Formation, Kuhe-Kurkhud, north Bash-Kalateh, Koppeh Dagh, northeast Iran (Schairer et al. 1999, p. 27, pl. 2, fig. 1).

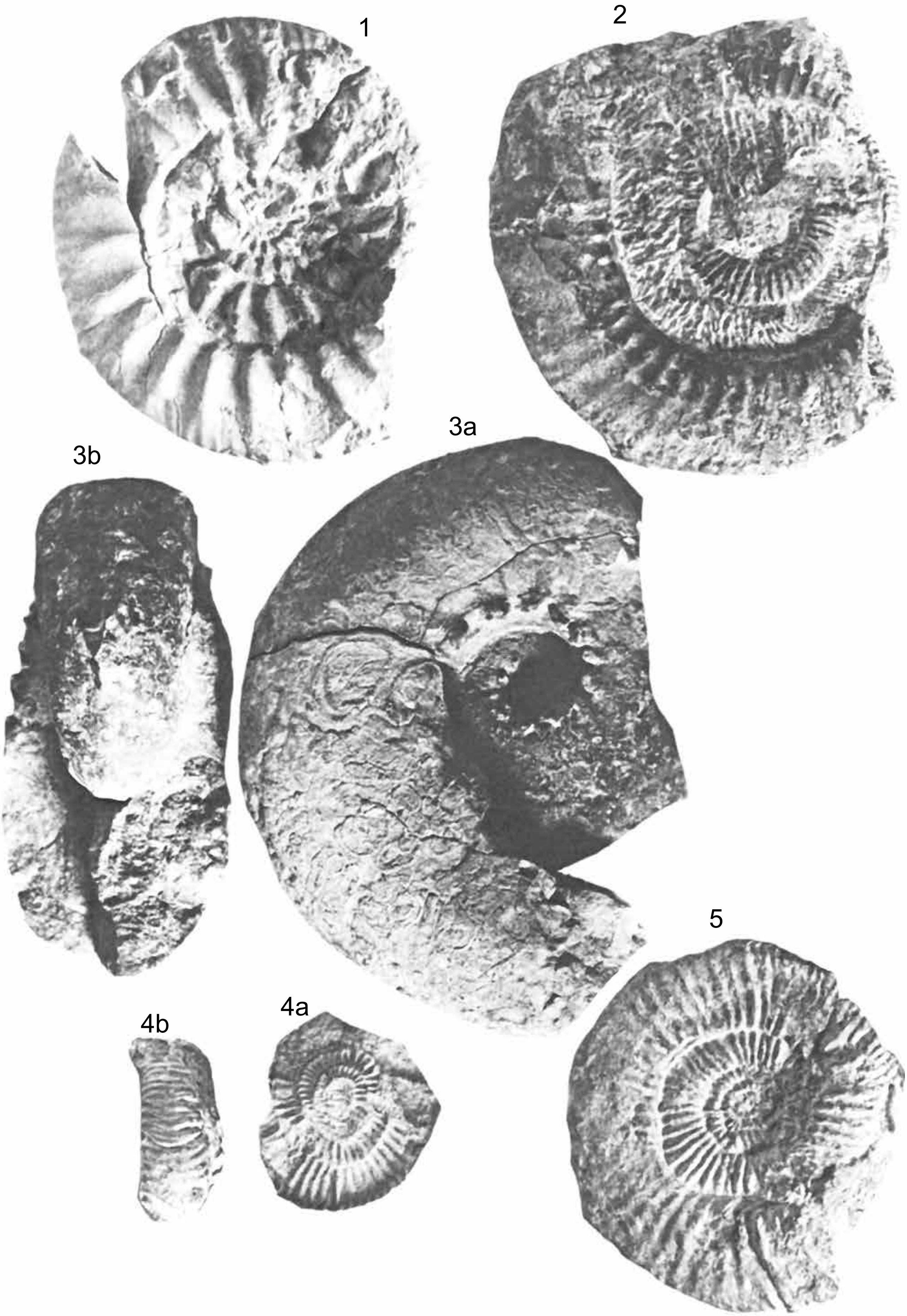
1
2
3a
3b
4a
4b
5

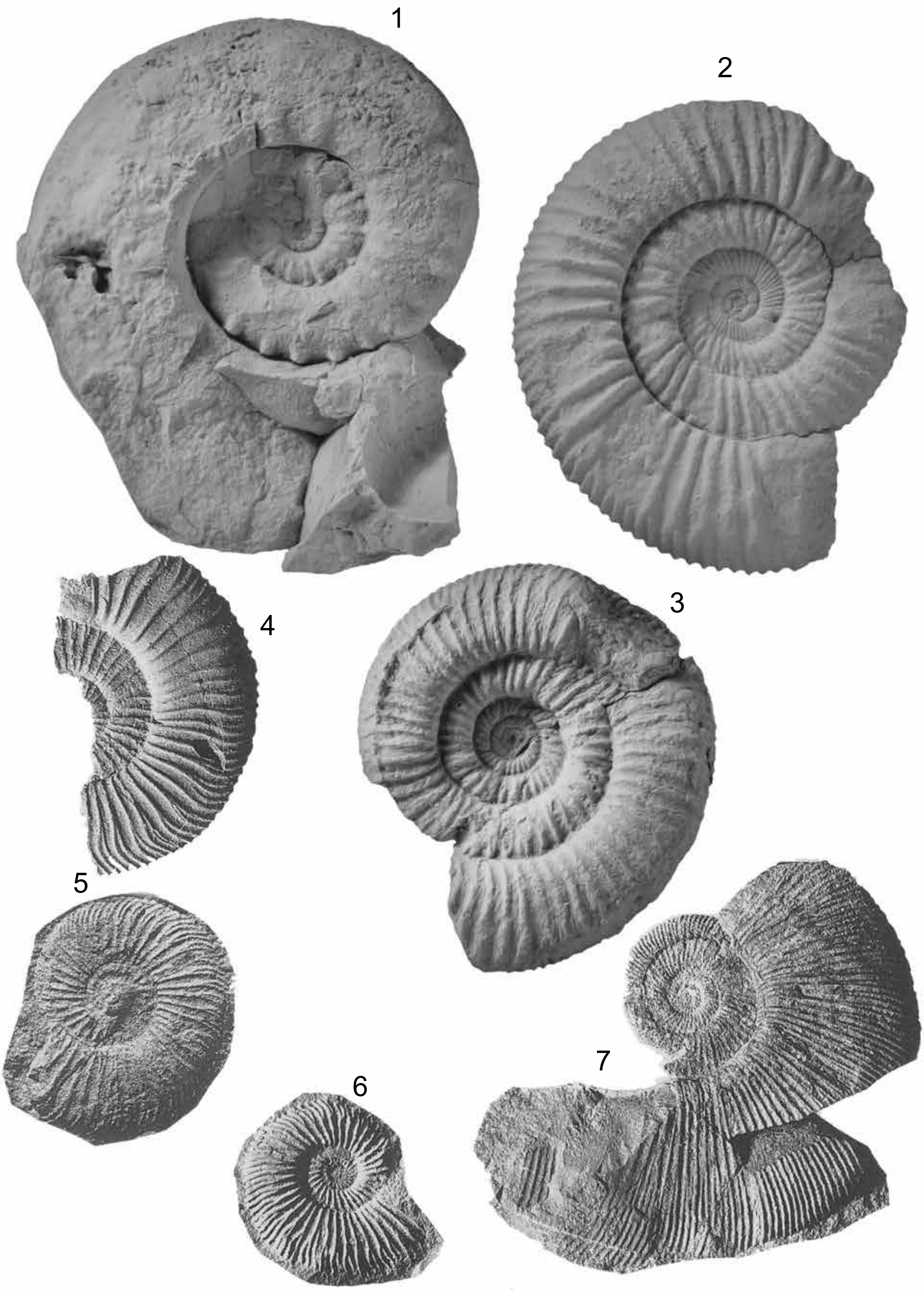
1
2
4
3
5
7
6

the Parvadeh and Baghamshah formations in East-Central Iran). Hand in hand with this change, there is a noticeable shifts in faunal composition, and the Tethyan (Mediterranean) influence on the ammonite faunas becomes much stronger (Seyed-Emami et al. 2001; Seyed-Emami & Schairer 2010, 2011a, b). This indicates significant environmental and palaeogeographic changes such as variations in bathymetry and temperature, the opening of new migration routes, and shifts in the palaeogeographic position. Consequently, palaeogeographic reconstructions for the Early Jurassic place the Iran Plate at a latitude of about N 45° (Fig. 9), but throughout the Middle and Late Jurassic, the Iran Plate shifted southward to a position about N 30° (Dercourt et al. 2000; Barrier & Vrielynck 2008; Mattei et al. 2015) (Fig. 1a).

The Middle and Late Jurassic ammonite faunas of North and Central Iran are closely related to those of epicontinental seas bordering the northern margin of the western Tethys and occupy a position intermediate between the Mediterranean and Submediterranean Faunal Province (Cariou et al. 1997; Page 2008), although some Subboreal elements may also be present. Typical Boreal ammonites, such as Cardioceratidae, are nearly absent. However, the north Iranian ammonite fauna differs from that of the Submediterranean and Subboreal provinces by their high percentage of Phylloceratidae, occasionally totaling up to 50% of the fauna. In this respect, the fauna exhibits closer affinities to the Mediterranean Province (Seyed-Emami & Schairer 2010, 2011a, b). Commonly, Perisphinctidae and Phylloceratidae account for more than 80% of the ammonite fauna. In contrast to Mediterranean ammonite faunas, Lytoceratidae are, except at a few levels, extremely rare in Middle and Upper Jurassic strata of North and Central Iran (Seyed-Emami & Schairer 2010). According to Page (2008, p. 40), “Lytoceratina have very similar distribution patterns to those of Phylloceratina, the two groups commonly associated in deeper-water facies. There is, however, some suggestion that latitudinal controls may have been more important for the Lytoceratina, as high-latitude records seem to be less common than for the Phylloceratina, and Lytoceratina are typically only abundant in low-latitude Tethyan faunas”.

The close palaeobiogeographic relationship of the North and Central Iranian ammonite faunas with those of Northwestern Europe and the northwestern Tethys during the Jurassic and Cretaceous periods indicate the existence of direct marine connections and episodic faunal exchange between the two areas (Seyed-Emami 1988a). Remarkably, there is no or little faunal relationship with Southwest Iran (Zagros) and the southern Tethys throughout the Jurassic Period, suggesting that wide and deep oceanic areas in fact formed physical barriers for ammonite dispersal.

7 Conclusions

The Jurassic System in North and Central Iran (Iran Plate) is represented by a very thick sedimentary succession representing two tectono-stratigraphic megacycles, bounded by three important unconformities produced by the Main-, Mid- and Late Cimmerian tectonic events. The older cycle starts after the Late Triassic closure of the Palaeotethys and the collision of the Iran Plate with the southern margin of Eurasia (Turan Plate) with an abrupt uplift of the Cimmerian Mountains around the Triassic–Jurassic boundary (Main-Cimmerian Event). The important Mid-Cimmerian Tectonic Event around the Early/Late Bajocian terminates this older tectono-stratigraphic cycle, the sediments of which are accommodated in the Ab-e-Haji Subgroup of the (upper) Shemshak Group. The Ab-e-Haji Subgroup consists largely of thick, partly coal-bearing siliciclastic strata and also records some important marine ingressions, especially during the Toarcian and Aalenian ages.

The younger tectono-stratigraphic cycle begins with an extensive marine transgression in the Late Bajocian and ends around the Jurassic-Cretaceous boundary with the Late Cimmerian Tectonic Event. After the Mid-Cimmerian Tectonic Event, the Iran Plate became fragmented into several structural units, the geological histories of which differed and so did their facies patterns. Thus, in North Iran two main sedimentary areas developed, namely the Alborz and Koppeh Dagh (Kopet Dagh) basins, which show some, but not very strong, differences with respect to lithology and thickness. Differences are much more pronounced on the Central-East Iranian Microcontinent (CEIM), which comprises three N–S-oriented and differently acting structural units (blocks). These are from east to west the Lut, Tabas and Yazd blocks. During the Jurassic Period, the sea mostly covered the Tabas and Lut blocks, whereas the Yazd Block remained largely emergent.

Palaeobiogeographic studies of the ammonite faunas of North and Central Iran show that they are closely related to the Northwest European (Subboreal) ammonite faunas in the Early to Early Middle Jurassic, allowing a similar biozonation. Remarkable is the scarcity of Phylloceratidae (less than one per cent) and the total absence of Lytoceratidae. After the Late Bajocian transgression, there is an abrupt change in faunal composition, and the Tethyan (Mediterranean) influence on the ammonite faunas becomes much stronger. The Middle and Late Jurassic ammonite faunas of North and Central Iran are closely related to those of epicontinental seas bordering the northern margin of the western Tethys and occupy an intermediate position between the Mediterranean and Submediterranean Province, although some Subboreal elements may also be present. Typical Boreal ammonites, such as Cardioceratidae, are nearly absent. The results of the studies on ammonoid palaeobiogeography are in line with reconstructions of the Early

Jurassic palaeogeography that place the Iran Plate at a fairly high palaeo-latitude of about 45°N, followed by a rapid southward shift throughout the Middle and Late Jurassic to a position of about 30°N.

Acknowledgements

KSE expresses deep thanks to Prof. Dr. G. Wörheide and B. Schellenberger (both SNSB-BSPG Munich) for providing research facilities and technical support. He also acknowledges a Research Fellowship granted by the Alexander-von-Humboldt-Stiftung. Furthermore, we are indebted to the Geological Survey of Iran for continuous logistic support. A National Geographic project (grant 5888-97), the Middle East Basin Evolution (MEBE) Programme and the German Research Foundation (DFG, grant FU 131/32) provided additional financial funding. Edition-inchief Prof. Dr. M. Krings (SNSB-BSPG Munich), is thanked for the professionel editorial handlind.

8 References

Afshar-Harb A. 1994. Geology of the Kopet Dagh. Treatise on the Geology of Iran 11, 1–275 5. [in Farsi]

Aghaei A, Mahboudi A, Moussavi-Harami R, Heubeck C, Nadjafi M. 2013. Facies interpretation and sequence stratigraphy of Upper Jurassic carbonates in the Eastern Alborz Range and Binalud Mountains, NE Iran. Facies 59, 863–889.

Aghaei A, Zand-Moghadam H, Moussavi-Harami R, Mahboudi A. 2019. Sequence stratigraphic analysis and sea-level history of the Upper Jurassic deposits (Mozduran Formation), south of Aghdarband, NE Iran. Historical Biology 31, 1097–1114.

Aghanabati SA. 1977. Étude géologique de la région de Kalmard (W. Tabas). Geological Survey Iran Report 35, 1–230.

Aghanabati SA. 1996. Introducing Parvadeh Formation. Geosciences Scientific Quarterly –Journal of the Geological Survey of Iran 5(19), 2–13. [in Farsi]

Aghanabati SA. 1998. Jurassic Stratigraphy of Iran, vols 1 and 2. Geological Survey of Iran, Tehran, 726 p. [in Farsi]

Assereto R. 1966a. The Jurassic Shemshak Formation in Central Elburz (Iran). Rivista Italiana di Paleontologia e Stratigrafia 72(4), 1133–1182.

Assereto R. 1966b. Geological map of upper Djajerud and Lar Valleys (Central Elburz, Iran), scale 1: 50 000, with explanatory notes. Instituto di Geologia dell'Universita di Milano, Serie G 232, 1–86.

Assereto R, Barnard PDW, Fantini-Sestini N. 1968. Jurassic stratigraphy of the Central Elburz (Iran). Rivista Italiana di Paleontologia e Stratigrafia 74(1), 3–21.

Barrier E, Vrielynck B. (eds) 2008. Palaeotectonic maps of the Middle East – Tectono-sedimentary-palinspastic maps from the Late Norian to Pliocene. Commission for the Geological Map of the World (CGMW/CCGM), Paris.

Benzaggagh M, Fabrizio C, Schnyder J, Seyed-Emami K, Majidifard MR. 2012. Calpionellids and pelagic microfaunas of Upper Jurassic–Lower Cretaceous Shal and Kolur formations (Talesh Mountains, Alborz Chain, North-West Iran). Stratigraphic distribution, new species, systematic revision and regional comparisons. Annales de Paléontologie 98, 253–301.

Brunet M-F, Korotaev MV, Ershov AV, Nikishin AM. 2003. The South Caspian Basin: a review of its evolution from subsidence modelling. Sedimentary Geology 156, 119–148.

Cariou E, Enay R, Hantzpergue P, Rioult M. 1997. Oxfordian. In: E Cariou, P. Hantzpergue (Eds), Biostratigraphie du Jurassique oust-Européen et Méditerranéen. Bulletin du Centre de Recherches Elf Exploration et Production, Mémoires 17, 79–86.

Davies RG, Jones CR, Hamzepour B, Clark GC. 1972. Geology of the Masuleh sheet, 1:100000, NW Iran. Geological Survey of Iran Report 24, 1–110.

Dercourt J, Gaetani M, Vrielynck B, Barrier E, Biju-Duval B, Brunet M-F, Cadet J, Crasquin S, Sandulescu M. (Eds) 2000. Atlas Peri-Tethys palaeogeographical maps. CCGM/CGMW, Paris, 24 maps and explanatory notes: i–xx, 269 p.

Dietze V, Seyed-Emami K, Raoufian A. 2014. *Morphoceras* Douvillé, 1880 and *Ebrayiceras* Buckman, 1920 from the Dalichai Formation (Lower Bathonian) North and Northeast of Damghan (Northeast Alborz, Iran). Zitteliana A54, 15–22.

Eftekharnezhad J, Behroozi A. 1991.Geodynamic significance of recent discoveries of ophiolites in Late Paleozoic rocks in NE Iran (including Kopet Dagh). Abhandlungen der geologischen Bundesanstalt 38, 89–100.

Fantini-Sestini N, Assereto R. 1970. The Lar Limestone and its ammonite fauna (Upper Oxfordian–Lower Kimmeridgian). Rivista Italiana di Paleontologia e Stratigrafia 76(2), 199–232.

Fürsich FT, Wilmsen M, Seyed-Emami K, Majidifard MR. 2003a: Evidence of synsedimentary tectonics in the northern Tabas Block, East-Central Iran: The Callovian (Middle Jurassic) Sikhor Formation. Facies 48, 151–170.

Fürsich FT, Wilmsen M, Seyed-Emami K, Schairer G, Majidifard MR. 2003b. Platform-Basin Transect of a Middle to Late Jurassic Large-Scale Carbonate Platform System (Shotori Mountains, Tabas Area, East-Central Iran). Facies 48, 171–198.

Fürsich FT, Wilmsen M, Seyed-Emami K, Cecca F, Majidifard MR. 2005. The upper Shemshak Formation (Toarcian-Aalenian) of the Eastern Alborz (Iran): Biota and palaeoenvironments during a transgressive-regressive cycle. Facies 51, 365–384.

Fürsich FT, Wilmsen M, Seyed-Emami K, Majidifard MR. 2009a. Lithostratigraphy of the Upper Triassic-Middle Jurassic Shemshak Group of Northern Iran. In: MF Brunet, M Wilmsen, JW Granath (Eds), South Caspian to Central Iran Basins. Geological Society of London, Special Publication 312, 129–160.

Fürsich F.T., Wilmsen M., Seyed-Emami K., Majidifard M.R. 2009b. The Mid-Cimmerian tectonic event (Bajocian) in the Alborz Mountains, Northern Iran: Evidence of the break-up unconformity of the South Caspian Basin. In: MF Brunet, M Wilmsen, JW Granath (Eds), South Caspian to Central Iran Basins. Geological Society London, Special Publication 312, 189–203.

Fürsich FT, Pan Y-H, Wilmsen M, Majidifard MR. 2016. Biofacies, taphonomy and palaebiogeography of the Kamar-e-Mehdi Formation of east-central Iran, a Middle to Upper Jurassic shelf lagoon. Facies 62(2), 23 p.

Golonka J. 2007. Late Triassic and Early Jurassic palaeogeography of the world. Palaeogeography, Palaeoclimatology, Palaeoecology 244, 297–307.

Hardenbol J, Thierry J, Farley MB, Jaquin T, de Graciansky P, Vail PR. 1998. Mesozoic and Cenozoic sequence chronostratigraphic framework of European basins. Chart 6: Jurassic sequence chronostratigraphy. In: P de Graciansky, J Hardenbol, T Jaquin, PR Vail (Eds), Mesozoic and Cenozoic sequence stratigraphy of European basins. Society of Economic Palaeontologists and Mineralogists Special Publication 60.

Hoseiniun M. 1995. Stratigraphy and biostratigraphy of the Kashafrud Formation based on ammonites. M.Sc.Thesis, Azad University Tehran. [in Farsi with English abstract]

Hosseinyar G, Moussavi-Harami R, Abdollahie Fard I, Mahboubi A, Noemani Rad R, Ebrahimi M-H. 2019. Facies analyses and depositional setting of the Lower Cretaceous Shurijeh–Shatlyk formations in the Kopeh Dagh–Amu Darya Basin (Iran and Turkmenistan). Geological Journal 54, 1715–1729.

Huber H, Stöcklin J. 1954. Hojedk coal geology. Iran Oil Corporation, Geological Report 116, 1–65. [unpublished]

Huckriede R, Kürsten M, Venzlaff H. 1962. Zur Gelogie des Gebietes zwischen Kerman und Sagand (Iran). Beihefte zum Geologischen Jahrbuch 51, 1–197.

Immel H, Seyed-Emami K, Afshar-Harb M. 1997. Kreide-Ammoniten aus dem iranischen Teil des Koppeh-Dagh (NE-Iran). Zitteliana 21, 159–190.

Kavoosi MA, Lasemy Y, Sherkati S, Moussavi-Harami R. 2009. Facies analysis and depositional sequences of the Upper Jurassic Mozduran Formation, a carbonate reservoir in the Kopet Dagh basin, NE Iran. Journal of Petroleum Geology 32, 235–260.

Kluyver HM, Griffis R, Tirrul R, Chance PN, Meixner HM. 1983a. Explanatory text of the Lakar Kuh Quadrangle Map 1:250 000. Geological Survey of Iran, Geological Quadrangle Map 19, 1–175.

Kluyver HM, Griffis R, Tirrul R, Chance PN, Johns GW, Meixner HM. 1983b. Explanatory text of the Naybandan Quadrangle Map 1:250 000. Geological Survey of Iran, Geological Quadrangle Map J8, 1–143.

Krystyn L, Malini M, Aghababalou BS, Hairapetian V. 2019. Norian ammonoids from the Nayband Formation (Iran) and their bearing on Late Triassic sedimentary and geodynamic history of the Iran Plate. Rivista Italiana di Paleontologia e Stratigrafia 125, 231–248.

Lassemi Y. 1995. Platform carbonates of the Upper Jurassic Mozduran Formation in the Kopet Dagh Basin, NE Iran-facies, paleoenvironments and sequences. Sedimentary Geology 99, 151–164.

Madani M. 1977. A study of the sedimentology, stratigraphy and regional geology of the Jurassic rocks of eastern Kopet Dagh (NE Iran). Unpublished Ph.D. Thesis, Royal School of Mines, Imperial College London, 246 p.

Majidifard MR. 2003. Biostratigraphy, lithostratigraphy, ammonite taxonomy and microfacies analysis of the Middle and Upper Jurassic of Northeastern Iran. Ph. D. Thesis, Julius-Maximilians Universität Würzburg, Germany, 201 p. [https://opus.bibliothek.uni-wuerzburg.de/frontdoor/index/index/year/2004/docId/683]

Majidifard MR. 2008. Stratigraphy and facies analysis of the Dalichai and Lar formations (Middle – Upper Jurassic) of NNE Iran. Beringeria 39, 3–49.

Majidifard MR. 2015. Late Bajocian–Bathonian ammonites from northeast Iran. Acta Paleontologica Romaniae 11(2), 25–41.

Majidifard MR, Fürsich FT, Keupp H, Seyed-Emami K. 2017. Lower Tithonian ammonites from the Chaman Bid Formation in northeastern Iran, Koppeh-Dagh Basin. Geopersia 7(1), 11–26.

Mattei M, Cifelli F, Muttoni G, Rashid H. 2015. Post-Cimmerian (Jurassic–Cenozoic) palaeogeography and vertical axis tectonic rotations of Central Iran and the Alborz Mountains. Journal of Asian Earth Sciences 102, 92–101.

Moussavi-Harami R, Brenner RL. 1990. Lower Cretaceous (Neocomian) fluvial deposits in eastern Kopet-Dagh Basin, northeastern Iran. Cretaceous Research 11, 163–174.

Mossavi-Harami R, Mahboubi A, Nadjafi M, Brenner RL, Mortazavi M. 2009. Mechanism of calcrete formation in the Lower Cretaceous (Neocomian) fluvial deposits, northeastern Iran based on petrographic, geochemical data. Cretaceous Research 30, 1146–1156.

Mosavinia A, Lehmann J, Wilmsen M. 2014. Upper Albian ammonites from the Aitamir Formation (Koppeh Dagh, NE Iran). Cretaceous Research 50, 72–88.

Nabavi MH, Seyed-Emami K. 1977. Sinemurian ammonites from the Shemshak Formation of North Iran (Semnan area, Alborz). Neues Jahrbuch für Geologie und Paläontologie, Abhandlungen 53(1), 70–85.

Page KN. 2008. The evolution and geography of Jurassic ammonoids. Proceedings of the Geologists' Association 119, 35–57.

Parent H, Raoufian A, Seyed-Emami K, Ashouri AR, Majidifard MR. 2014. The Bajocian–Kimmeridgian ammonite fauna of the Dalichai Formation in the SE Binalud Mountains, Iran. Informes del Insitituto de Fisiografía y Geología 1, 60 p.

Porsoltani MR. 2017. Sea-level change and deep sea sequence stratigraphy: A Middle Jurassic siliciclastic strata (Kashfrud Formation), NE Iran. Iranian Journal of Earth Sciences 9, 17–30.

Pourmotamed F, Motamed A. 1976. Sur l'existence du Domérian marin dans l'Elbourz central (Iran). Compte Rendu sommaire des Séances de la Société géologique de France, fascicule 3, 105–107.

Raoufian A. 2014. Investigations on the Middle and Upper Jurassic strata along the Binalud Range based on stratigraphy, paleontology (ammonite fauna) and sedimentary environment. Unpublished Ph.D. Thesis, University of Mashhad, Iran. 380 p. [in Farsi with English abstract]

Raoufian A, Joly B, Seyed-Emami K, Ashouri AR, Majidifard MR, Ameri H. 2014. Phylloceratoidea from Middle and Late Jurassic of North East Iran (Binalud Ranges). Annales de Paléontologie 100(4), 311–325.

Raoufian A, Zand-Moghadam H, Seyed-Emami K. 2019. Depositional history of Middle-Upper Jurassic succession at the Binalud Mountains, NE Iran: implications of ammonites, trace fossils and stable isotopes in palaeoenvironmental analysis. Historical Biology, DOI: 10.1080/08912963.2018.1563078, 18 p.

Robert MM, Letouzey J, Kavoosi MA, Sherkati S, Müller C, Vergés J, Aghababaei A. 2014. Structural evolution of the Kopeh Dagh fold-and-thrust belt (NE Iran) and interactions with the South Caspian Sea Basin and Amu Darya Basin. Marine and Petroleum Geology 57, 68–87.

Ruttner A, Nabavi MH, Hajian M. 1968. Geology of the Shirgesht area (Tabas area, East Iran). Geological Survey Iran Report 4, 1–133.

Ruttner A. 1991. The Triassic of Aghdarband (Aq Darband) NE Iran and its pre-Triassic frame. Abhandlungen der Geologischen Bundesanstalt 38, 1–252.

Sabbagh Bajestani M, Mahboubi A, Moussavi-Harami R, Al-Aasm I, Nadjafi M. 2017. Facies analysis and sequence stratigraphy of the Qal'eh Dokhtar Formation (Middle–Upper Jurassic) in the west of Boshrouyeh, east central Iran. Acta Geological Sinica 91, 1797–1819.

Salehi MA, Moussavi-Harami SR, Mahboubi A, Wilmsen M, Heubeck C. 2014. Tectonic and palaeogeographic implications of compositional variations within the siliciclastic Ab-Haji Formation (Lower Jurassic, east-central Iran). Neues Jahrbuch für Geologie und Paläontologie 271, 21–48.

Salehi MA, Moussavi-Harami R, Mahboubi A, Fürsich FT, Wilmsen M, Heubeck C. 2018. A tectono-stratigraphic record of an extensional basin: the Lower Jurassic Ab-Haji Formation of east-central Iran. Swiss Journal of Geosciences 111, 51–78.

Sardar Abadi M, Da Silva A-C, Amini A, Aliabadi AA, Boulvain F, Sadar Abadi MH. 2014. Tectonically controlled sedimentation: impact on sediment supply and basin evolution of the Kashafrud Formation (Middle Jurassic, Kopeh-Dagh Basin, northeast Iran). International Journal of Earth Sciences 103, 2233–2254.

Schairer G, Seyed-Emami K, Zeiss A. 1991. Ammoniten aus der oberen Dalichai-Formation (Callov) östlich von Semnan (SE-Alborz, Iran). Mitteilungen der Bayerischen Staatssammlung für Paläontologie und historische Geologie 31, 47–67.

Schairer G, Seyed-Emami K, Majidifard MR, Mohammadi Monfared M. 1999. Erster Nachweis von Untertithon in der Chaman Bid Formation an der Typus-Lokalität bei Bash Kalateh (Zentral-Koppeh Dagh, NE-Iran). Mitteilungen der Bayerischen Staatssammlung für Paläontologie und historische Geologie 39, 21–32.

Schairer G, Seyed-Emami K, Fürsich FT, Senowbari-Daryan B, Aghanabati SA, Majidifard MR. 2000. Stratigraphy, facies analysis and ammonite fauna of the Qal'eh Dokhtar Formation (Middle -Upper Jurassic) at the type locality west of Boshrouyeh (east-Central Iran). Neues Jahrbuch für Geologie und Paläontologie, Abhandlungen 260(1), 35–66.

Schairer G, Fürsich FT, Wilmsen M, Seyed-Emami K, Majidifard MR. 2003. Stratigraphy and ammonite fauna of Upper Jurassic basinal sediments at the eastern margin of the Tabas Block (east-central Iran). Geobios 36, 195–222.

Sengör AMC, Altiner D, Cin A, Ustaömer T, Hsü KJ. 1988. Origin and assembly of the Tethyside orogenic collage at the expense of Gondwana Land. In: MG Audley-Charles, A Hallam (Eds), Gondwana and Tethys. Geological Society London, Special Publication 37, 119–181.

Seyed-Emami K. 1967: Zur Ammoniten-Fauna und Stratigraphie der Badamu-Kalke (unteres Toarcium bis mittleres Bajocium) bei Kerman. Unpublished Ph.D-Thesis Ludwig-Maximilians Universität München, 180 p.

Seyed-Emami K. 1971. The Jurassic Badamu Formation in the

Kerman region, with some remarks on the Jurassic stratigraphy of Iran. Geological Survey of Iran Report 19(15), 1–180.
Seyed-Emami K. 1975. Jurassic – Cretaceous boundary in Iran. Bulletin of the American Association of Petroleum Geologists 59(2), 231–238.
Seyed-Emami K. 1987. Hammatoceratinae (Ammonoidea) aus der Shemshak Formation östlich von Shahmirzad (SE-Alborz, Iran). Neues Jahrbuch für Geologie und Paläontologie, Abhandlungen 87(6), 371–384.
Seyed-Emami K. 1988a. Jurassic and Cretaceous ammonite faunas of Iran and their paleobiogeographic significance. In: J. Wiedmann, J Kullmann (Eds), Cephalopods – Present and Past. Stuttgart, Schweizerbart, 599–606.
Seyed-Emami K. 1988b. Eine Ammoniten-Fauna aus der Badamu-Formation (Unterbajocium, sauzei-Zone) westlich von Kerman (Zentraliran). Paläontologische Zeitschrift 62(1–2), 71–86.
Seyed-Emami K. 1999. New informations on the evaporitic (Ravar Formation) and the stratigraphic position of the Middle and Upper Jurassic strata in the Ravar-Kerman area (Central Iran). Journal of the Faculty of Engineering, University of Tehran 33(2), 81–95. [in Farsi with english abstract]
Seyed-Emami K. 2003. Triassic in Iran. Facies 48, 91–106.
Seyed-Emami K, Nabavi MH. 1985. *Dumortieria* und *Pleydellia* (Ammonoidea) aus der Shemshak Formation (Obertrias bis mittlerer Jura) östlich von Shahmirzad (SE-Alborz, Iran). Neues Jahrbuch für Geologie und Paläontologie, Abhandlungen 170, 243–272.
Seyed-Emami K, Alavi-Naini M. 1990. Bajocian Stage in Iran. Memorie del Descrizione della Carta Geologica d'Italia 40, 215–221.
Seyed-Emami K, Schairer G. 2010. Late Jurassic (Oxfordian, Bimammatum Zone) ammonites from the eastern Alborz Mountains, Iran. Neues Jahrbuch für Geologie und Paläontologie, Abhandlungen 257(3), 267–281.
Seyed-Emami K, Schairer G. 2011a. Late Jurassic (Oxfordian, Bifurcatus and Bimammatum zones) ammonites from the eastern Alborz Mountains, Iran. Neues Jahrbuch für Geologie und Paläontologie, Abhandlungen 260, 11–20.
Seyed-Emami K, Schairer G. 2011b. New Middle and Upper Jurassic ammonites from the Binalud Mountains (Mashhad region, NE Iran). Neues Jahrbuch für Geologie und Paläontologie, Abhandlungen 261, 373–380.
Seyed-Emami K, Wilmsen M. 2016. Leymeriellidae (Cretaceous ammonites) from the lower Albian of Esfahan and Khur (Central Iran). Cretaceous Research 60, 78–90.
Seyed-Emami K, Raoufian A. 2017. Ammonites from Bathonian and Callovian (Middle Jurassic) North of Damghan, Eastern Alborz, North Iran. Zitteliana A89, 253–270.
Seyed-Emami K, Schairer G, Bolourchi MH. 1985. Ammoniten aus der unteren Dalichay Formation (ob. Bajocium–unt. Bathonium) in der Umgebung von Abe-Garm (Avaj, NW Ira). Zitteliana 12, 57–85.
Seyed-Emami K, Schairer G, Alavi-Naini M. 1989. Ammoniten aus der unteren Dalichai-Formation (Unterbathon) östlich von Semnan (SE-Alborz, Iran). Münchner Geowissenschaftliche Abhandlungen A15, 79–91.
Seyed-Emami K, Schairer G, Aghanabti S. A, Fazl M. 1991. Ammoniten aus dem Bathon von Zentraliran (Tabas-Naiband Region). Münchner Geowissenschaftliche Abhandlungen A19, 65–100.
Seyed-Emami K, Schairer G, Aghanabti SA, Hajmolaali A. 1993. Einige Ammoniten aus der Badamu-Formation (oberes Toarc bis unteres Bajoc) SW von Ravar (N-Kerman, Zentraliran). Mitteilungen der Bayerischen Staatssammlung für Paläontologie und historische Geologie 33, 13–30.
Seyed-Emami K, Schairer G, Behroozi A. 1994. Einige Ammoniten aus der Kashafrund-Formation (mittlerer Jura) E Mashhad (NE-Iran). Mitteilungen der Bayerischen Staatssammlung für Paläontologie und historische Geologie 34, 145–158.
Seyed-Emami K, Schairer G, Zeiss A. 1995. Ammoniten aus der Dalichai-Formation (Mittlerer bis Oberer Jura) und der Lar-Formation (Oberer Jura) N Emamzadeh-Hashem (Zentralalborz, Nordiran). Mitteilungen der Bayerischen Staatssammlung für Paläontologie und historische Geologie 35, 39–52.
Seyed-Emami K, Schairer G, Behroozi A. 1996. Ammoniten aus dem Oberen Bajoc (Mittlerer Jura) des SE-Koppeh-Dagh und SE-Alborz (NE-Iran). Mitteilungen der Bayerischen Staatssammlung für Paläontologie und historische Geologie 36, 87–106.
Seyed-Emami K, Schairer G, Aghanabati SA. 1997. Ammoniten aus der Baghamshah Formation (Callov, Mittlerer Jura) von NW-Tabas (Zentraliran). Mitteilungen der Bayerischen Staatssammlung für Paläontologie und historische Geologie 37, 27–40.
Seyed-Emami K, Schairer G, Aghanabati SA. 1998a. *Bullatimorphites* aus Oberbathon (Mittlerer Jura), SW Tabas (Zentraliran). Mitteilungen der Bayerischen Staatssammlung für Paläontologie und historische Geologie 38, 121–134.
Seyed-Emami K, Schairer G, Fürsich FT, Senowbari-Daryan B, Majidifard MR. 1998b. *Cadomites* aus der unteren Baghamshah-Formation (Oberbathon, Mittlere Jura) SW Tabas (Zentraliran). Mitteilungen der Bayerischen Staatssammlung für Paläontologie und historische Geologie 38, 111–119.
Seyed-Emami K, Schairer G, Mohammadi-Monfared M. 1998c. Ammoniten aus dem Oberen Jura des Nordiran. Mitteilungen der Bayerischen Staatssammlung für Paläontologie und historische Geologie 38, 97–110.
Seyed-Emami K, Schairer G, Fürsich FT, Wilmsen M, Majidifard MR. 2000. First record of ammonites from the Badamu Formation at the Shotori Mountains (Central Iran). Eclogae geolgicae Helveticae 93, 257–263.
Seyed-Emami K, Fürsich FT, Schairer G. 2001. Lithostratigraphy, ammonite faunas and paleoenvironments of Middle Jurassic strata in North and Central Iran. Newsletters on Stratigraphy 38, 163–184.
Seyed-Emami K, Schairer G, Fürsich FT, Wilmsen M, Majidifard MR. 2002. Reineckeidae (Ammonoidea) from the Callovian (Middle Jurassic) of the Shotori Range (East-Central Iran). Neues Jahrbuch Geologie Paläontologie, Monatshefte 3, 184–192.
Seyed-Emami K, Fürsich FT, Wilmsen M. 2004a. Documentation and significance of tectonic events in the northern Tabas Block (east Central Iran) during the Middle and Late Jurassic: structural, sedimentary and stratigraphic evidence. Rivista Italiana di Paleontologia e Stratigrafia 110, 163–171.
Seyed-Emami K, Fürsich FT, Wilmsen M, .Schairer G, Majidifard MR. 2004b. Jurassic (Toarcian to Bajocian) ammonites from the Lut Block, east-central Iran. Acta Geologica Polonica 54(1), 77–94.
Seyed-Emami K, Fürsich FT, Wilmsen M, Schairer G, Majidifard MR. 2005. Toarcian and Aalenian (Jurassic) ammonites from the Shemshak Formation of the Jajarm area (eastern Alborz, Iran). Paläontologische Zeitschrift 79(3), 349–369.
Seyed-Emami K, Fürsich FT, Wilmsen M, Majidifard MR, Cecca F, Shekarifard A. 2006. Stratigraphy and ammonite fauna of the upper Shemshak Formation (Toarcian-Aalenian) at Tazareh, eastern Alborz. Journal of Asian Earth Sciences 28, 259–275.
Seyed-Emami K, Fürsich FT, Wilmsen M, Majidifard MR, Shekarifard A. 2008. Lower and Middle Jurassic ammonites of the Shemshak Group in Alborz, Iran and their palaeobiogeographical and biostratigraphical importance. Acta Palaeontologica Polonica 53(2), 237–260.
Seyed-Emami K, Schairer G, Raoufian A, Shafeizad M. 2013. Middle and Upper Jurassic ammonites from the Dalichai Formation east of Shahrud (East Alborz, North Iran). Neues Jahrbuch für Geologie und Paläontologie, Abhandlungen 267, 43–66.
Seyed-Emami K, Raoufian A, Mönnig E. 2015. Macrocephalitinae (Ammonoidea, Middle Jurassic) from North and Central Iran. Neues Jahrbuch für Geologie und Paläontologie, Abhandlungen 278(3), 257–279.
Seyed-Emami K., Raoufian, A., Zand-Moghadam H. 2018. Late Bajocian and Bathonian (Middle Jurassic) ammonites from the Dalichai Formation north of Damghan (Alborz, North Iran). Neues Jahrbuch für Geologie und Paläontologie, Abhandlungen 288(2), 183–2003.
Smith PL, Tipper HW, Ham DM. 2001. Lower Jurassic Amaltheiidae (Ammonitina) in North America: Paleobiogeography and tectonic implications. Canadian Journal of Earth Sciences 38, 1439–1449.
Stampfli GM. 1978. Étude géologique generale de l'Elbourz oriental

au sud de Gonbad-e-Qabus (Iran NE). PhD thesis 1868, Université Genève, 329 p.

Steiger R. 1966. Geologie der West-Firuzkuh-Area (Zentralelburz, Iran). Mitteilungen aus dem Geologischen Institut der Eidgenössischen Technischen Hochschule und der Universität Zürich, Neue Folge 68, 1–145.

Stöcklin J. 1961. Lagoonal formations and salt domes in East Iran. Bulletin of the Iranian Petroleum Institute 3, 29–46.

Stöcklin J. 1972. Iran central, septentronal et oriental. Lexique Stratigraphique International, v. III, Asie, Fascicule 9b, 1–238.

Stöcklin J. 1974. Possible ancient continental margin in Iran. In: CA Burke, CL Drake (Eds), The Geology of Continenal Margins. New York, Springer, 873–887.

Stöcklin J, Eftekhar-Nezhad J, Hushmand-Zadeh A. 1965. Geology of the Shotori Range (Tabas Area, East Iran). Geological Survey of Iran Report 3, 1–69.

Taheri J. 2009. Stratigraphy, ichnology, and sedimentary environments of the Late Bajocian-Late Bathonian Kashafrud Formation, northeastern Iran. PhD thesis University of Würzburg, 257 p. [https://opus.bibliothek.uni-wuerzburg.de/frontdoor/index/index/year/2009/docId/3334]

Taheri J, Fürsich FT, Wilmsen M. 2009. Stratigraphy, depositional environments and geodynamic significance of the Upper Bajocian-Bathonian Kashafrud Formation (NE Iran). In: MF Brunet, M Wilmsen, JW Granath (Eds), South Caspian to Central Iran Basins. Geological Society Londen, Special Publication 312, 205–218.

Takin M. 1972. Iranian geology and continental drift in the Middle East. Nature 235 (5334), 147–150.

Thierry J. 2000. Middle Callovian (157–155 Ma). 1n: J Dercourt, M Gaetani, B Vrielynck, E Barrier, B Biju-Duval, MF Brunet, JP Cadet, S Crasquin, M Sandulescu (Eds), Atlas Peritethys Palaegeographical Maps. Paris, CCGM/CGMW, 71–97.

Wilmsen M, Fürsich FT, Seyed-Emami K. 2003. Revised lithostratigraphy of the Middle and Upper Jurassic Magu Group of the northern Tabas Block, east-central Iran. Newsletters on Stratigraphy 39, 143–156.

Wilmsen M, Fürsich FT, Seyed-Emami K, Majidifard MR, Taheri J. 2009a. The Cimmerian orogeny in northern Iran: tectono-stratigraphic evidence from the foreland. Terra Nova 21, 211–218.

Wilmsen M, Fürsich FT, Seyed-Emami K, Majidifard MR. 2009b. An overview of the lithostratigraphy and facies development of the Jurassic System on the Tabas Block, east-central Iran. In: MF Brunet, M Wilmsen, JW Granath (Eds), South Caspian to Central Iran Basins. Geological Society London, Special Publication 312, 323–344.

Wilmsen M, Fürsich FT, Taheri J. 2009c. The Shemshak Group (Lower-Middle Jurassic) of the Binalud Mountains, NE Iran: stratigraphy, depositional environments and geodynamic implications. In: MF Brunet, M Wilmsen, JW Granath (Eds), South Caspian to Central Iran Basins. Geological Society London, Special Publications 312, 175–188.

Wilmsen M, Fürsich FT, Seyed-Emami K, Majidifard MR, Zamani-Pedram M. 2010. Facies analysis of a large-scale Jurassic shelf-lagoon: The Kamar-e-Mehdi Formation of east-central Iran. Facies 56, 59–87.

Wilmsen M, Fürsich FT, Majidifard, MR. 2015. An overview of the Cretaceous stratigraphy and facies development of the Yazd Block, western Central Iran. Journal of Asian Earth Sciences 102, 73–91.

Zamani-Pedram M. 2011. Source, facies, and sedimentary environments of the Middle to Upper Jurassic strata in the Kerman and Tabas areas, east-central Iran. PhD Thesis University of Würzburg, 212 p. [https://opus.bibliothek.uni-wuerzburg.de/frontdoor/index/index/docId/4840]

Zand-Moghadam H, Moussavi-Harami R, Mahboudi A, Aghaei A. 2016. Lithofacies and sequence stratigraphic analysis of the Upper Jurassic siliciclastics in the eastern Kopet-Dagh Basin, NE Iran. Journal of African Earth Sciences 117, 48–61.